The University of Texas MD Anderson Cancer Center UTHealth Graduate School of Biomedical Sciences Dissertations and Theses (Open Access)

The University of Texas MD Anderson Cancer Center UTHealth Graduate School of Biomedical Sciences

8-2019

TRACKING TREATMENT RESPONSE AND RESISTANCE TO PARP INHIBITION (TALAZOPARIB) IN HEREDITARY PANCREATIC CANCER.

Jennifer Goldstein

Follow this and additional works at: https://digitalcommons.library.tmc.edu/utgsbs_dissertations

Part of the Neoplasms Commons, and the Oncology Commons

TRACKING TREATMENT RESPONSE AND RESISTANCE TO PARP INHIBITION

(TALAZOPARIB) IN HEREDITARY PANCREATIC CANCER.

A

DISSERTATION

Presented to the Faculty of

The University of Texas

MD Anderson Cancer Center UTHealth

Graduate School of Biomedical Sciences

In Partial Fulfillment

of the Requirements

for the Degree of

DOCTOR OF PHILOSOPHY

by

Jennifer B Goldstein, M.D.

Houston, Texas

August, 2019

Dedicated to My Family

Acknowledgments

I would like to thank Dr. Andy Futreal for his excellent mentorship over the last six years. and my Advisory Committee members, Drs. Giulio Draetta, Scott Kopetz, Gheath Al-Atrash, and Paul Scheet for their guidance. I would like to express my appreciation to Drs. Hannah Beird, Whijae Roh, Sabitha Prabhakaran, and Akash Mitra for their extreme kindness and patience, helping me with various projects. In addition, I thank of the other members of the Futreal laboratory including, Curtis Gumbs, Latasha Little, Marcus Coyle, Joshua Baguley, Christigale Mandapat, Samantha Tippen, and Rebecca Thornton who all graciously supported me by teaching me techniques and helping me process samples. I would also like to thank Dr. Chang-Gong Liu, Dr. Linghua Wang, Yuanxin Wang and Sahil Seth and all the members of Dr. John Zhang's laboratory, including Drs. Henry Song, Ethan Mao, and Lily Zhao for their sequencing and bioinformatics support. I would additionally like to thank Drs. Michael Peoples and Ale Carugo with IACS who have always been so willing to answer all of my questions, provide protocols and reagents. I would also like to think Dr. Robert Wolff and Dr. Robert Bast for allowing me to participate in the GSBS program during my hematology/oncology fellowship. I am also forever indebted to Dr. Waun K Hong who was one of my biggest fans and biggest supporters at MD Anderson.

I would also like to thank my parents Joyce and Rick, as well as my sister Kimberly, my uncle Dave, and cousins Aaron and Leon for always being there for me. A tremendous thank you goes to my husband, Adolfo, for his constant patience and loving support during my training. Lastly, I would like to dedicate this thesis to my Aunt Lynn and cousin Sarah who were my very first cancer patients. Always loved, never forgotten.

IDENTIFYING AND TRACKING TREATMENT RESPONSE AND RESISTANCE

MECHANISMS TO PARP INHIBITION (BMN-673, TALAZOPARIB) IN

HEREDITARY PANCREATIC CANCER

Jennifer B Goldstein, M.D.

Advisor Professor: Andrew Futreal, Ph.D.

polyADP ribose polymerase (PARP) inhibitors are a class of drugs that block the PARP enzymes, involved in the repair of singe-stranded DNA breaks through the base excision repair pathway. PARP inhibition leads to replication-associated double stranded DNA breaks, which are repaired by homologous recombination (HR). In tumors with HR defects (i.e. *BRCA* mutants), there is a shift to error-prone DNA repair and subsequent genomic instability and cell death.

In 2014, Olaparib became the first FDA-approved PARP inhibitor for the treatment of *BRCA*-mutant ovarian cancer. In the phase III POLO (Pancreas cancer OLaparib Ongoing) trial presented at the American Society for Clinical Oncology (ASCO) conference in 2019, maintenance therapy with Olaparib significantly delayed the progression of metastatic *BRCA* mutant pancreatic adenocarcinoma (PDAC) compared to placebo (7.4 months vs 3.8 months). Talazoparib, a second generation PARP inhibitor, is 20-200-fold more efficacious compared to older PARP inhibitors. In 2018, Talazoparib was FDA approved to treat *BRCA*-mutant, HER2-negative breast cancer and is still in early phase trials for PDAC. While these inhibitors show tremendous promise, not all hereditary PDAC patients respond to PARP inhibitors, and resistance has been observed.

In order to explore resistance to PARP inhibitors in PDAC and I hypothesized that: 1. Genomic alterations are responsible for response and resistance to PARP inhibitor

(Talazoparib) treatment in pancreatic patient-derived xenograft (PDX) tumors; and 2. The use of shRNA technology on pancreatic PDX tumors can elucidate synthetic lethal partners to overcome therapeutic resistance to PARP inhibition. To test this hypothesis, I set out to first further characterize the hereditary PDAC population with germline sequencing and then second, find novel resistance mechanisms and potential rational drug combination therapies to overcome this resistance.

I demonstrated the results of a large-scale germline sequencing project of 133 metastatic PDAC patients. In Chapter 2, I show that the incidence of hereditary pancreatic cancer is nearly 20% in this cohort as well as a TCGA validation patient data set. Patients with DNA damage repair gene (*ATM*, *BRCA1*, *BRCA2*, *ERCC4, PALB2*) alterations have a statistically significant near doubling of overall survival compared to those without mutations (17.9 versus 9.6 months, *P* = 0.03). I show that although strong family history of multiple breast, ovarian, and pancreatic cancers is associated with improved survival, mutational profile is a better indicator of overall survival.

I tested the efficacy of Talazoparib in *BRCA*-mutant PDAC PDX models. Using colony formation assays, I show a differential response in *BRCA*-mutant and wild type cell lines; and found unexpected resistance in one *BRCA2*-mutant PDX model (PATC55). I found a truncating *RIF1* DNA mutation at the BRCA interacting site. Additional shRNA targeted knockdown of *RIF1* did not induce resistance, however single cell RNA sequencing of Talazoparib-treated cells did demonstrate high expression levels of SHFM1, known to facilitate Rad51 loading of RPA. Elevated SHFM1 levels has been associated with aggressive breast cancer and platinum resistance and may be playing a part in PARP resistance in hereditary PDAC as well[1,2].

Pancreatic cancer is a difficult disease to treat with limited possibility for cure. Some hereditary pancreatic cancers with deficiencies in DNA repair appear sensitive to treatment with PARP inhibitors, although not all cancers respond as expected. This data, provides rationale to pursue drug combination therapies, to mitigate resistance to PARP inhibitors and bring about novel treatment options to hereditary PDAC patients.

Table of Contents

List of Illustrations

List of Tables

Abbreviations

AACR – American Academy of Cancer Research

ABS – Applied Biosystems

ADEX - aberrantly differentiated endocrine exocrine

AJCC - American Joint Committee on Cancer

ATCC - American Type Culture Collection

BER – base excision repair

BME - 2-Mercaptoethanol

BWA - Burrows-Wheeler Aligner

CCF – cancer cell fraction

CI – confidence interval

CR – complete response

CT - Computed Tomography

DDR – DNA damage repair

DDROme - DNA damage RepairOme

DEGs – differentially expressed genes

DMEM - Dulbecco's Modified Eagle Medium

DMSO – dimethyl sulfoxide

DNA - deoxyribonucleic acid

DR – damage reversal

ECOG - Eastern Cooperative Oncology Group

ESP – exome sequencing project

EUS – endoscopic ultrasound

EXAC - Exome Aggregation Consortium

FA – Fanconi's anemia

FBS – fetal bovine serum

FDA- Food and Drug Administration

FOLFIRINOX – 5-fluorouracil, irinotecan, oxaliplatin

H&E – hematoxylin and eosin

HGMD – human gene mutation database

IACS – Institute for Applied Cancer Science

IACUC - Institutional Animal Care and Use Committee

IC – inhibitory concentration

INDEL – insertion and deletion

IPMN - intraductal papillary mucinous neoplasm

H6PD - Hexose-6-Phosphate Dehydrogenase

HR – homologous recombination

MCN - mucinous cystic neoplasm

MDACC – MD Anderson Cancer Center

MMR – mismatch repair

NCCN - National Comprehensive Cancer Network

NER – nucleotide excision repair

NHEJ – non-homologous end joining

NMF - Nonnegative matrix factorization

NSG - NOD scid gamma

ORR – overall response rate

OR – odds ratio

OS – overall survival

PanIN - pancreatic intraepithelial neoplasia

PARP - polyADP ribose polymerase

PBS – phosphate buffered saline

PCR – polymerase chain reaction

PD – progressive disease

PDAC – pancreatic ductal adenocarcinoma

PDX – patient-derived xenograft

POLO – Pancreas cancer OLaparib Ongoing

PR – partial response

QC – quality control

RIN – RNA integrity number

RIPA - Radioimmunoprecipitation assay

RNA - ribonucleic Acid

RPA – replication protein A

RPMI - Roswell Park Memorial Institute

SD – stable disease

SDS - Sodium dodecyl sulfate

SEER - Surveillance, Epidemiology, and End Results Program

shRNA – short-hairpin RNA

SNN – shared nearest neighbor

SOC – standard of care

SPSS - Statistical Package for the Social Sciences

ssGSEA - single sample GSEA

TBST – Tris buffered saline Tween

TCGA – The Cancer Genome Atlas

TIC – tumor initiating cell

TSNE - t-distributed stochastic neighbor embedding

UMAP - uniform manifold approximation and projection

UMD – universal mutation database

UCSC – University of California at Santa Cruz

UCSD - University of California at San Diego

V – volts

VAF – variant allele frequency

VUS – variant of unknown significance

WES – whole exome sequencing

WGS – whole genome sequencing

WT – wild type

XRT – radiation

XPO - exportin

Chapter 1

Introduction

1.1 Pancreatic Cancer Diagnosis is Often Delayed and Found Late in the Disease Process

Pancreatic cancer is characterized by its aggressive nature and therapeutic resistance. Although pancreatic cancer only makes up 3% of all cancers diagnosed each year, pancreatic ductal adenocarcinoma (PDAC) is the 4th leading cause of cancer death in the United States[3] According to the Surveillance, Epidemiology, and End Results Program (SEER) registry there are estimated to be 56,770 new cases in 2019 and the current five-year-survival rate is approximately 9%[4]. However, it has been projected that by 2020, pancreatic cancer will become the second leading cause of cancer-related deaths, second only to lung cancer[5].

Pancreatic cancer predominantly effects the elderly with a median age of diagnosis of 70 years[4]. The etiology and inciting factors associated with PDAC are poorly understood. Cigarette smoking, family history of pancreatic cancer, heavy alcohol consumption, diabetes and history of pancreatitis have been shown to increase risk of disease[6]. Symptoms of pancreatic cancer are often vague and include abdominal pain, jaundice and weight loss[7]. Presentation to physicians is often delayed and cancer is commonly found late in the disease process[8].

Diagnosis of pancreatic cancer is usually made by Computed Tomography (CT) imaging followed by Endoscopic ultrasound (EUS)-guided biopsy and tumor markers[9]. Pancreatic cancer is rarely staged using the traditional American Joint Committee on Cancer (AJCC) staging system. Rather, clinical oncologists frequently stage patients based on their ability to undergo curative resection[10]. Surgical feasibility is determined based on proximity to the major vasculature and adjacent structures[11]. It is estimated that

only 20% of patients will meet criteria for surgery[12]. Standard-of-care is limited to surgical resection, if feasible, followed by adjuvant chemotherapy with the oral antimetabolite, capecitabine, and intravenous gemcitabine[13]. Locally advanced, borderline resectable, or metastatic disease is even more difficult to treat with limited treatment choices outside of clinical trials.

Pancreatic cancer precursor lesions have been described. These include the intraductal papillary mucinous neoplasm (IPMN), mucinous cystic neoplasm (MCN), and the pancreatic intraepithelial neoplasia (PanIN1, PanIN2, and PanIN3)[14]. There appears to be a temporal progression of mutation acquisition in PanIN leading to pancreatic cancer, beginning with telomere shortening and *KRAS* mutation, followed by *p16/CDKN2A* loss and later mutations of *DPC4/SMAD4, TP53,* and *BRCA2*[15]. Once cancer has developed, molecular subtyping may be performed based on DNA mutational and RNA expression data.

1.2 Molecular Subtyping of Pancreatic Cancer Can Be Performed with Gene Expression Profiling and Assessment of Structural Variation Patterns

Molecular subtyping of pancreatic cancer has been performed based on gene expression profiling with four molecular subtypes having been described: squamous; pancreatic progenitor; immunogenic; and aberrantly differentiated endocrine exocrine (ADEX)[16]. Squamous tumors have a poor prognosis. They are characterized by frequent somatic mutations in *TP53* and *KDM6A*, TP63ΔN transcriptional network upregulation, and hypermethylation and downregulation of endodermal cell-fate determining genes such as *GATA6*, *HNF1B*, *MNX1*, and *PDX1*. Pancreatic progenitor tumors have

upregulation of early pancreatic development genes such as *FOXA2/3*, *MNX1*, and *PDX1*. Immunogenic tumors demonstrate upregulation of immune networks involved in acquired immune suppression. ADEX tumors display upregulation of genes that regulate KRAS activation, endocrine (*NEUROD1* and *NKX2-2*), and exocrine differentiation (*NR5A2* and *RBPJL*)[16]. Pathologic germline and somatic *BRCA* mutations were found in all subtype groups[16]. Although these molecular subtypes have been delineated, they are infrequently used clinically to inform on treatment decisions.

In 2015, Waddell and colleagues published a groundbreaking study, that significantly enhanced our understanding of PDAC[17]. Whole genome sequencing (WGS) and copy number variation analysis classified PDAC based on patterns of structural variations. Four distinct subtypes emerged, including stable, locally rearranged, scattered and unstable tumors. The proportion of patients (14%) with an "unstable" phenotype, characterized by cases with over 200 somatic variants per sample, were thought to represent the *BRCA* mutant and other hereditary PDAC patients, as a large portion of these tumors were found to have mutations in DNA repair pathway genes or harbored *BRCA* mutational signatures[17]. Interestingly, structural variant patterns for *BRCA1* and *BRCA2* mutants are different with *BRCA1*-deficient cancers predominantly containing short (< 10 kb) tandem duplications, while *BRCA2*-inactive cancers usually show deletions[18]. The inherent genomic instability in some of these hereditary tumors lead to a unique disease phenotype and possibly differential response to treatment.

1.3 Hereditary Pancreatic Cancer is Caused by Germline Mutations Which May Alter Response to Treatment

Sporadic cancers are those that are not caused by an inherited germline cancer predisposition gene but may have acquired somatic gene mutations or other genomic alterations that lead to cancer progression. On the other hand, familial pancreatic cancer may be due to multifactorial risks of low penetrance genetic mutations or even environmental influence combined with germline genomic alterations. Hereditary pancreatic cancer is the result of germline mutations (i.e. *BRCA1* and *BRCA2*) in specific genes that increase the susceptibility to pancreatic cancer[19-21]. PDAC has been over-represented in families with history of breast and ovarian cancers[22,23]. Also, those individuals with a first-degree relative with PDAC have 2.3 times increased risk of developing pancreatic cancer[24]. Iqbal and colleagues reported a near doubling of PDAC in those with *BRCA1* and *BRCA2* mutations[25]. In those of Ashkenazi Jewish decent, two predominant mutations in *BRCA1* (185delAG, 5382InsC) and one in *BRCA2* (6174delT) are identified in the large majority of high-risk families[26,27]. The prevalence of *BRCA2* mutations in hereditary PDAC in non-Jewish, ethnically diverse populations has been reported to range from 6% to 17%[28-30].

Hereditary PDAC patients are thought to represent a unique population with characteristic molecular patterns and improved response to both standard of care and certain experimental therapeutics[17,31,32]. Previous mutations studies in PDAC have focused on a limited set of genes, mostly dedicated to those genes within the DNA damage repair (DDR) pathway (*ATM, BRCA1, and BRCA2*). A provocative family history of cancer or Ashkenazi Jewish heritage may prompt some physicians to order further genetic testing. However, often gene carriers have incomplete penetrance, some patients with germline *BRCA* mutations will not have a strong family history of cancer.

Goggins and colleagues showed that about 10% of patients who appeared to have sporadic disease had pathologic germline *BRCA2* mutations[33]. Recent studies have also shown that family history of PDAC is not always predictive of germline mutations[34,35]. In fact, the National Comprehensive Cancer Network (NCCN) guidelines recommend all pancreatic cancer patients undergo germline DNA sequencing, regardless of risk profile[36]. Expanded genome-wide assessment of tumor and germline DNA and RNA may provide insight into drug selection.

In 2015, 549 patients at MD Anderson Cancer Center (MDACC) and Johns Hopkins University, Fogelman and colleagues showed that platinum therapy in patients with 3 or more family members with history of breast, ovarian, or pancreatic cancers, was associated with a longer survival. These findings suggest that family history may serve as a predictive marker for platinum use in patients with metastatic PDAC[32]. In February 2019, my colleagues and I followed up on this study with a paper accepted for publication in Clinical Cancer Research, where we assessed the prevalence of deleterious germline mutations in metastatic PDAC[37]. Our goal was to identify novel genomic alterations leading to hereditary pancreatic cancer in an unselected cohort of PDAC patients. As will be further demonstrated in the results section in Chapter 2, we have expanded on our current understanding of the causes of hereditary pancreatic cancer.

1.4 PARP Inhibitors Show Promise in Treatment of Hereditary Cancers

PolyADP ribose polymerase (PARP) enzymes contain 18 family members, the most well characterized of which are PARP1 and PARP2[38]. PARP enzymes participate in multiple diverse cellular functions including the metabolism of nucleic acids,

modification of chromatin structure, and participation in DNA synthesis and repair[39]. PARP1 was first described for its role in orchestrating single stranded DNA breaks through its role in the base excision repair (BER) pathway[40]. Upon detection of single stranded DNA breaks, PARP1 is activated and binds to the DNA. PARP1 then uses NAD+ to create polymers of poly(ADP-ribose) and transfers it to other DNA repair proteins, including PARP itself[41]. The auto-poly(ADP-ribosyl)ation recruits other proteins to the damaged DNA site initiating DNA repair[42]. Eventually, PARP1 undergoes a conformational change and it is released from the site of damage.

PARP inhibitors are a class of agents that have shown some promise in the treatment of hereditary PDAC. PARP inhibitors block the PARP enzymes. This inhibition can then lead to stalling at replication forks, conversion to replication-associated double stranded breaks and subsequent repair via homologous recombination. In tumors with homologous recombination defects (i.e. germline or somatic *BRCA* mutants), there is an increased use of error prone DNA repair mechanisms and subsequent genomic instability and cell death[43]. PARP inhibitors do have varying binding profiles to members within the PARP protein family[44]. The majority of PARP inhibitors currently in clinical use such as Rucuparib and Olaparib show selective binding to PARP1-4[44]. Cross-sensitivity has been shown between platinum and PARP inhibitor therapy in pancreatic cancer[45].

In 2014, Olaparib became the first FDA approved PARP inhibitor indicated to treat *BRCA*-mutant ovarian cancer[46]. In the randomized phase III POLO trial presented at ASCO 2019, it was shown that maintenance therapy with olaparib significantly delayed the progression of metastatic pancreatic cancer in those patients with a germline *BRCA*

mutation compared with placebo (median progression-free survival = 7.4 months vs 3.8 months, respectively)[47]. Newer generation PARP inhibitors, such as Talazoparib (BMN-673), also have a PARP-trapping mechanism that has been shown to increase the efficacy of the agent 20-200-fold compared to older PARP inhibitors[48]. In 2018 Talazoparib was FDA approved to treat *BRCA*-mutated, HER2-negative breast cancer[49].

It has been described that response to PARP inhibitors may be dependent on specific driver mutations and response in *BRCA1* versus *BRCA2* mutants may even differ[50,51]. Additionally, certain classes of PARP inhibitors may have off target effects (i.e. PARP1-independent, p21 dependent mitotic arrest) that may contribute to their therapeutic potential[52]. These mechanisms are thought to be independent of their activity on PARP-1 as these effects are seen in only specific PARP inhibitors. For example, rucaparib has also been shown to target Hexose-6-Phosphate Dehydrogenase (H6PD). H6PD is an enzyme that generates NADPH via the pentose phosphate pathway inside the endoplasmic reticulum[53,54]. Targeting of the protein has been shown to induce apoptosis and increase sensitivity of cells to PARP inhibtion[55]. Yet, resistance still exists against these agents and therapeutic resistance to newer generation PARP inhibitors has yet to be explored in depth.

1.5 Resistance has Been Demonstrated to both Platinum and PARP Inhibitor Treatment

In the Waddell study described above, five of the 24 (20%) patients with evidence of defective DNA repair pathways were treated with DNA-damaging platinum therapy. Two had complete radiographic responses and normalization of CA19-9 and two had

robust partial responses of the five treated[17]. Although it appeared that all 5 patients should have been sensitive to the platinum agent, not all responses were equal.

There have been multiple mechanisms of resistance to both platinum and PARP inhibitor therapy described in the literature. Some reports show secondary mutations in *BRCA1* or *BRCA2* allow restoration of the open reading frame and restore homologous recombination[56,57]. This leads to increased genomic stability and PARP inhibitor resistance. This mechanism has also been shown to cause cross-resistance to platinum therapy as well[58].

Double stranded DNA breaks may be repaired by three main mechanisms including homologous recombination, microhomology-mediated end joining, and non-homologous end joining[59]. CtIP interacts with the MRN (Mre11/Rad50/Nbs1) complex to recognize double stranded DNA breaks[60]. This promotes the resection of 5' strands to generate 3' single-stranded intermediates that are necessary for homologous recombination[61]. CtIP therefore promotes DNA repair via homologous recombination while inhibiting non-homologous end joining[62,63]. Several proteins are known to suppress the CtIP-mediated DNA end resection pathway and thereby inhibit homologous recombination. REV7, PTIP, 53BP1, and RIF1 are among these proteins[64]. CtIP-mediated DNA end resection is blocked by 53BP1 via downstream effectors like RIF1 and PTIP and DNA repair is diverted to C-NHEJ[65]. With loss of 53BP1, homologous recombination is partially restored in *BRCA1* mutants and results in resistance to DNA-damaging agents[66,67].

SLFN11 is a protein that promotes the destabilization of the RPA‑ssDNA complex thereby inhibiting checkpoint maintenance and homologous recombination.

Cancer cell lines with high levels of endogenous SLFN11 are sensitive to DNA-damage inducing agents[68]. Murai and colleagues, however, showed that inactivation of SCLFN11 led to resistance to PARP inhibition therapy, not by activation of homologous recombination, but rather, SLFN11-induced irreversible and lethal replication inhibition[69]. SLFN11 expression levels have therefore been used as a biomarker to predict response to PARP therapy.

In Chapter 3 below I rule out these mechanisms in our Talazoparib-resistant model with DNA and single cell sequencing and look at alternative mechanisms of resistance to PARP inhibitor therapy.

1.6 BRCA2 Antagonizes RIF1-dependent alt-NHEJ to Prevent Gross Genomic Instability

RIF1 protein acts downstream of 53BP1 to translocate to sites of double-stranded DNA damage via an ATM-dependent 53BP1 phosphorylation. Loss of RIF1 rescues initial DNA end resection and checkpoint activation in *BRCA1* mutated cells[70]. However, loss of RIF1, unlike loss of 53BP1, cannot fully rescue RAD51 foci formation and restore defects in homologous recombination. This is likely because of RIF1's dual function in regulation of the foci formation and chromatin loading of BLM. Therefore, one the one hand, RIF1 deficiency facilitates BRCA1-mediated DNA end processing and on the other hand impairs BLM-EXO1 mediated DNA end resection[70,71].

A recent study showed that in BRCA2-depleted cells, the 53BP1–RIF1 complex may promote toxic c-NHEJ and alt-NHEJ events by facilitating the retention of Artemis at sites of DNA damage. BRCA2 antagonizes RIF1-dependent alt-NHEJ to prevent gross

genomic instability in a RAD51-independent manner[72].   We therefore examined whether the loss of RIF1 could lead to restoration in genomic stability in either BRCA1 or BRCA2-deficient cells, thereby reducing their hypersensitivity to PARP inhibition and DNA-damaging agents.

1.7 High SHFM1 Expression Levels are Associated with Worse Prognosis and Platinum Resistance

SHFM1 (DSS1) is a component of the 26S proteasome, a complex involved in the ATP-dependent degradation of ubiquinated proteins[73]. However, SHFM1 has also been shown to bind to and stabilize BRCA2 thereby promoting the BRCA2-dependent loading of RAD51 filament formation on RPA-covered single-stranded DNA. *BRCA2* mutants with impaired DSS1 binding have impaired HR, demonstrating at least part of the HR function is dependent on DSS1's interaction with BRCA2[74]. In budding yeast, lacking a BRCA2 homolog, the DSS1 homolog localizes to double stranded breaks and promote HR- and NHEJ-mediated repair. This suggests a BRCA2-independent function of DSS1 in DNA repair as well which may play a part in *BRCA2* mutants[75].

High expression levels of SHFM1 has been shown to be associated with worse prognosis and shorter relapse-free survival in breast cancer and increased resistance to platinum agents[1,76]. Given the frequent cross-resistance of *BRCA*-mutant cancers to both platinum and PARP inhibitor therapies, in chapter 3, I further explore this as a possible novel mechanism of resistance to Talazoparib treatment in pancreatic cancer.

1.8 XPO1 is a Nuclear Exporter of BRCA1 and Other Tumor Suppressors and Oncoproteins

Exportin1/XPO-1 (CRM1) Is a nuclear export protein responsible for the nuclear export of proteins and messenger RNAs allowing for regulation of key sub cellular molecules. Included in the transport cargo are multiple tumor suppressor and oncoproteins including APC, p53, BRCA1, BRCA2, and Survivin[77]. It has been shown both in ovarian and pancreatic cancer that patients with high CRM1 levels survived less time than those with low CRM1 expression levels[78,79]. KPT-330 or Selinexor is an XPO-1 inhibitor that has been widely tested in phase 1 and phase 2 clinical trials[80,81]. We postulated that in PDAC cells with *BRCA2* defects, blocking the XPO-1 inhibitor would lead to decreased BRCA1 exportation from the nucleus, partial restoration of homologous recombination and resistance to PARP inhibitor treatment.

The goal of this dissertation was to first broaden our understanding of the genomic alterations contributing to hereditary pancreatic cancer. In Chapter 2, I used germline sequencing of an unselected cohort treated here at MDACC to further elucidate underlying pathologic molecular aberrations contributing to disease. I will discuss the finding that DNA damage repair gene mutations (*ATM*, *BRCA1/2*, *CDKN2A*, *CHEK2*, *ERCC4*, and *PALB2*) had a statistically significant improved overall survival as compared to those patients without. In Chapter 3, I describe novel response and resistance mechanisms to PARP inhibitor treatment by using PDX cell line model systems of hereditary PDAC and evaluating for alterations at the DNA, RNA, and protein level. I show that elevated levels of SHFM1 may contribute to primary Talazoparib resistance.

Chapter 2

Germline DNA Sequencing of

Pancreatic Cancer Patients Reveals

Novel Pathologic Hereditary Pancreatic

Cancer Mutations

Chapter 2 is based upon Goldstein J, Zhao L, Wang X, Ghelman Y, Overman M, Javle M, Shroff R, Varadachary G, Wolff R, McAllister F, Futreal PA, Fogelman D, Germline DNA Sequencing Reveals Novel Mutations Predictive of Overall Survival in a Cohort of Pancreatic Cancer Patients. Clinical Cancer Research. 2019, Accepted for Publication. Authors of articles published in AACR journals are permitted to use their article or parts of their article in the following ways without requesting permission from the AACR. All such uses must include appropriate attribution to the original AACR publication. Authors may do the following as applicable:

1. Reproduce parts of their article, including figures and tables, in books, reviews, or subsequent research articles they write;

2. Submit a copy of the article to a doctoral candidate's university in support of a doctoral thesis or dissertation.

2.1 Introduction

Familial pancreatic cancer, defined as having two or more first degree family members who have been diagnosed with pancreatic cancer, is thought to account for 5 to 10% of pancreatic adenocarcinoma[82]. Previous studies of mutation prevalence in familial pancreatic cancer, however, have focused on a limited set of genes, mostly dedicated to those genes within the DNA damage repair (DDR) pathway (*ATM*, *BRCA1* and *BRCA2*) or related to hereditary Lynch syndrome (*MLH1*, *MSH2*, *MSH6, PMS2*)[83-88]. The National Comprehensive Cancer Network (NCCN) currently endorses genetic counseling for all pancreatic cancer patients[89]. A provocative family history of cancer or Ashkenazi Jewish heritage may prompt some physicians to order further genetic testing. Recent studies have

shown that pancreatic cancer family history is not predictive of germline mutations[35,88], highlighting the value of broad sequencing in unselected groups. Specific genes are frequently tested on the basis of known cancer syndromes[90]. The prevalence of mutations among patients with pancreatic cancer, who are unselected for specific risk factors such as age at diagnosis or family cancer history, is a current topic of interest amongst oncologists. Next-generation sequencing enables testing for both commonly described familial mutations, as well as rarely described variants.

We previously reported family history as a biomarker for survival in pancreatic cancer[32]. We found that patients with a strong family history of *BRCA*-related cancers (three or more 1st to 3rd generation relatives with breast, ovarian, or pancreas cancer) had an overall survival (OS) nearly double of those with no such family history. Family history, however, is a subjective measure and surrogate for the underlying disease biology leading to predisposition to pancreatic cancer in families.

Additionally, despite evidence for a predictive benefit to platinum agents in familial PC, most practitioners use performance status as the main determinate for treatment regimen decisions. In metastatic pancreatic cancer patients with poorer performance status (PS > 1) often receive treatment with gemcitabine plus nab-paclitaxel (gem/nab-paclitaxel), rather than the more difficult to tolerate platinum-based regimen 5-fluoruracil, irinotecan, and oxaliplatin (FOLFIRINOX)[91,92].

In this study, we assessed the prevalence of deleterious germline mutations using a 263-gene panel in a population of pancreatic cancer patients, treated with current SOC chemotherapy, who presented to a large academic cancer institution. We also used a secondary cohort, the pancreatic cancer genome atlas (TCGA) research network germline

data, to confirm the validity of some of our findings[24]. Our goal was to identify additional underlying genomic alterations leading to familial pancreatic cancer in an unselected cohort including their link to family history, clinical implications, response to SOC treatment and survival outcomes.

2.2 Materials and Methods

2.2.1 Patient Selection of MDACC Cohort

All patients with metastatic pancreatic adenocarcinoma who were seen at MD Anderson Cancer Center (MDACC) between January 2010 and January 2016, and who received first-line SOC chemotherapy, were eligible for chart review (Figure 1). Cases were identified retrospectively. All patients had consented for DNA banking for clinical research. Samples were obtained from the MDACC pancreas cancer tissue bank and the Center for Translational and Public Health Genomics at Duncan Family Institute of MDACC and Patient History database Program. Clinical and pathological information was abstracted from chart review from the MDACC electronic medical record including cancer stage, cancer histology, family history, and record of clinical genetic testing. Family history was defined as 1st through 3rd degree (out to first cousins) relatives with breast, ovarian, or pancreas cancer diagnosed at any age. The gastrointestinal pathologists in the MDACC Department of Pathology and Laboratory Medicine reviewed all pancreatic cancer tumors. All patients consented to DNA banking and clinical research. Of the 233 patients identified, blood samples for germline DNA testing were available from 133 cases including 95 and 38 patients treated with first-line FOLFIRINOX and gem/nab-paclitaxel,

respectively. When available, outside germline mutation testing results were incorporated into our database.

Figure 1: Consortium diagram of metastatic PDAC cohort (adapted from Goldstein et al, Clinical Cancer Research accepted 2019).
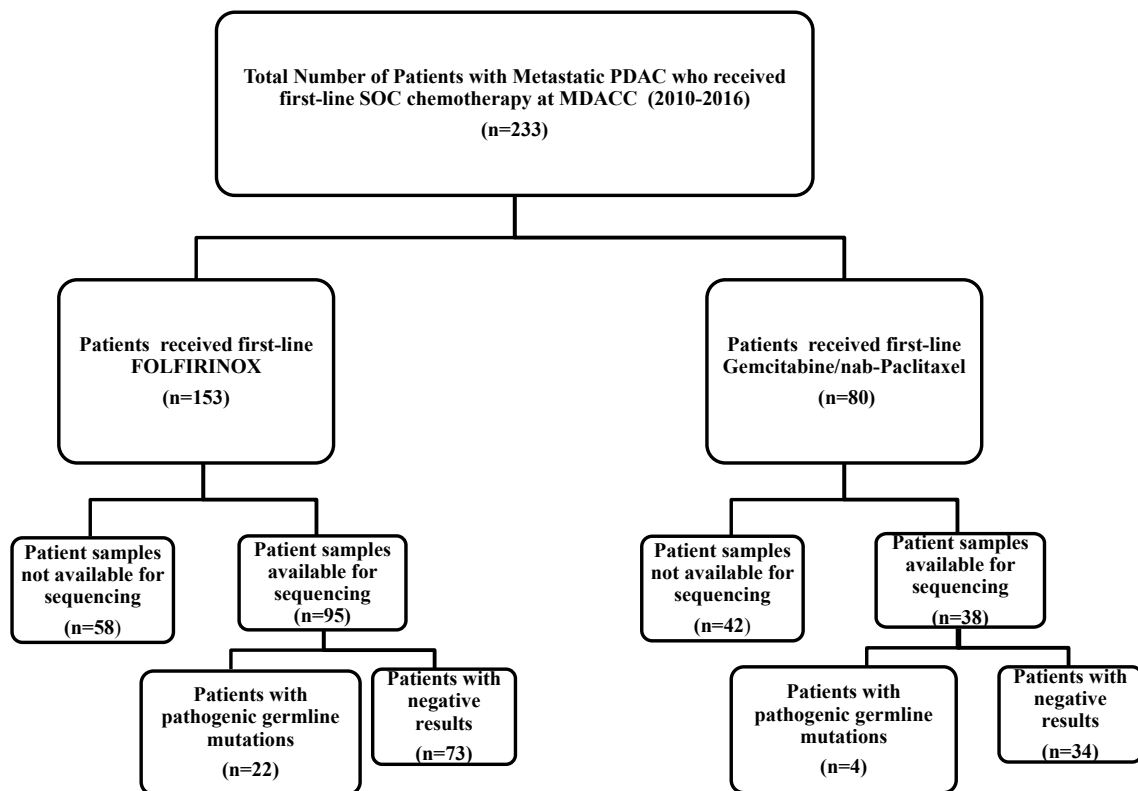
As specimens were used for research purpose alone, testing was not performed under Clinical Laboratory Improvement Amendments regulations. Results were not returned to the families of study participants or used to make clinical decisions. The study was conducted under the auspice of the MDACC Institutional Review Board. A consort diagram is available in Figure 1.

2.2.2 Validation Cohort

De-identified germline genomic data was obtained from TCGA, pancreatic adenocarcinoma cohort. DNA sequencing data as well as a limited amount of clinical information was collected on all 127 patients.

2.2.3 Next Generation Germline Sequencing

Peripheral blood leukocytes were used to collect germline DNA. DNA was extracted using a QIAGEN DNA extraction kit (51306, Qiagen Inc., Valencia, CA). Targeted panel capture was performed on 500 ng of genomic DNA per sample based on KAPA library prep (KAPA Biosystems, Wilmington, MA) using the T200.1 Solid Tumor Cancer gene panel (263 genes) and paired-end multiplex sequencing of samples was performed using the Illumina HiSeq 2500 sequencing platform[93]. Average coverage was 450X.

2.2.4 Germline Sequencing Variant Calling

Paired end reads in FastQ format generated by the Illumina platform were aligned to the human reference genome (UCSC Genome Browser, hg19) using Burrows-Wheeler Aligner[94] by allowing 3 mismatches with 2 in the first 40 seeding regions and aligned reads processed using the GATK Best Practices of duplicate removal, indel (insertion and deletion) realignment, and base recalibration[95]. Germline single-nucleotide substitutions were detected using Platypus[96]. The following filtering criteria were used: (a) total read coverage of the variant >=20, (b) the variants should be on-target, exonic and non-silent, (c) a population frequency threshold of 1% was used to filter out common variants in the

databases of dbSNP129 (PMID: 11237013), 1000 Genomes Project (PMID: 23128226), Exome Aggregation Consortium (Exac) (PMID: 27535533) and ESP6500 (PMID: 23201682). Specifically, variants with a population frequency larger than 3% in any individual ethnicity group in Exac were also filtered out. A schema of variant calling and number of variants seen at each filtering step are provided in Figure 2.

Figure 2: Variant classification pipeline (A), number of variants at each level of variant filtering (B).
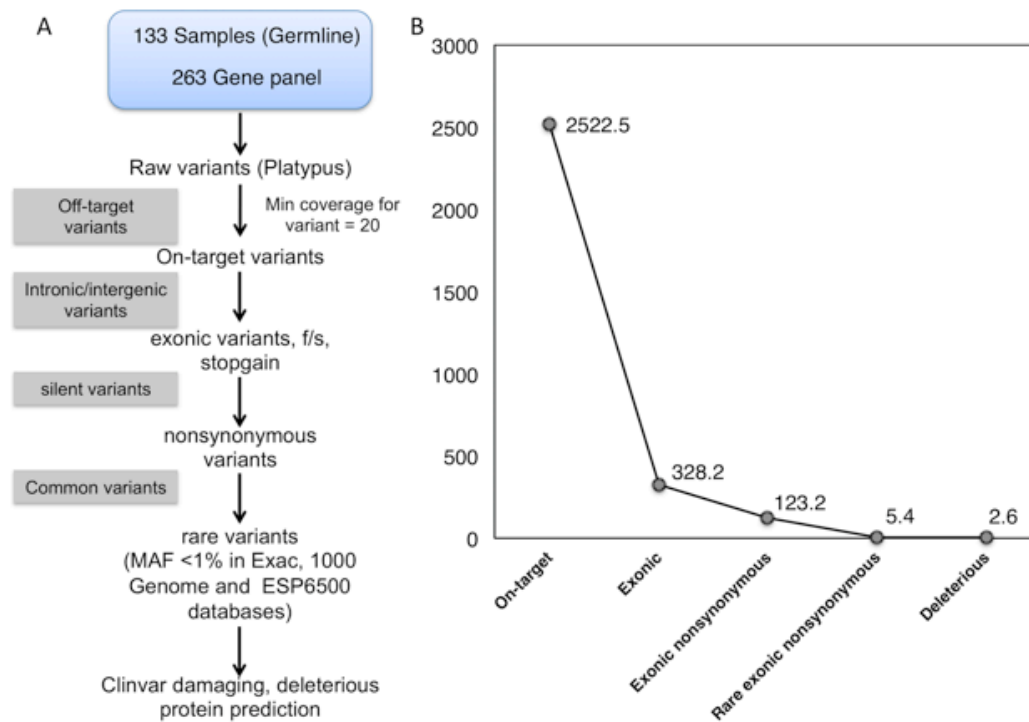
2.2.5 Variant Classification

Gene variants deemed deleterious were considered mutations as were private, non-silent variants not filtered out by the criteria shown in Figure 2A. Those variants suspected as deleterious without evidence of validation in the literature were classified as variants of

unknown significance (VUS). Variants were classified using American College of Medical Genetics and Genomics recommendations. Supporting data was obtained from literature review using linkage, biochemical, clinical, functional, and statistical research for specific alterations[97,98]. Variants were cross-referenced to Clinvar, HGMD and UMDBRCA genomic data banks for further variant determination[99-101].

2.2.6 Statistics

Patient clinical characteristics of categorical variables such as race and gender are reported given frequencies and percentages. Continuous data and sequencing results were summarized with descriptive statistics. The *chi*-squared test and Fisher's exact test were used to evaluate the association between two categorical variables. Wilcoxon's rank sum test was used to compare the distributions of continuous variables between two different groups. Univariate and multivariable logistic regression models were used to evaluate the association between the outcomes of interest and patient demographic covariates. All tests are two-sided and *P* values < 0.05 are considered statistically significant. All analyses were conducted using SPSS version 24 (SPSS, Armonk, NY).

2.3 Results

2.3.1 Characterization of Study Patients Shows Germline Mutation Rate of Nearly 20%

We identified 233 patients that met our study cohort selection criteria as shown in Figure 1. The median and mean ages at diagnosis of the entire cohort were 62 and 61 years (range, 36-84 years), respectively. One hundred thirty-six patients were male (58.4%) and all patients were metastatic at diagnosis. One hundred and fifty-five patients had a baseline

ECOG score of 0-1, 12 with 2, and in 15 patients, the score was unknown. One hundred and seventy-eight (76.4%) patients had liver metastases at diagnosis. Nineteen patients had secondary cancers (8.2%) that included breast (n = 3), colorectal cancer (n = 3), lung (n = 3), prostate (n = 3), bladder (n = 2), ovarian (n = 1), melanoma (n = 1) and various hematologic malignancies (n = 3), as well as other cancers. Four (1.7%) of these patients had multiple cancers including two patients with lung cancer, both heavy smokers, one with bladder cancer and one with squamous cell carcinoma of the maxilla.

Blood samples for germline DNA testing were available from 133 cases. The median and mean ages of the sequenced cohort at diagnosis were 61 and 60 years (range, 36-84 years), respectively. Sequenced patients were more likely to have received front-line FOLFIRINOX than gem/nab-paclitaxel (95 versus 38 patients, $P = 0.03$). Otherwise, no other significant differences were observed between the two groups. A summary of these patients is presented in Table 1. A comparison of the sequenced versus unsequenced patients is found in Appendix Table A1.

Table 1: Patient clinical and pathologic characteristics of sequenced cohort.

Characteristic	No. of Patients Sequenced Cohort (n = 133)	Percent (%)
Age at diagnosis of disease, years		
Median	61	
Range	36-84	
Gender		
Male	78	58.6

Female	55	41.4
ECOG PS		
0-1	97	72.9
2+	13	9.8
Unknown	23	17.3
Ethnicity		
Caucasian	111	83.4
Black	11	8.3
Hispanic	7	5.3
Asian	2	1.5
Other	2	1.5
Formal Genetic Screening		
Yes	18	13.5
No	115	86.5
Ashkenazi Jewish		
No	122	91.7
Yes	7	5.3
Unknown	4	3
BRCA relatives		
0-1	114	85.7
2	13	9.8
3+	6	4.5

Second Cancer		
No	124	93.2
Yes	9	6.8
Median Baseline CA 19-9	940	
Frontline Chemotherapy		
FOLFIRINOX	95	71.4
Gem/nab-paclitaxel	38	28.6
Response to Chemotherapy		
Partial Response	37	27.8
Stable Disease	49	36.9
Progressive Disease	33	24.8
Not evaluable	14	10.5

Of the 133 sequenced patients, 29 deleterious mutations were found in 26 (19.6%) patients (Table 2). Of those patients with a deleterious mutation, the median and mean ages were 56 and 55 years (range, 36-70 years), respectively. Seventy-eight (58.6%) patients were male, 111 (84%) were Caucasian and 7 (5.3%) were of Ashkenazi Jewish descent. Of the 6 (4.5%) sequenced patients with a family history of 3 or more first through third degree *BRCA*-related relatives, 3 (50%) were found to have a deleterious mutation and one of these patients had two inherited mutations. Conversely, of the 26 patients with a deleterious mutation, 2 (7.7%) patients had no family history of cancer.

There were 21 patients with 0-1, 2 patients with 2 and 3 patients with 3 affected first, second, or third-degree relatives with a *BRCA*-associated cancer (breast, ovarian, or

pancreas). Twenty-two of the 26 patients received first-line therapy with FOLFIRINOX. Clinical and tumor pathologic features for the patients with a deleterious mutation are provided in Table 3.

2.3.2 At Least One Variant of Unknown Significance was Identified per Patient

We identified at least one variant of uncertain significance in 123 (93.2%) patients, with as many as ten variants found per patient. On average, patients had 2.6 variants per patient (Figure 2B). The most commonly seen VUSs were in *FANCA* (n = 8, [6%]), *NOTCH1* (n = 8, [6%]), *ERCC4* (n = 7, [5%]), and *FGFR4* (n = 7, [5%]), respectively. Seven patients had VUSs in known pancreatic cancer predisposition genes including 2 (1.5%) patients with *PALB2* variants, 2 (1.5%) patients with *PMS2* variants, and 3 (2.3%) patients with *POLE* variants, including two recurrent variants. All VUSs identified are listed in Appendix Table A2.

2.3.3 Patients with a DDR Mutation had a Significantly Longer Overall Survival and Had Better Overall Response Rates

The median overall survival (OS) from date of diagnosis of the 133 sequenced patients was 10.0 months (95% CI: 8.5-11.5 months). Of the sequenced patients with a family history of 0-1, 2, or 3 or more first, second, or third-degree relatives with a *BRCA*-associated cancer (breast, ovarian, or pancreas), the median OS was 9.6, 8.4, and 23.7 months, respectively ($P = 0.13$, Figure 3A). The median OS in patients with versus without a deleterious mutation was 10.2 versus 9.9 months ($P = 0.25$, Figure 3B). The median OS of the 10 patients with a deleterious DDR (*ATM, BRCA1, BRCA2, ERCC4,*

Table 2: MDACC cohort list of deleterious mutations and associated clinical characteristic

Patient ID	Gene	Mutation	Mutation Effect	Recurrent in Germline Pancreatic TCGA Cohort	Age at Dx (Years)	Askenazi Jewish	Personal Cancer History	Family History of Cancer	Referred to Genetic Counselor	OS
FamilyH x21	*AR*	c.T170A	nonsynonymous SNV	Y	70	N	None	Endometrial (S)	N	297
FamilyH x45	*AR*	c.C2395G	nonsynonymous SNV	N	55	N	None	Breast (M), colorectal (PA), gastric (MU), prostate (F, B)	N	229
FamilyH x36	*ATM*	c.1024_10 27del	frameshift deletion	N	62	Y	None	Male breast(F)	Y	77
FamilyH x49	*ATM*	c.5352del C	frameshift deletion	N	63	N	None	Esophageal (S), lung(M)	N	694
FamilyH x17	*ATM*	c.4736dup A	frameshift insertion	N	42	N	None	Colorectal(MGM, MU)	N	287
FamilyH x24	*BRCA 1*	c.2576del C	frameshift deletion	N	40	N	None	Breast (M, MA x 2), endometrial (MGM), ovarian(M)	Y	457
FamilyH x107	*BRCA 1*	c.6749del C	frameshift deletion	N	36	N	None	Glioblastoma (MC), pancreatic(B)	Y	1320
FamilyH x108	*BRCA 2*	c.5578del AA	frameshift deletion	N	53	Y	None	Breast(S), gastric(PA), head and neck(B), melanoma (F, B), ovarian(PA x 2), prostate (F)	Y	540
FamilyH x109	*BRCA 2*	*	frameshift deletion	N	43	Y	None	Breast (S), lung(MU)	Y	1307
FamilyH x41	*CHEK 2*	c.C254T	nonsynonymous SNV	N	67	N	None	Breast (S), leukemia (F, S x 2), unknown gynecologic (S)	N	96
FamilyH x20	*CHEK 2*	c.C1412T	nonsynonymous SNV	N	50	N	None	None	N	96
FamilyH x3217	*CHEK 2*	c.T599C	nonsynonymous SNV	N	62	N	None	Glioblastoma (PGC), leukemia (PGU), lung (F), pancreatic (PU), prostate (PGF), unknown(PGA)	Y	925
FamilyH x12	*CHEK 2*	c.1229del C	frameshift deletion	N	50	N	None	Hepatocellular carcinoma (MA), lung (MA), pancreatic (M)	N	253
FamilyH x3413	*CDKN 2A*	c.131insA A	Frameshift insertion	Y	58	N	None	Bladder (PC), breast (PA), colorectal (MC), melanoma (PA, PC x 2), pancreatic (M, B), prostate (MU), ovarian (MC)	Y	723
FamilyH x27	*CYP2 C19*	c.A1G	nonsynonymous SNV	Y	65	N	None	Lung (M)	N	44
FamilyH x3198	*CYP2 C19*	c.A1G	nonsynonymous SNV	Y	56	N	None	Hepatocellular carcinoma (PU), Prostate (F)	N	922
FamilyH x42	*ERCC 4*	c.C2395T	nonsynonymous SNV	N	64	N	None	Lung (PGF)	N	88
FamilyH x3460	*ERCC 4*	c.C2395T	nonsynonymous SNV	N	65	N	None	Colorectal (MGM), Unknown type skin (PGF)	N	497
FamilyH x95	*HNF1 A*	c.G92A	nonsynonymous SNV	N	59	N	Prostate	Bladder (F), colorectal, lung (F, PGF, PC), pancreatic (PA)	N	424
FamilyH x12	*IL7R*	c.G617A	nonsynonymous SNV	N	50	N	None	Hepatocellular carcinoma (MA), lung (MA), pancreatic (M)	N	253
FamilyH x3413	*IL7R*	c.G214C	nonsynonymous SNV	Y	58	N	None	Bladder (PC), breast (PA), colorectal (MC), melanoma (PA, PC x 2), pancreatic (M, B), prostate (MU), ovarian (MC)	Y	723
FamilyH x3728	*NF1*	c.T2C	nonsynonymous SNV	N	48	N	None	Breast (S, PA), prostate (F, PU)	N	192

Family Hx110	*PALB2*	c.G3A	nonsynonymous SNV	N	58	N	None	Breast (PC), colorectal (MU x 2, PA), Kidney (MU, PC), Lung (F, B, PU, PGF, PC), head and neck (B), pancreatic (PA), prostate (MU), unknown (MC, PGM)	Y	737
FamilyHx95	*RET*	c.A2372T	nonsynonymous SNV	Y	59	N	None	Bladder (F), colorectal, lung (F, PGF, PC), pancreatic (PA)	N	424
FamilyHx33	*SDHD*	c.C33A	stopgain	N	50	N	None	Carney's triad: paraganglioma, chondrosarcoma, and GIST (M), pheochromocytoma (M), urothelial(M), prostate (F)	N	350
FamilyHx59	*TERT*	c.C1234T	nonsynonymous SNV	N	68	N	None	None	N	37
Family Hx88	*TERT*	c.C1234T	nonsynonymous SNV	N	62	N	None	Colorectal (F)	N	224
FamilyHx1	*TERT*	c.G2371A	nonsynonymous SNV	N	50	N	None	Endometrial (M), osteosarcoma (F), thyroid (M)	N	178
FamilyHx2	*TP53*	c.G229T	stopgain	N	39	N	Bilateral breast cancer	Breast (M), melanoma (F), neuroendocrine tumor (PC), sarcoma (S), unknown (MGF, MU)	Y	268

Table 3: Summary of sequenced patient characteristics by deleterious mutation status.

Covariate	Levels	Deleterious mutation= No	Deleterious mutation= Yes	*P*-value
Sex	Male	63(58.9%)	15(57.7%)	0.91
	Female	44(41.1%)	11(42.3%)	.
Age at Diagnosis	>60	57(53.3%)	10(38.5%)	0.18
	<=60	50(46.7%)	16(61.5%)	.
Age at Diagnosis	>45	99(92.5%)	21(80.8%)	0.07
	<=45	8(7.5%)	5(19.2%)	.
ECOG	0,1	77(86.5%)	20(95.3%)	0.27
	>=2	12(13.5%)	1(4.7%)	.
First-line Treatment	F	73(68.2%)	22(84.6%)	0.10
	G	34(31.8%)	4(15.4%)	.
BRCA Group>=3	N	104(97.2%)	23(88.5%)	0.05
	Y	3(2.8%)	3(11.5%)	.
Family history breast cancer	N	78(72.9%)	16(61.5%)	0.25
	Y	29(27.1%)	10(38.5%)	.

Covariate	Levels	Deleterious mutation= No	Deleterious mutation= Yes	P-value
Family history ovarian cancer	N	102(95.3%)	25(96.2%)	0.86
	Y	5(4.7%)	1(3.8%)	.
Family history pancreatic cancer	N	94(87.9%)	20 (76.9%)	0.15
	Y	13(12.1%)	6 (23.1%)	.
Family history any cancer	N	25(23.4%)	5(19.2%)	0.96
	Y	82(76.6%)	21(80.8%)	.
Ashkenazi Jewish	N	99(96.1%)	23(88.5%)	0.12
	Y	4(3.9%)	3(11.5%)	.
Recurrent_VUS	N	58(54.2%)	22(84.6%)	0.005
	Y	49(45.8%)	4(15.4%)	.
Personal_Hx_Cancer	N	100(93.5%)	25(96.2%)	0.51
	Y	7(6.5%)	1(3.8%)	.

PALB2) gene mutation versus other sequenced patients was significantly longer than patients without a DDR mutation (17.9 versus 9.6 months, P = 0.03, Figure 3C). There was no difference in survival for those patients who were 60 years old or less compared to those over 60 (10.0 versus 9.4 months, P = 0.91, data not shown). The median OS from the date of the start of chemotherapy was 9.6 versus 8.9 months (P = 0.47, Figure 3D), in those sequenced patients who were treated with FOLFIRINOX versus gem/nab-paclitaxel, respectively.

On univariate analysis, ECOG PS > 1, family history of pancreatic cancer, family history of any cancer, and presence of 3 or more affected family members with a BRCA-associated cancer, were all significant determinants of survival (Appendix Table A3). However, on multivariate analysis, ECOG PS >2 (HR 2.37, 95% CI; 1.28 – 4.37, P = 0.006) and a family history of pancreatic cancer remained significant (HR 0.55, 95% CI; 0.32 –

0.93, *P* = 0.03, Table 4). Univariate analysis of all 233 patients is provided in Appendix Table A4, however the only significant predicting factor on multivariate analysis was ECOG PS (data not shown).

Of the patients who underwent sequencing, there were 0 complete responses (CR), 37 partial responses (PR), 49 patients with stable disease (SD), 33 with progressive disease (PD) and 14 that were not evaluable due to lack of follow up imaging or other reasons (Table 1). The overall response rate (ORR) was 27.8% (37 of 133 patients). The ORR of patients without deleterious mutations was 29% (31 of 107 patients). Of the 26 patients with deleterious mutations, 22 were treated with FOLFIRINOX and 4 patients were treated with gem/nab-paclitaxel (Appendix Table A5). There were 0 CRs, 6 PRs, 8 SDs, 8 PDs, and 4 were not evaluable with an ORR of 23.1% (6 of 26 patients). However, of the patients with DDR mutations, there were 0 CRs, 5 PRs, 6 SDs, 3 PDs, and 1 was not evaluable (ORR = 33.3%, 5 of 15 patients) compared to 0 CRs, 1 PR, 1 SD, 4 PD, and 2 who were not evaluable in those without DDR mutations (ORR = 12.5%).

2.3.4 Recurrent VUS was the Only Predictor of Deleterious Pathologic Germline Mutation

The prevalence of deleterious mutations decreased with increasing age at pancreatic cancer diagnosis, with frequencies of 41.7% (5/12), 20.4% (11/54), and 14.9% (10/67) for age groups younger than 45 years, 45 to 60 years, and older than 60 years, respectively. In a univariate analysis, age less than 45 nearly reached statistical significance (OR 2.94, 95% CI 0.88 – 9.91, *P* = 0.08) (Appendix Table A6). Nearly half of all sequenced patients (56/133) had a family history of a *BRCA*-related cancer. There was a trend among those

Figure 3: Overall survival of sequenced cohort stratified by the number of family members with *BRCA*-related tumors (A), overall survival of sequenced cohort stratified by deleterious mutation (B), overall survival of sequenced cohort stratified by DDR or DDR cell cycle checkpoint mutation (C), overall survival of sequenced cohort stratified by treatment (D).
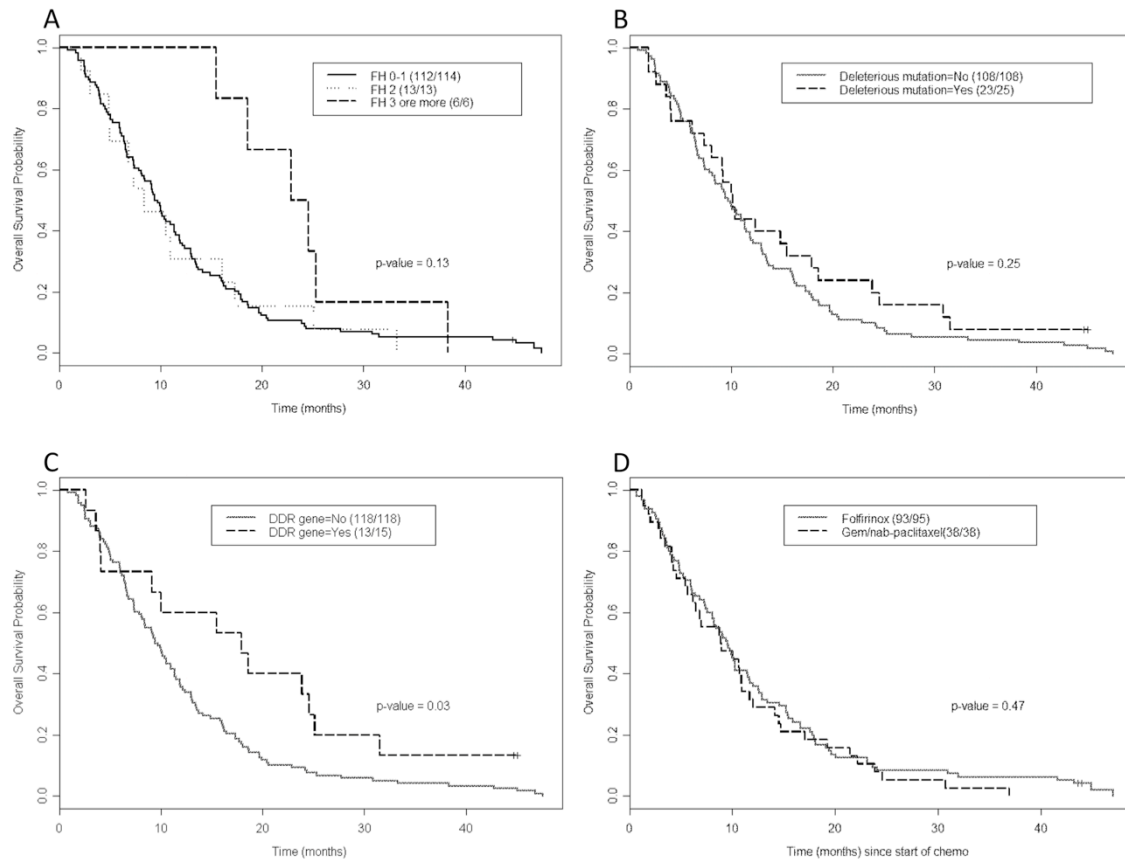
Table 4: Multivariate analysis of determinants of overall survival.

Covariate	Hazard Ratio	95% CI		*P* value
ECOG ≥ 2 (vs. 0, 1)	2.37	1.28	4.37	0.006
Family history pancreatic cancer = Yes (vs. No)	0.55	0.32	0.93	0.03

patients with three or more relatives with a *BRCA*-related cancer to have a deleterious mutation, however, this did not reach the level of statistical significance (OR = 4.53, 95% CI 0.86 – 23.85, *P* = 0.08, Appendix Table A5. Of all sequenced patients, 6.8% (9/133) had a personal history of an additional malignancy, including three patients with breast cancers. Personal history, however, did not predict for deleterious mutations (*P* = 0.96, Appendix Table A6). There was a trend towards increased number of mutations in those with Ashkenazi Jewish heritage, although this did not reach statistical significance on univariate analysis. Other correlates are presented in Appendix Table A5. On multivariate analysis, only recurrent VUS was associated with a deleterious mutation (OR = 0.20, 95% CI 0.06-0.62, *P* = 0.005, Appendix Table A7).

2.3.5 The Cancer Genome Atlas Validation Cohort Shows Similar Incidence of Pathological Germline Mutations

We additionally performed a similar query with the limited clinical data and germline sequencing data from the pancreatic cancer patients in TCGA. Median and mean age at diagnosis for this cohort was 61 (35-88 range, years) and sixty-five (51.2%) were male. Using the same variant calling pipeline (Figure 2A), we identified 26 deleterious mutations in 24 (18.9%) patients of the 127 patients tested. There were no *BRCA1* mutations and 2 (1.6%) *BRCA2* mutations. Five (3.9%) patients had mutations in *ATM*, three (2.4%) patients had mutations in *MUTYH*, two patients each (1.6%) had mutations in *AR*, *CHEK2*, *DNMT3A* and one (0.8%) patient each had a mutation in *CDKNA, CYP2C19, ERCC2, FANCA, IL7R, MEN1, NBN, PALB2, RET* and *TERT*. Recurrent deleterious mutations that overlapped with our own study cohort were seen in 6 (4.7%) patients (Table

2). The median OS from date of diagnosis was 19.8 months in this cohort. We see that the median survival of patients with a DDR mutation exceeds that of those without DDR mutations (24.2 versus 19.7 months, P= 0.024, data not shown).

2.4 Discussion

Our current understanding of the prevalence of familial pancreatic cancer is largely limited to twelve genes previously described by Grant and colleagues in the Journal of Gastroenterology in 2015[83]. The incidence of damaging mutations in these genes, including *ATM*, *BRCA1*, *BRCA2*, and *TP53* is thought to occur in 5 to 10% of pancreatic cancer patients and is mainly limited to particular genes in the DDR pathways. In this study, we have evaluated for a larger variety of mutations that may predispose to familial pancreatic cancer and found a mutation rate of almost 20% when testing 263 cancer-associated genes in this unselected cohort.

Here, we have also provided additional evidence that family history of 3 or more *BRCA*-related cancers is a determinate of OS, however, this was not statistically significant. The small number of patients in this group and the subjective nature of family history may contribute to the lack of significance. Interestingly, patients with mutations in genes involved in DDR or the cell cycle check point (*ATM*, *BRCA1*, *BRCA2*, *CDKN2A*, *CHEK2*, *PALB2*, and *ERCC4*) had a near doubling of the OS (17.9 versus 9.6 months, $P = 0.03$) compared to those that did not have a mutation in one of these genes. Perhaps not all deleterious mutations are beneficial. As seen in Table 3, there is a trend towards better outcomes in those with *BRCA* mutations than those with *ERCC4*.

Familial pancreatic cancer due to mutations in mismatch repair genes may demonstrate overlapping tumor biology with those with DNA repair defects. We did not find any pathological mutations in MMR genes other than 2 VUSs in *PMS2*. In previous studies of familial pancreatic cancer, the estimated incidence of MMR gene mutations was very low at 0.1-1%[102,103]. With a larger study cohort, we may have observed mutations in these genes. Future study may also include a broader range of genes related to DNA repair such as *MREIIA*, *NBN*, and *BARD1*.

The frequency of each DDR mutation in the TCGA cohort differs from our own discovery cohort. This is consistent with findings from Johns Hopkins University that showed a large amount of heterogeneity among familial pancreatic cancer patients[104]. However, when taken as a whole, the TCGA patients with DDR mutations also demonstrated prolonged OS (24.2 versus 19.7 months, P= 0.024), confirming our own findings. In 2019, a group at Memorial Sloan Kettering Cancer Center published a study in the journal, *Genetics in Medicine* where they found a 10% incidence of germline pathogenic mutations in a cohort of familial pancreatic cancer patients[103]. They tested a larger cohort of patients, but used a smaller panel of genes to test both germline and somatic mutations. Importantly, we confirm that patients with pathogenic germline defects in DNA repair genes have a better overall survival. This may argue for a biologically based survival benefit in these patients either due to improved treatment response or less aggressive tumor biology. In the future we plan to compare germline and somatic variants in our patient cohort.

In the clinic, decisions whether to treat patients with either of the current SOC regimens, FOLFIRINOX or gem/nab-paclitaxel, is largely based on performance status.

Those in better condition tend to receive the more difficult to tolerate, yet arguably more effective, FOLFIRINOX. We did find that the majority of patients identified as carrying deleterious mutations in predisposition genes were treated with front-line FOLFIRINOX (85%). Of the 4 patients with mutations that received front-line gemcitabine and nab-paclitaxel, only two were evaluable for response. This may be due to the fact that FOLFIRINOX had become SOC by 2011 for first-line metastatic pancreatic cancer and it wasn't until 2013 that gem/nab-paclitaxel became FDA approved.

In those with *BRCA* mutated cancers, previous predictive data has largely been based on treatment with cisplatin, a chemotherapeutic agent that is less frequently used with current SOC chemotherapy regimens[17]. Due to this widely held perspective, patients with a stronger family history, which may be more likely to represent those with a deleterious mutation, were placed on FOLFIRINOX. If patients with deleterious mutations in DDR genes have a better prognosis, they may be in better physical condition at presentation, and given the more difficult to tolerate regimen by their oncologist. Unfortunately, we did not have enough patients to characterize the effectiveness of these regimens among patients with inherited mutations.

One of the limitations of this study is that the vast majority of sequenced patients were deceased. This introduces a retrospective bias, as patients who lived longer might not undergo genetic testing. Therefore, the actual overall survival of mutated patients may be longer than what we report in this study. We would ideally perform a prospective study looking at an unselected pancreatic cancer cohort where all-comers are sequenced for germline mutations. Additionally, mutations, although predicted to be deleterious, may

not necessarily be causative of pancreatic adenocarcinoma. Furthermore, in this study we focused on metastatic patients. We therefore, cannot speak to the germline mutation spectrum of resectable or locally advanced patients.

Only 13.5% of sequenced patients underwent formal genetic screening. Of those that underwent screening, mutations were found in 50% (9/18) of these patients. This was due to lack of follow through in sending blood for sequencing or a determination that sequencing was not necessary. We additionally compared our profiling with commercial tests. Two commercial labs, which omit testing for *ERCC4* and *CHEK2*, would have missed 6 patients with DDR mutant cancers. The age of these affected patients ranged from 50 to 66. As these mutations occurred in patients over the age of 45, their omission would have potentially failed to predict cancers in relatives. The prevalence of *ERCC4* and *CHEK2* mutations among patients 50 and older suggests that commercial platforms should be expanded to include these genes. This also demonstrates the need for a more universal approach to evaluating familial pancreatic cancer.

In conclusion, we have better characterized the germline mutational profile in hereditary pancreatic cancer. We have shown that deleterious mutations in either DDR genes or cell cycle checkpoint genes confer a better prognosis over those without these mutations. Available commercial testing omits genes that may confer prognostic information. This study highlights the need for continued family counseling, preventative imaging, and early detection in those unaffected carriers via genetic testing.

Additionally, identifying patients to refer to clinical trials with targeted therapies is important. In the following chapter, I used PDX models of hereditary pancreatic cancer to test a class of drugs, PARP inhibitors, which have shown to have promise in this patient

population. I examined genomic alterations leading to sensitivity and response to therapy,

exploring treatment options in the patient population I have studied here in Chapter 2.

Chapter 3

Characterization of BRCA Pathways in PDX Cell Lines Determines Mechanisms of Sensitivity and Resistance to PARP Therapy

3.1 Introduction

polyADP ribose polymerase (PARP) inhibitors are a class of agents that block the PARP enzymes and are involved in the repair of singe-stranded DNA breaks through the Base excision repair (BER) pathway. This inhibition can then lead to replication-associated double stranded breaks that normally would be repaired using homologous recombination. In tumors with homologous recombination defects (i.e. *BRCA* mutants), there is an increased use of error prone DNA repair mechanisms and subsequent genomic instability and cell death[43].

In 2014, Olaparib became the first FDA approved PARP inhibitor indicated to treat *BRCA*-mutant ovarian cancer[46]. In the randomized phase III POLO trial presented at ASCO 2019, it was shown that maintenance therapy with olaparib significantly delayed the progression of metastatic pancreatic cancer in those patients with a germline *BRCA* mutation compared with placebo (median progression-free survival = 7.4 months vs 3.8 months, respectively)[47]. Newer generation PARP inhibitors, such as Talazoparib (BMN-673), also have a PARP-trapping mechanism that has been shown to increase the efficacy of the agent 20-200-fold compared to older PARP inhibitors[48]. In 2018 Talazoparib was FDA approved to treat *BRCA*-mutated, HER2-negative breast cancer[49].

It has been described that response to PARP inhibitors may be dependent on specific driver mutations and response in *BRCA1* versus *BRCA2* mutants may even differ[50,51]. There have been multiple mechanisms of resistance to PARP inhibitor therapy described in the literature including secondary mutations in *BRCA1* or *BRCA2* to restore the open reading frame and restore homologous recombination, loss of 53BP1, and high

levels of SLFN11 results in resistance to DNA-damaging agents and PARP inhibitors[56,57,66,67].

RIF1 protein acts downstream of 53BP1 to translocate to sites of double-stranded DNA damage via an ATM-dependent 53BP1 phosphorylation. Loss of RIF1 rescues initial DNA end resection and checkpoint activation in *BRCA1* mutated cells[70]. However, loss of RIF1, unlike loss of 53BP1, cannot fully rescue RAD51 foci formation and restore defects in homologous recombination. This is likely because of RIF1's dual function in regulation of the foci formation and chromatin loading of BLM. Therefore, one the one hand, RIF1 deficiency facilitates BRCA1-mediated DNA end processing and on the other hand impairs BLM-EXO1 mediated DNA end resection[70,71].

A recent study showed that in BRCA2-depleted cells, the 53BP1–RIF1 complex may promote toxic c-NHEJ and alt-NHEJ events by facilitating the retention of Artemis at sites of DNA damage. BRCA2 antagonizes RIF1-dependent alt-NHEJ to prevent gross genomic instability in a RAD51-independent manner[72]. We therefore hypothesized that the loss of RIF1 would lead to restoration in genomic stability in either BRCA1 or BRCA2-deficient cells, thereby reducing their hypersensitivity to PARP inhibition and DNA-damaging agents. We also looked at compensatory expression of RNA in response to Talazoparib treatment with single cell RNA sequencing. We particularly focused on the DNA repair pathway and ability to maintain genomic stability.

3.2 Materials and Methods

3.2.1 Patient-Derived Xenograft Cell Line Clinical Review

Briefly, PDX cell lines were derived from pancreatic cancer specimens obtained from patients admitted to the University of Texas at MD Anderson Cancer Center under a protocol approved by the institutional ethical committee and conducted in accordance with the Helsinki Declaration[105]. Informed consent was obtained from all patients. Chart review was performed to assess general clinicopathologic characteristics such as ethnicity, family and personal history of cancer of patients using the MDACC electronic medical record.

3.2.2 Cell Culture

ASPC-1 (BRCA wild type, KRAS and TP53 mutant), Capan-1 (germline BRCA2 c.6174delT, KRAS and TP53 mutant), and Capan-2 (BRCA wild type, KRAS mutant, TP53 wild type) were obtained from the American Type Culture Collection (ATCC)[106,107] and genotype confirmed. PATC53, 55, 69, 102, and 124, patient-derived xenograft (PDX) pancreas cancer cell lines were successfully derived from core biopsies of patients with PDAC and utilized.

AsPC-1 cells were cultured in McCoy's 5a (SH30200.01, Hyclone, Logan, UT) with 10% fetal bovine serum (FBS) (A3840101, Gibco, Grand Island, NY), penicillin G (100 U/mL), and streptomycin (100 µg/mL). Capan-1 cells were cultured in DMEM (SH30243.01, Hyclone) supplemented with 20% FBS, penicillin G (100 U/mL), and streptomycin (100 µg/mL). Capan-2 cells were cultured with RPMI (11875-093, Gibco) with 10% FBS, penicillin (100 U/mL), and streptomycin (100 µg/mL) as previously described[108-110]. All PDX cells from MDACC were expanded in DMEM culture medium with 10% FBS, penicillin (100 U/mL), and streptomycin (100 µg/mL) at 37 °C containing

5% (v/v) CO_2, in a humidified incubator. Cells were tested negative for mycoplasma contamination (MycoAlert, Lonza Walkersville, Walkersville, MD).

3.2.3 Cell Line Characterization by Whole Exome Sequencing

Genomic DNA was extracted using the QIAamp DNA Mini Kit (51306, Qiagen) from plated cell line samples and a common normal database was used as a germline DNA control. Exome capture was performed on 500ng of genomic DNA per sample based on KAPA library prep (Kapa Biosystems) using the Agilent SureSelect Human All Exon V4 kit according to the manufacturer's instructions and paired-end multiplex sequencing of samples was performed on the Illumina HiSeq 2000 sequencing platform. The average sequencing depth was 267X per cell line.

3.2.4 Somatic Variant Calling

Paired-end reads (2 x 75 bp) in FastQ format generated by the Illumina pipeline were aligned to the reference human genome (UCSC Genome Browser, hg19) using Burrows-Wheeler Aligner (BWA) on default settings except a seed length of 40, maximum edit distance of 3, and maximum edit distance in the seed of 2[94]. Aligned reads were further processed following the GATK Best Practices of duplicate removal, indel realignment, and base recalibration. Somatic single-nucleotide substitutions were detected by using MuTect[111]. In addition to MuTect's built-in filters, the following filtering criteria were applied: (i) total read count in tumor DNA ≥15; total read count in germ line DNA ≥ 10; (iii) variant present on both strands; (iv) VAF in tumor DNA ≥ 5%; (v) VAF in normal < 1%; (vi) variants in positions listed in 1000 Human Genomes, ESP

and EXAC databases were removed; (vii) variants predicted as damaging in at least one protein prediction program [PolyPhen-2 (http://genetics.bwh.harvard.edu/pph2/), SIFT (http://sift.jcvi.org/), or MutationTaster (http://www.mutationtaster.org/)] were kept. Small indels were identified using Pindel (Pindel 0.2.4t)[112]. Pindel outputs were furthered by applying (i) total tumor reads > 10; (19) total normal reads > 15; total number of 4 reads supporting a call > 4; (iii) VAF in tumor >2%; (iv) VAF in normal <2%. Different filtering criteria were applied to indels to increase sensitivity. Substitutions and indel were annotated using ANNOVAR based on UCSC known genes[113].

3.2.5 Detection of Copy Number Alterations

Copy number data were derived from whole exome sequencing reads. The Sequenza algorithm was used to estimate sample purity, ploidy, and absolute somatic copy numbers. Read counts in each exon region were determined using bedtools[114]. The log2 ratios of PDX cell lines versus common normal reads were calculated for each region after adjusting for the total mapped reads in that region. Manual inspection was applied to review all segments to make amplification and deletion calls.

3.2.6 RAD51 Foci Immunocytochemistry

Cells were plated on 96 well clear bottom plates and incubated in the dark at 37°C under an atmosphere of 5% (v/v) CO_2 in air. Once cells reached about 90% confluency, irradiation was performed at 0 vs. 10 Gy[115]. Six hours after irradiation, cells were washed twice with phosphate-buffered saline (PBS) and then fixed using 4% paraformaldehyde

in PBS-T (0.2% Triton-X-100 in PBS) for 10 minutes.   Cells were blocked with serum free protein block (X0909, Dako, Carpinteria, CA) for an hour and incubated with a Rad51 primary antibody (1:500, ab213, Abcam, Cambridge, UK) at 37 degrees for 1 hour. Cells were washed three times with PBS-T (0.05% Tween20 in PBS) and then incubated with anti-mouse Alexa Fluor 488-conjugated secondary antibody (1:1000, A-11001, Life Technologies, Carlsbad, CA) for 1 hour at room temperature[116]. Nuclei were counterstained with Hoechst (1:5000, H3570, Life Technologies).

Cells were imaged and analyzed with an Operetta system (Perkin-Elmer, Waltham, MA) using manual determination of sub cellular compartments. Foci were then visualized and positivity was determined if a cell had >10 foci present, a common threshold for positivity reported in the literature[117].

3.2.7 In Vitro Talazoparib Treatment and Colony Formation Assays

AsPC-1, Capan-1, Capan-2, PATC53, 55, 69, 102 and 124 PDX cell lines were grown separately in culture. Cells were plated in twelve well plates with the number of cells plated determined by cell density assays. To determine IC50 and IC 90 values, cells were treated at increasing concentrations of Talazoparib, ranging between 0.0001 and 10,000 nM, as previously described in the literature[48]. Cells were treated for 14 days and media was changed every 5 days. Following 14 days of treatment, cells were fixed and stained with cresyl violet and dried for 72 hours. Acetic acid (10%) was added to solubilize and plates were placed on the shaker for 20 minutes. The PheraStar detection system (BMG labtech, Cary, NC) was then used to measure the absorbance (590 nm) of Talazoparib-treated versus DMSO-treated control cells. Dose response curves to calculate

IC50 and IC90 values were plotted using Graph Pad Prism 8.0 Software (La Jolla, CA). All experiments were done in triplicate.

3.2.8 Animals

We used 24 NSG mice for shRNA DNA RepairOme experiments. Female NSG mice (NOD.Cg-Prkdcscid Il2rgtm1Wjl/SzJ, The Jackson Laboratory, Bar Harbor, MA) were 6 to 8 weeks old at time of PDX injection/implantation. All animal experiments were done in accordance with protocols approved by the Institutional Animal Care and Use Committee (IACUC) of MD Anderson Cancer Center and followed the National Institutes of Health guidelines for animal welfare.

3.2.9 Lentiviral Vector Systems Can be Used as a Stable Method of Gene Transfer

Lentiviral vectors have emerged as a powerful and reliable tool for stable gene transfer in a variety of mammalian cells. We created a custom lentiviral-based DNA Damage RepairOme (DDROme) short-hairpin (shRNA) library can targets up to 350 DNA repair related genes. In our lab, we have established the lentiviral-based shRNA system in multiple types of cancer including melanoma, pancreatic, and glioblastoma. We have used this model to determine the appropriate tumor-initiating cell (TIC) frequency that is then used to determine the number of cells needed to successfully yield a population of cells in which each individual cell is tagged with a unique lentiviral integrin. We have performed an initial screen in PDAC patient-derived xenograft (PDX) cell lines without treatment to pilot this system, (described further in Aim 3 below).

Here, we will use an shRNA screen and subsequent targeted hairpin shRNAs to explore potential synthetic lethal partners of PARP inhibition therapy.

3.2.10 Patient-Derived Xenografts shRNA DNA RepairOme Loss of Function Screen

PATC69 and PATC124 PDX cell lines were grown separately in culture. Briefly, 75 million cells were transduced with our custom loss of function shRNA DNA RepairOme library (IACS, Houston, TX), which contains targets against 350 DNA repair related genes. The infection process was optimized to deliver approximately one lentiviral particle per cell using calculated multiplicity of infection, deemed to be 0.3 and 0.15 for PATC69 and PATC124 respectively. Cells were supplemented with polybrene (final concentration; 10 μg/mL) and incubated at 37°C in a CO2 incubator for 3 days. Puromycin selection was not performed to avoid development of resistance due to protein synthesis inhibition by the antibiotic itself. Three million PATC69 and 5 million PATC124 cells were injected into the subcutaneous flank tissue of the mice. An uninjected population of cells was collected as a reference for each cohort.

Mice were weighed and tumors were measured twice weekly. After 6 weeks of tumor growth, mice were randomly divided into Talazoparib-treated and vehicle-treated cohorts. Talazoparib was formulated at a dose of 0.125mg/kg in 10% dimethylacetamide/5% Solutol HS 15/85% PBS and stored for up to 7 days at 4°C. Talazoparib was given once daily for 4 weeks via oral gavage. One triplicate of mice in each cohort were sacrificed after 4 weeks and an additional triplicate per cohort continued to grow tumors until tumors reached 2cm in any direction, had 1mm of ulceration, or were moribund per MDACC Veterinary department standards.

3.2.11 PCR of DNA for shRNA DNA RepairOme Loss of Function Screen

Barcodes were amplified starting with the total amount of genomic DNA, using the Titanium Taq DNA polymerase (639209, Takara Bio, Mountain View, CA), and pooling together the total material from the first PCR. The first PCR reactions were performed for 16 cycles with the forward primer (5'-TCGGATTCGCACCAGCACGCTA -3') and reverse (5'-AGTAGCGTGAAGAGCAGAGAA -3'). Two µL of the pooled 1st PCR material was used in the second PCR reaction. The second PCR was performed for 12 cycles with the primers forward (5'-CAAGCAGAAGACGGCATACGAGATCGCACCAGCACGCTACGCA -3') and reverse primers to include (5'-ACGGCGACCACCGAGATCTACACGCACGACGAGACGCAGACGAACGATGTAGAGAACGAGCACCGACAACAACGCAGA-3', 5'-ACGGCGACCACCGAGATCTACACGCACGACGAGACGCAGACGAAACAGTGAGAGAACGAGCACCGACAACAACGCAGA-3', 5'-ACGGCGACCACCGAGATCTACACGCACGACGAGACGCAGACGAAGCCAATAGAGAACGAGCACCGACAACAACGCAGA-3', 5'-ACGGCGACCACCGAGATCTACACGCACGACGAGACGCAGACGAACAGATCAGAGAACGAGCACCGACAACAACGCAGA-3', 5'-ACGGCGACCACCGAGATCTACACGCACGACGAGACGCAGACGAAGTTGTAAGAGAACGAGCACCGACAACAACGCAGA-3', 5'-ACGGCGACCACCGAGATCTACACGCACGACGAGACGCAGACGAAGTGAAAAGAGAACGAGCACCGACAACAACGCAGA-3', 5'-

ACGGCGACCACCGAGATCTACACGCACGACGAGACGCAGACGAATGACCAA
GAGAACGAGCACCGACAACAACGCAGA-3', 5'-
ACGGCGACCACCGAGATCTACACGCACGACGAGACGCAGACGAAAGTCAAA
GAGAACGAGCACCGACAACAACGCAGA-3', 5'-
ACGGCGACCACCGAGATCTACACGCACGACGAGACGCAGACGAAATGTCAA
GAGAACGAGCACCGACAACAACGCAGA-3').

Primers for the second PCR reaction were optimized to introduce the required adapters and indexes for Illumina NGS technology. The PCR amplifications were analyzed by agarose gel electrophoresis (2.5%, 17850, Thermo Fisher, Waltham, MA) to check for the expected 279 bp product. Two replicates of the second PCR reaction were pooled together and extracted from agarose gel with the QIAquick gel purification kit (28706, Qiagen Inc.). The purified PCR product was then quantified using the High Sensitivity DNA Assay (Agilent Technologies, Santa Clara, CA) with the Agilent 2100 Bioanalyzer. Next Generation Sequencing on an Illumina HiSeq2000 was performed with the FSeq16IND (5'-TCTGCGTTGTTGTCGGTGCTCGTTCTCT-3') and RSeq16IND (5'-ACACGCACGACGAGACGCAGACGAA-3') sequencing primers and barcode representation was measured. All primers were obtained from Sigma Aldrich (St. Louis, MO).

3.2.12 Sanger Sequencing

Sanger sequencing was used to confirm *RIF1* mutation (forward primer, 5'-ACTGTGGGCTAACCTCAGTTATGAT-3'; reverse primer, 3'-GAGAGAAGGGGATGAACAGAATTTA-5'). Samples were sequenced on the Applied

Biosystems (ABI) 3730XL DNA Analyzer using Big Dye Terminator Chemistry Version 3.1.

3.2.13 Statistical Inference of Clonal Population Structure

Pyclone was employed to infer the clonal population structure of all DNA samples from PDX cell lines[118]. Sequenza copy number information was used as the input for PyClone analysis[119,120]. The cancer cell fraction (CCF) was inferred and variants were clustered as previously described[118]. PyClone was run with 20,000 iterations and default parameters. Variants located in the cluster with greatest mean CCF were defined as clonal, the rest were subclonal[118].

3.2.14 shRNA Lentiviral Packaging and Infection

GIPZ shRNA (clone ID; V2LHS_102188, GE Dharmacon, Lafeyette, CO, clone ID; V3LHS_360712, GE Dharmacon, clone ID; V3LHS_360714, GE Dharmacon, clone ID; V3LHS_360715, GE Dharmacon, clone ID; V3LHS_360716, GE Dharmacon) lentivirus was packed in 293T cells using the psPAX2 and pM2DG system (https://www.addgene.org/viral-vectors/lentivirus/). Capan-1 and PATC124 cells were cultured separately and plated on 150 mm plates. Virus was harvested and transduced into Capan-1 and PATC124 cells. Forty-eight hours post-transduction, puromycin (2ug/ml) selection was performed over 3 days to establish stable cell lines.

3.2.15 shRNA RIF1 Colony Formation Assay

Capan-1 and PATC124 PDX cell lines were grown separately in culture. Cells

were transduced with lentiviral shRNA targeted against RIF1. Cells were plated in twelve well plates with the number of cells plated determined by cell density assays. Cells were treated at increasing concentrations of Talazoparib, ranging between 0.0001 and 10,000 nM, as previously described above. Cells were treated for 14 days and media was changed every 5 days. Following 14 days of treatment, cells were fixed and stained with cresyl violet as described above. Dose response curves to calculate IC50 were plotted using Graph Pad Prism 8.0 Software. Dose response curves were compared between Talazoparib-treated and vehicle (DMSO)-treated transduced cell lines.

3.2.16 PARP Inhibitor Resistance Assay

PATC55 PDX cells were grown in culture. Cells were plated on 150 mm plates at a seeding density of 3 million cells. Cells were treated at a concentration of 100 nM of Talazoparib, based on results of IC50 and IC90 experiments described above. Cells were treated for 14 days and media was changed every 5 days. Following 14 days of treatment, Talazoparib-treated and Vehicle-treated cells were harvested and DNA and RNA extraction were performed (Figure 4).

3.2.17 Cell Line Characterization by Single Cell RNA Sequencing

Experimental procedures of single cell RNA sequencing followed from established 10X genomics single cell RNA sequencing techniques using the Chromium single cell 3' library v2 kit (PN-120237, 10x Genomics; Pleasanton, CA) and Nextseq 500 (TG-160-2005, Illumina, San Diego, USA). Briefly, concentration of single cell suspension from cultured cells and cell viability were measured using Countess II

Automated Cell Counter combined with Trypan blue stain (15250061, Thermo Fisher).

Approximately 3000 input single live cells in cellular suspensions were loaded on a

Single-Cell Instrument (10x Genomics) to generate single-cell GEMs from 65%

recovered cells. Single-cell RNA-Seq libraries were prepared using Chromium single

cell 3' library & gel bead kit V2 (PN-120237, 10x Genomics). GEM-RT was performed

on the Applied Biosystems 9700 Thermal cycler to generate barcoded single-strand

Figure 4: PARP inhibitor resistance assay experimental design.
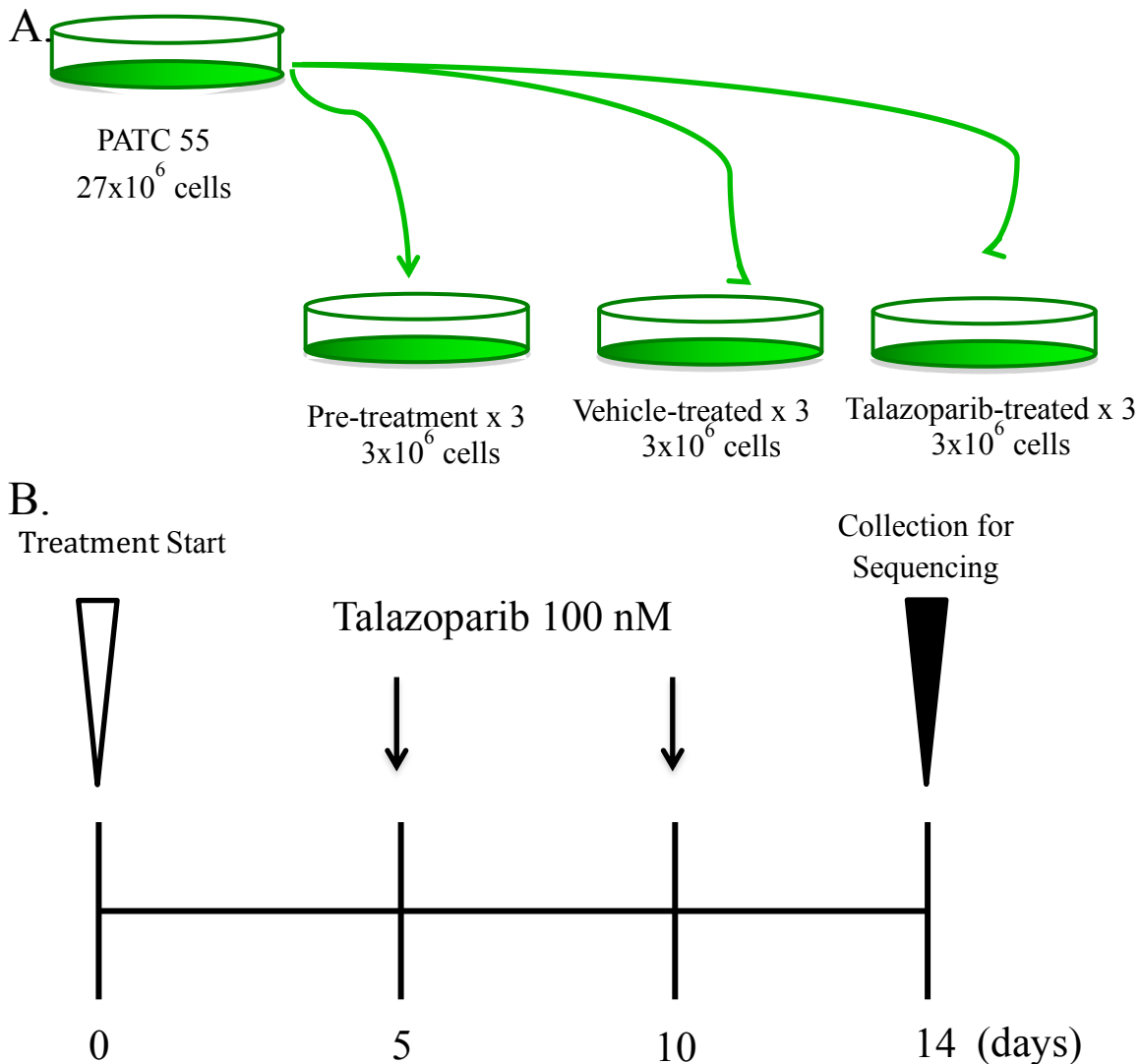
cDNAs were used to construct libraries. RNA-seq in paired-end, with R1 26nt and R2 98nt, was performed on pooled indexed samples (approximately 150 million reads/sample). The sample demultiplexing from i7 8nt index, barcode processing and single cell 3' gene counting were performed using the Cell Ranger single cell software suite (10X Genomics).

3.2.18 Single Cell Data Processing

The sequencing data was processed using package Seurat (v3.0.1) in R 3.5.0[121,122]. For each sample, cells with less than 200 unique genes or more than 10% mitochondrial genes were removed. Genes found in less than 3 cells were also filtered out. After removing low quality/dying cells, samples were merged together, and cell names were re-named as sample names plus the original cell names. Merged data was normalized, scaled and heterogeneity caused by mitochondrial contamination was regressed out. The top 2,000 most variable genes were found for principal component analysis and the top 15 principal components were used for unsupervised clustering using shared nearest neighbor (SNN) and clusters were defined with resolution 0.8 (Figure 5).

To visualize the data, Uniform Manifold Approximation and Projection (UMAP), a non-linear dimensional reduction method, was used to present it on 2D[123]. Differentially expressed genes (DEGs) were found using function 'FindMarkers' with default parameters. DEGs with adjusted p value < 0.05 and absolute average log fold change value > log(1.5) were selected for heatmap visualization.

Figure 5: Single cell RNA sequencing principal component analysis plots to determine optimal number of principal components to perform unsupervised SNN clustering.
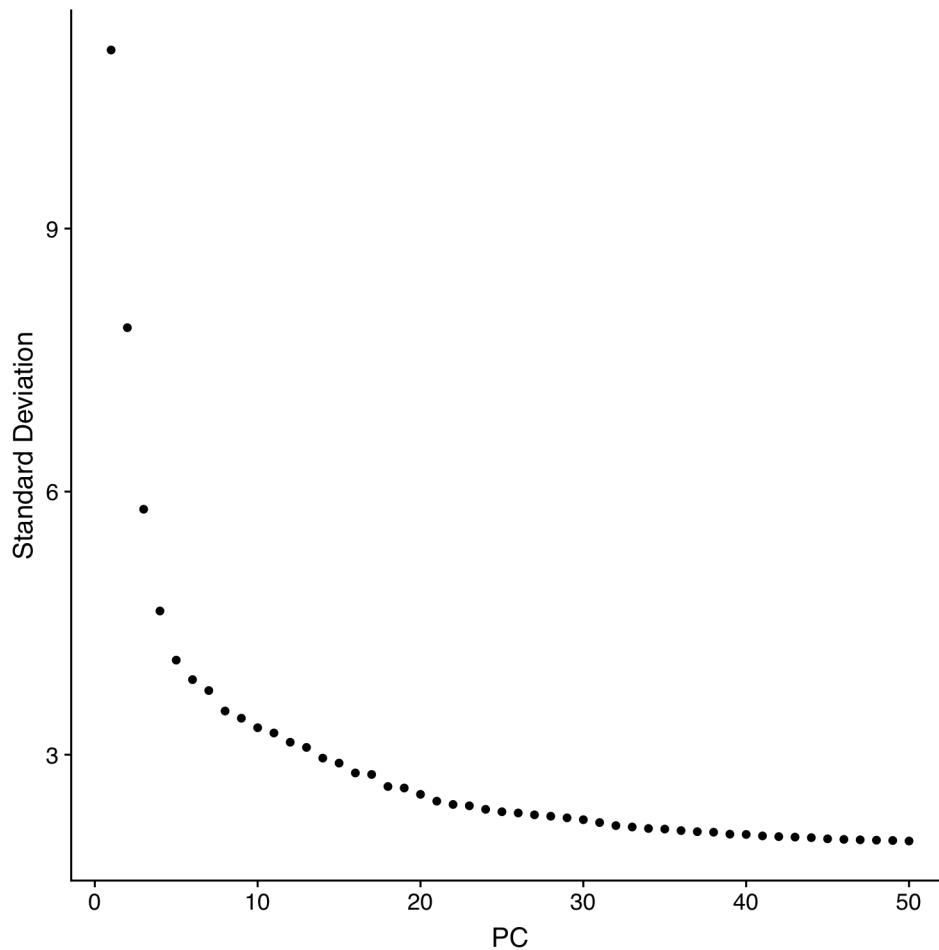
3.2.19 Pathway Enrichment Analysis

The R package GSVA (v1.30.0) was used for enrichment analysis[124]. We included HALLMARK, KEGG and REACTOME gene sets collections and used Single sample GSEA (ssGSEA) method to calculate an enrichment score per cell as described previously by Hänzelmann et al. To find significant pathways, we combined Pre-treated and Vehicle-treated cohorts as a control group and compared it with the Talazoparib-treated group. Linear model in limma (v3.38.3) was used for finding the significant pathways.

3.2.20 Identification of Molecular Patterns Within Each Treatment Group

Nonnegative matrix factorization (NMF) was used to identify distinct molecular patterns within each sample between two different clusters identified by SNN and UMAP. Details of this algorithm were described by Brunet et al[125]. We split the data into 2 to 10 unsupervised clusters, and calculated cophenetic correlation for each rank[126]. Rank k=3 was finally chosen for downstream analysis. DEGs among 3 clusters with adjusted p value < 0.05 and absolute average log fold change value > log(1.5) were selected for heatmap visualization.

3.2.21 Pseudotime Analysis

We used Monocle (v2.10.1) to see the "state" transitions of cells in response to different stimuli[127-129]. Differentially expressed genes among the three treatment groups with adjusted p value < 0.01 were used for learning the trajectory. DDRTree method was used to reduce the space into 2D for visualization.

3.2.22 DNA Repair Pathway and Gene Analysis

Boxplots were created in R to assess differential expression of genes. Statistical differences were calculated using the Wilcox test and correction for multiple hypothesis testing using the Bonferroni adjustment.

3.2.23 Antibodies

Rabbit polyclonal Anti-RIF1 (1:1000, ab229656), Rabbit monoclonal anti-53BP1 (1:20,000, ab175188), and anti-GAPDH (1:10,000, ab181602) primary antibodies were

purchased from Abcam. Rabbit monoclonal anti-BRCA2 (1:1000, 10741) primary antibody was purchased from cell signaling technology. Goat anti-Rabbit IgG H&L (HRP) (1:3000, ab6721) secondary antibody was also purchased from Abcam.

3.2.24 Western Blots

Cells were cultured on 60 mm culture plates. After experimental procedure, cells were washed two times with cold PBS. Radioimmunoprecipitation assay (RIPA) buffer (BP-115, Boston Bio Products, Ashland, MA) with Complete mini (3418550, Roche, Basel, CH) protease and phosphatase inhibitors were added to the plate and placed on ice. Plates were shaken continuously for 20 minutes. A cell scraper was used to scrape and collect cells and place into a 1.5 mill Eppendorf tube. Cells were centrifuged at 14,000 rpm for 10 minutes at 4° and supernatant was collected.

Protein quantification was performed using the Pierce BCA protein assay kit (23225, Thermo Fisher) to perform Bradford analysis. Using albumin for reference, samples were normalized with RIPA buffer to 1 μg per microliter. Protein was denatured by adding protein loading buffer (161-0747, Biorad, Hercules, CA) with SDS and BME and boiled for five minutes. For RIF1 and 53BP1 assays and BRCA2 assay, 20 μg and 75 μg of protein was loaded into each well, respectively. Gels were run using the Biorad Mini-Protean Tetra system (1658004) at 100 V for one to two hours. A semi dry blot was performed at 1.3A, 25V 15 to 20 minutes using Biorad Transblot Turbo Transfer Pack (1704158, Biorad) with 0.2 μm nitrocellulose paper (1704158, Biorad). Block was performed for 1 hour at room temperature with 5% milk in TBST (0.05% Tween 20 in Tris buffer solution). Blot paper was then washed with TBST until buffer was clear.

Primary antibody was diluted in Odyssey Blocking buffer (927-50000, Li-cor, Lincoln, NE) at 4° overnight on the shaker. Blot paper was then washed with TBST for three times 5 minutes on the shaker. Secondary antibody was diluted in 5% milk in TBST for 1 hour at room temperature on the shaker. Blot paper was then washed with TBST for three times 5 minutes on the shaker. Super Signal West Femto (34096, Thermo Fisher) was used to expose the horseradish peroxidase signal using a GE Imagequant LAS 4000 system for detection.

3.2.25 XPO-1 Inhibitor (Selinexor) and PARP Inhibitor (Talazoparib) Combination Assay

PATC55 and PATC124 PDX cell lines were grown separately in culture. Cells were plated in twelve well plates with the number of cells plated determined by cell density assays. Cells were treated at increasing concentrations of Talazoparib, ranging between 0.0001 and 10,000 nM, as previously described above in combination with Selinexor at concentrations ranging between 0.1 and 10,000 nM. Cells were treated for 14 days and media was changed every 5 days. Following 14 days of treatment, cells were fixed and stained with cresyl violet as described above. Dose response curves to calculate IC50 were plotted using Graph Pad Prism 8.0 Software. Dose response curves were compared between Talazoparib-treated, Selinexor-treated, and combination-treated cell lines.

3.3 **Results**

3.3.1 Clinico-Pathologic Assessment and Initial Genetic Profiling Identifies BRCA Mutant PDX Tumor Models

Dr. Jason Fleming and colleagues in the department of Surgical Oncology at MD Anderson, have established a bank of patient-derived xenografts isolated from core biopsies and resection specimens from patients with a diagnosis of PDAC. These PDXs have been used *in vivo* and cell lines have been established for *in vitro* experimentation[130].

We utilized the PATC53, 55, 69, 102, and 124 patient-derived xenograft pancreatic cancer cell lines that have been successfully derived from core biopsies of patients treated at MD Anderson Cancer Center (Table 5)[130]. We additionally used genotyped control lines ASPC-1 (*BRCA* wild type, *KRAS* and *TP53* mutant), Capan-1 (germline *BRCA2* c.6174delT, *KRAS* and *TP53* mutant), and Capan-2 (*BRCA* wild type, *KRAS* mutant, *TP53* wild type) from the American Type Culture Collection (ATCC) (Table 6)[106,107]. Whole-exome sequencing (WES) identified both somatic and germline DNA alterations. These included single nucleotide variants, small indels, and somatic copy-number alterations.

Significant recurrent somatic mutations were identified in *KRAS*, *TP53*, *CDKN2A*, *SMAD4* as reported in Table 5. PATC55 and PATC124 were identified to have a *BRCA2* (6219del5) mutation and *BRCA1* (5083del19) mutation, respectively. Although germline DNA was not available for these patients, these BRCA mutations were thought to be germline in nature due to strong family and personal history of *BRCA*-related cancers (breast, ovarian, and pancreatic) as shown in Table 5. Further detailed clinical and pathologic characteristics of the MDACC PDX model cohort were also collected.

Table 5: Clinical and pathologic characteristics of patient-derived xenograft models.

PDX Model	Molecular aberrations	Ashkenazi Jewish	Known Family History	Hx other Cancer
PATC53	*KRAS G12D, TP53 p.R306X, CDKN2A WT, SMAD4 WT, BRCA 1/2 WT*	No	Brother: lung	None
PATC55	*KRAS Q61H, TP53 p.M237I, CDKN2A WT, SMAD4 WT, BRCA 2 germline positive (6219del5)*	No	Mother: ovarian, maternal grandmother: breast, maternal grandfather: prostate, maternal great uncle: bladder, maternal great aunt: gastric, paternal uncle: colon, paternal uncle: leukemia	B/l breast cancer
PATC69	*KRAS G12D, TP53 p.Y236delinsNY, CDKN2A p.R115fs, SMAD4 WT, BRCA 1/2 WT*	No	Brother: lung	None
PATC102	*KRAS G13D, TP53 p.R248W, CDKN2A WT, SMAD4 WT, BRCA 1/2 WT*	No	Brother: lung, sister: lung	None
PATC124	*KRAS G12D, TP53 p.R333fs,CDKN2A WT, SMAD4 WT, BRCA 1 germline positive (5083del19)*	No	Daughter: ovarian, sister: breast, father: pancreas, paternal aunt: breast, paternal cousin: breast, paternal grandmother: ovarian, paternal second cousin: breast, paternal great grandfather: brain, maternal great aunt: ovarian	None

3.3.2 Significant Rad51 Induction is Observed in Response to XRT in BRCA Wild Type Over Mutant Cell Lines

Rad51 nuclear foci have been shown to localize to areas of double stranded DNA repair during DNA damage events. As a surrogate to homologous recombination

function, we assessed the induction of Rad51 foci in response to DNA damage by radiation in both *BRCA* wild type and deficient models. Figure 6 shows robust nuclear foci formation in wild type cell lines AsPC-1, Capan-2, PATC53, PATC69, and PATC102 whereas induction is absent or dampened in *BRCA* mutants Capan-1 and PATC124. This difference is statistically significant ($P = 2.55$ x 10^{-7}, Figure 6B).

Table 6: Molecular aberrations of ATCC cell lines.

PDX Model	Molecular aberrations
AsPC-1	*KRAS G12D, TP53 p.C135fs, CDKN2A p.S92fs, SMAD4 p.R100T, BRCA 1/2 WT*
Capan-1	*KRAS p.G12V, TP53 p.A159V, CDKN2A HD, SMAD4 p.S343X, BRCA 1 WT, BRCA 2* germline positive (5946delT)
Capan-2	*KRAS G12V, TP53 WT, CDKN2A WT, SMAD4 WT, BRCA 1/2 WT*

Response to Talazoparib Varies Among BRCA Mutants

In order to test the degree of response to the second generation PARP inhibitor, Talazoparib, I performed colony formation assays with Talazoparib testing occurring over a 14-day period. Treatment occurred every 5 days. At the end of the treatment period, cells were stained with Cresyl Violet and IC50 values calculated. *BRCA* wild type cell lines showed poor response with IC50 values in the 100-1000 nM range, whereas *BRCA* mutant cell lines showed robust response to treatment with IC50 values between 1-5 nM. PATC55, a *BRCA2* mutant, however, demonstrated a tail of cells resistant to treatment (Figure 7).

Figure 6: Varying Rad51 foci induction observed in *BRCA* wild type versus mutant cell lines in response to radiation (XRT) (A) Boxplot of percent cells with percentage of cells with > 10 Rad51 foci (B).
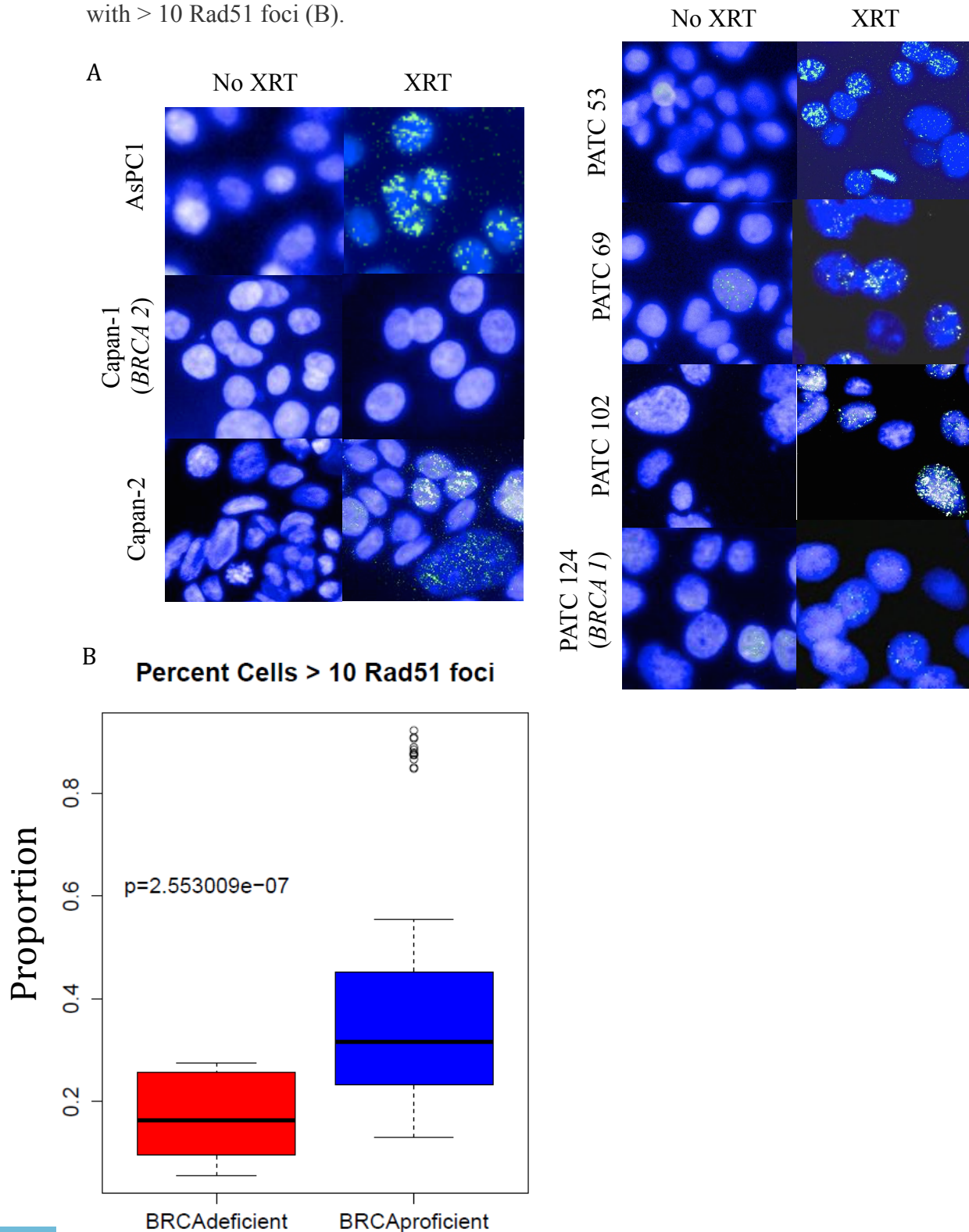
Figure 7: Colony formation assays show variable response to Talazoparib treatment

based on *BRCA* wild type (A) or mutant status (B).
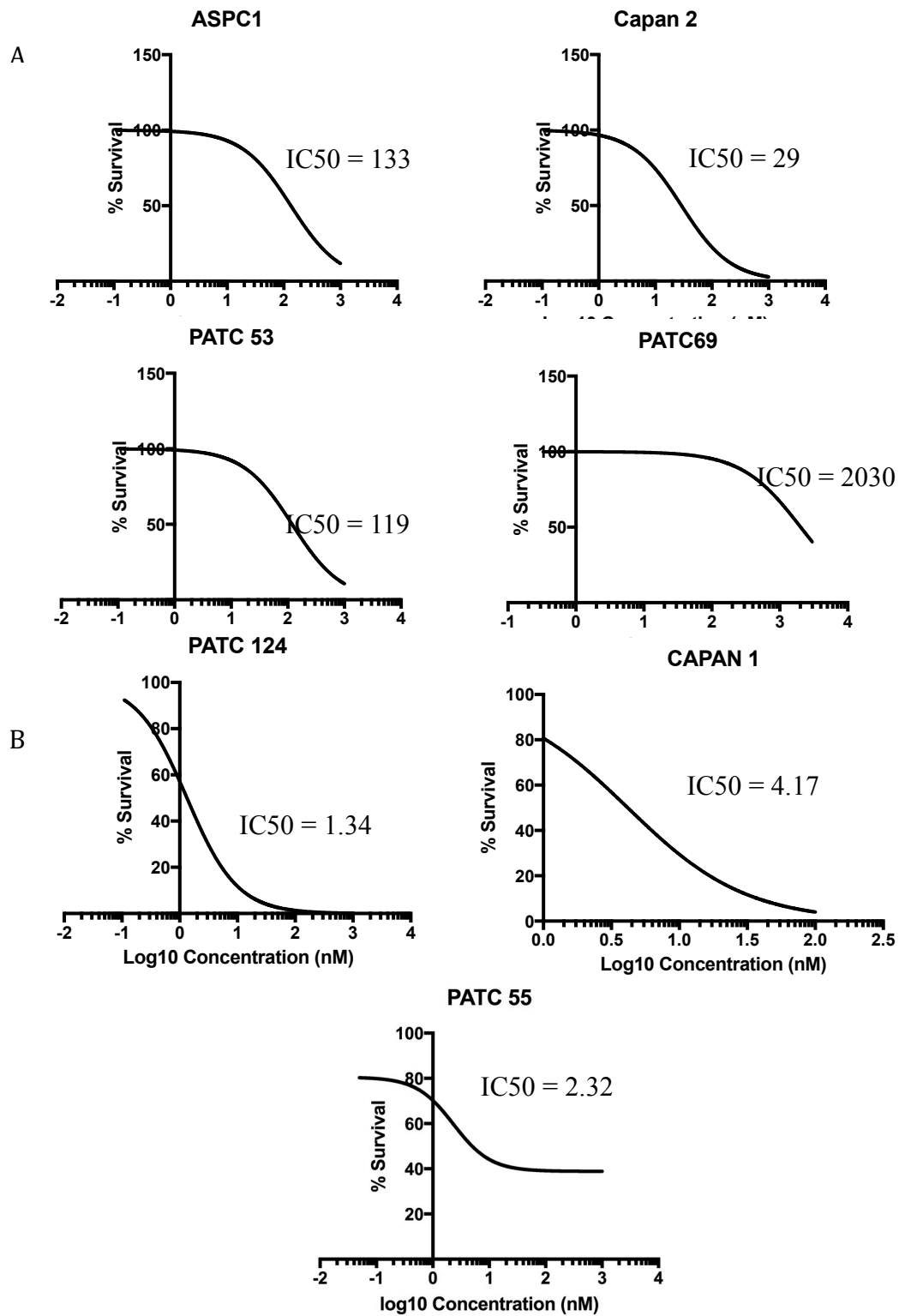
3.3.3 Investigation of Synthetic Lethal Partners to Talazoparib Treatment, with shRNA DNA RepairOme Loss of Function Screen, Fails Secondary to Tumor Necrosis

To test for synthetic lethal partners in the context of Talazoparib therapy, I conducted a loss of function shRNA screen encompassing 350 target genes involved in DNA repair. PATC69 (*BRCA* wild type) and PATC124 (*BRCA1* mutant) PDX cells were transduced with the custom library and injected into the flank of the mice. At 6 weeks, mice were randomly assigned to the Vehicle or Talazoparib (0.125mg/kg/day) treatment groups. Talazoparib-treated mice injected with PATC124 showed delayed tumor growth curves compared to vehicle-treated mice and lived for a shorter duration although this was not statistically significant with Anova testing ($P = 0.13$, Figure 8A). Growth curves were essentially overlapping in the PATC69 cohorts (Figure 8B). Note, PATC69 mice in the Talazoparib-alone group without shRNA library were all sacrificed at treatment end due to excessive tumor growth.

After 4 weeks of treatment, triplicates from each cohort were sacrificed while an additional triplicate were monitored until moribund from tumor growth. At sacrifice, there was no visible areas of necrosis on gross inspection. Tumors were digested and DNA extracted and sequenced for shRNA target reads. Initial QC of PATC124 showed a drop-out of control shRNAs (Luc, PSMA1, and RPL30) at a rate of 20-30% per sample, over the threshold of 10%. Z factor scores were less than zero for each sample representing an unacceptable assay without separation of positive and negative controls (Figure 9). Density plots also showed a left shift consistent with excessive barcode drop-out (Figure 10). H&E was performed of tumors and showed 20-30% necrosis (data not shown). All these factors lead to the determination that the shRNA loss of function

Figure 8: shRNA loss of function screen *in vivo* tumor growth curves for PATC124 (A) and PATC69 (B).

A. PATC 124 Effect of Talazoparib +/- shRNA on Tumor Growth

B. PATC 69 Effect of Talazoparib+/- shRNA on Tumor Growth
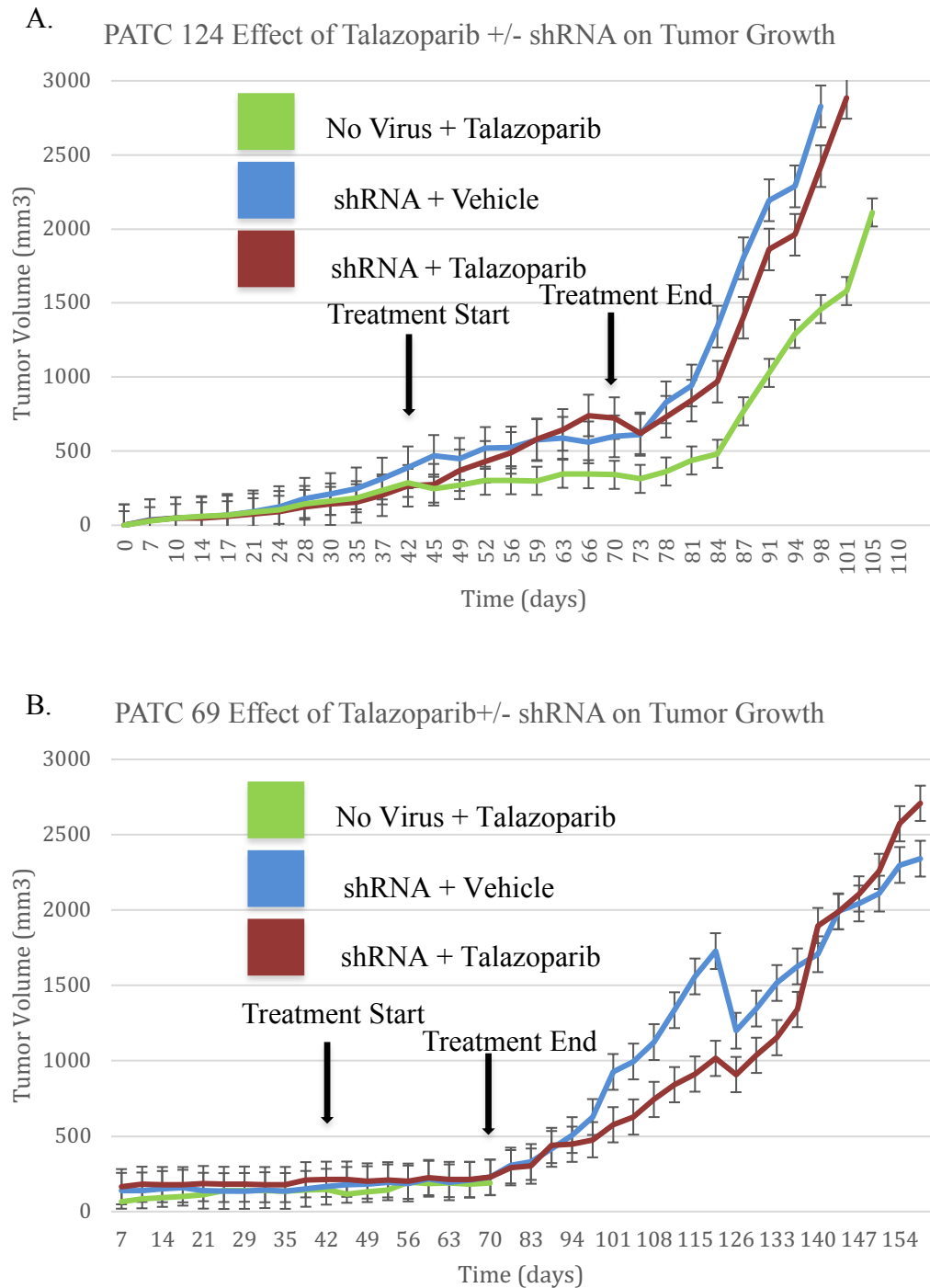
screen failed and further mechanisms of sensitivity and resistance needed to be
investigated.

Figure 9: Z factor scores for PATC124 shRNA DNA RepairOme loss of function screen.
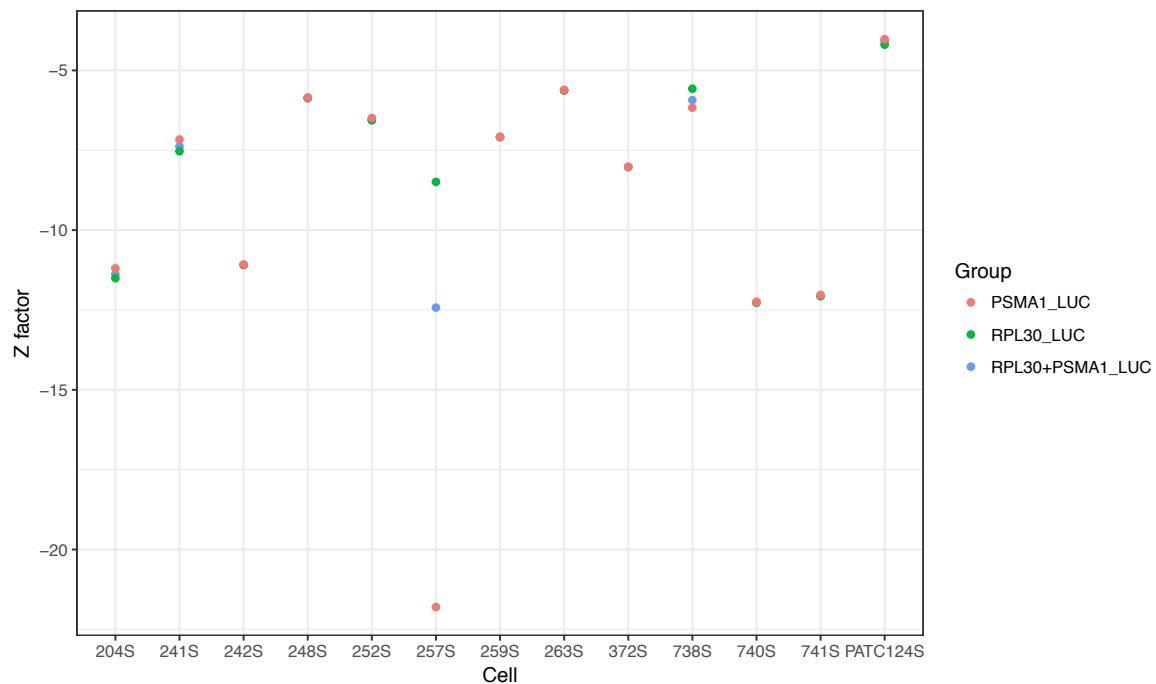
3.3.4 Genomic sequencing of PDAC Cell Lines Identifies RIF1 Mutation in PATC55, Primary Talazoparib-resistant BRCA2 Mutant Cell Line

We detected a 23-bp frameshift deletion in exon 34 (c.7032_7053del) of the *RIF1* gene. This corresponded to a region in the C-terminal known to interact with *BRCA2* (Figure 11). The variant allele frequency of the mutation was 0.28. Sanger sequencing validated the frameshift deletion. (Figure 12). Primers used are listed in the methods section. Sequenza and Pyclone showed the *RIF1* mutation to be present in a sub-clonal fraction present in a fraction of the cells (Figure 13).

Figure 10: PATC124 barcode density plots show left shift representative of barcode drop-out.
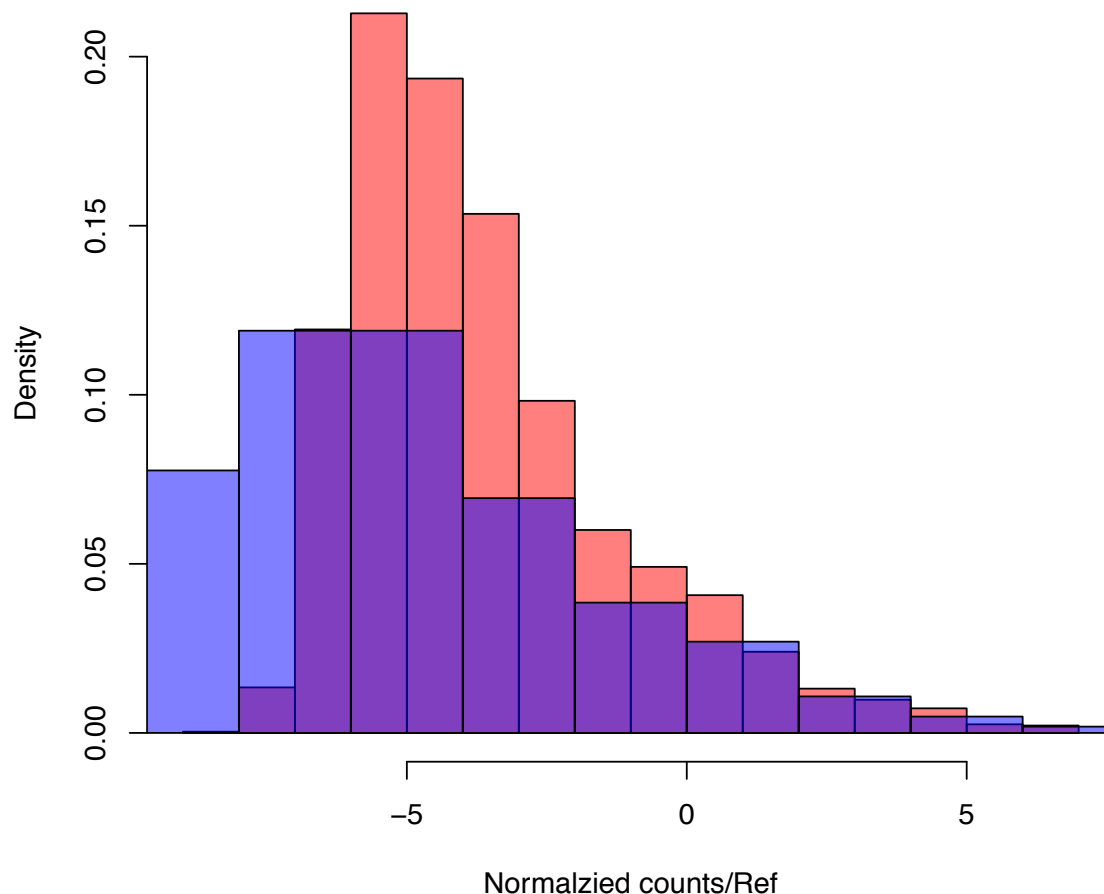
In a clonogenic assay, the PATC55 *RIF1* and *BRCA2* double mutant cell line showed primary Talazoparib-resistance *in vitro* (Figure 7).   In order to select for resistant colonies, cells were treated with Talazoparib at 100 nM over 14 days. Cells were harvested and DNA extracted and WES was performed on the resistant population. *RIF1* VAF decreased from 0.385 to 0.245 (Table 7) in Talazoparib compared to vehicle-treated control.

3.3.5 Loss of RIF1 Does Not Cause Talazoparib Sensitivity in BRCA1 and BRCA2 mutants

We next tested whether inactivation of *RIF1* is causal to PARP inhibitor resistance and whether this was specific to *BRCA1* or *BRCA2* loss. We then transduced 2 cell lines, PATC124 and Capan-1, with *BRCA1* and *BRCA2* mutations, respectively with lentiviral vectors encoding 2 individual shRNAs against *RIF1*. Western blot was used to confirm shRNA efficacy in PATC124 and Capan-1, *BRCA1* (Figure 14) and *BRCA2* (Figure 15) mutants, respectively. A silencing of *RIF1* did not result in reduced sensitivity to Talazoparib in either *BRCA1* (Figure 16A) or *BRCA2* (Figure 16B) mutants, indicating that *RIF1* loss does not cause Talazoparib resistance.

Figure 11: IgV viewer demonstrates *RIF1* p.L2344fs frameshift deletion.
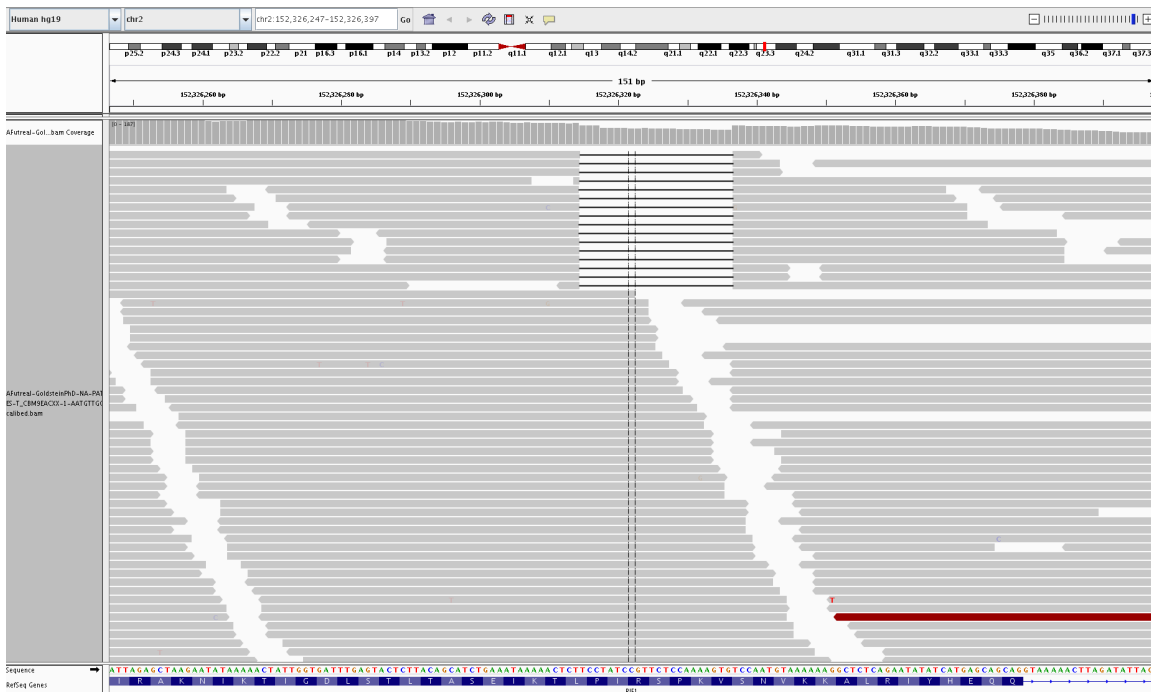
Figure 12: Sanger sequencing confirms *RIF1* mutation.

TCTTCACTGTGGGCTAACCTCAGTTATGATTGAGCTTAAATGGGGAAATTGAACTGGATAAACCCTTGCAAATAGCATAT
AAATAAAACTATATAATTATAATTTCCTGTTTCTGTTTTGTTTAGGGCAAGAGGCCTGGGACAACTCATTAGAGCTAAGA
ATATAAAAACTATTGGTGATTTGAGTACTCTTACAGCATCTGAAATAAAAACTCTTCCTATCCGTTCTCCAAAAGTGTCC
AATGTAAAAAAGGCTCTCAGAATATATCATGAGCAGCAGGTAAAAACTTAGATATTAGCTATGATGTATATTAATAAATG
ATGTAGCAGTACAGTTACAGAAGTTTGTTAAAAGATCACTTCATAATGGCACAGGGAAATTGATTCATTTATTTTGTACT
GTCTTTATGCATTGCACCTCAGATAAATTTTTAAATTGTTTTTTCATTAAATTCTGTTCATCCCCTTCTCTCTTTCATTTT

Forward

Reverse

Figure 13: Density plot of cellular prevalence shows *RIF1* in a fraction of subclones.
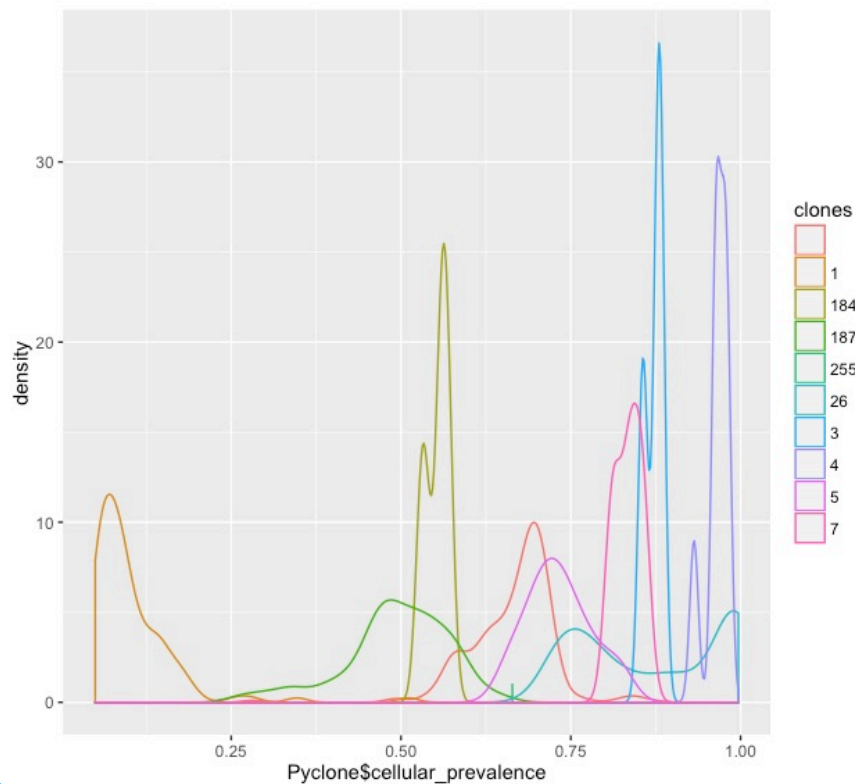
Table 7: Change in *RIF1* VAF between pre, vehicle, and Talazoparib treated PATC55 cells.

Condition	VAF	Average VAF	Std. Dev
Pre-tx 1	0.4348		
Pre-tx 2	0.3333		
Pre-tx 3	0.3571	0.375	0.053
Veh 1	0.217		
Veh 2	0.4		
Veh 3	0.5385	0.385	0.161
Talazoparib 1	0.32		
Talazoparib 2	0.2		
Talazoparib 3	0.2143	0.245	0.065

Figure 14: Western blot demonstrating shRNA silencing of *RIF1* in PATC124 BRCA1 mutant cell line.
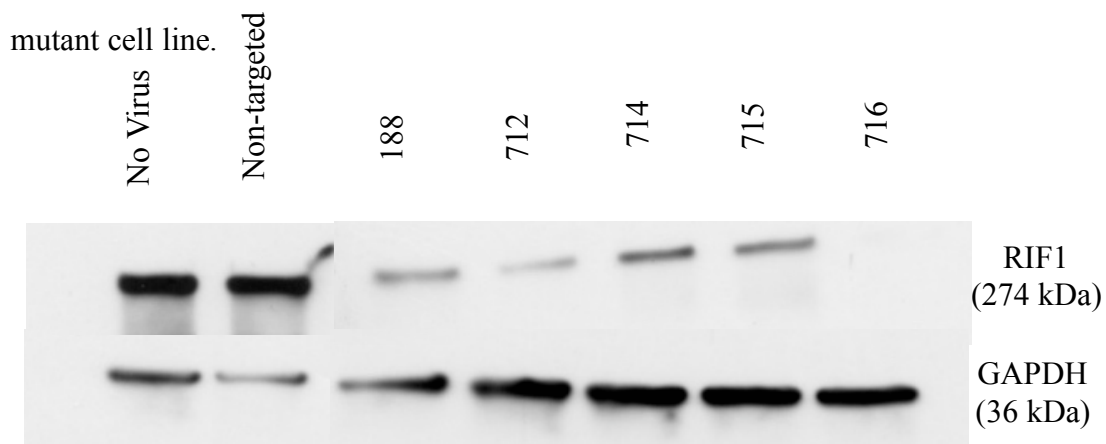
Figure 15: Western blot demonstrating shRNA silencing of *RIF1* in Capan-1 BRCA2 mutant cell line.
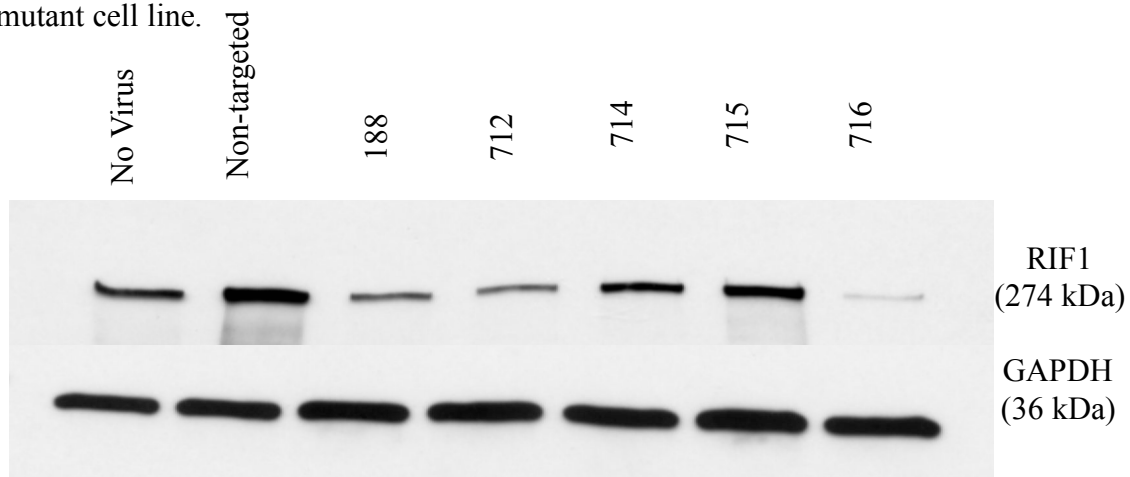
Figure 16: Colony formation assay of *RIF1* shRNA transduced BRCA1 (A) and BRCA2 (B) mutants.

Capan1 IC50

	IC50
No virus	0.620
Non-targeted	0.095
712	1.446
716	1.178
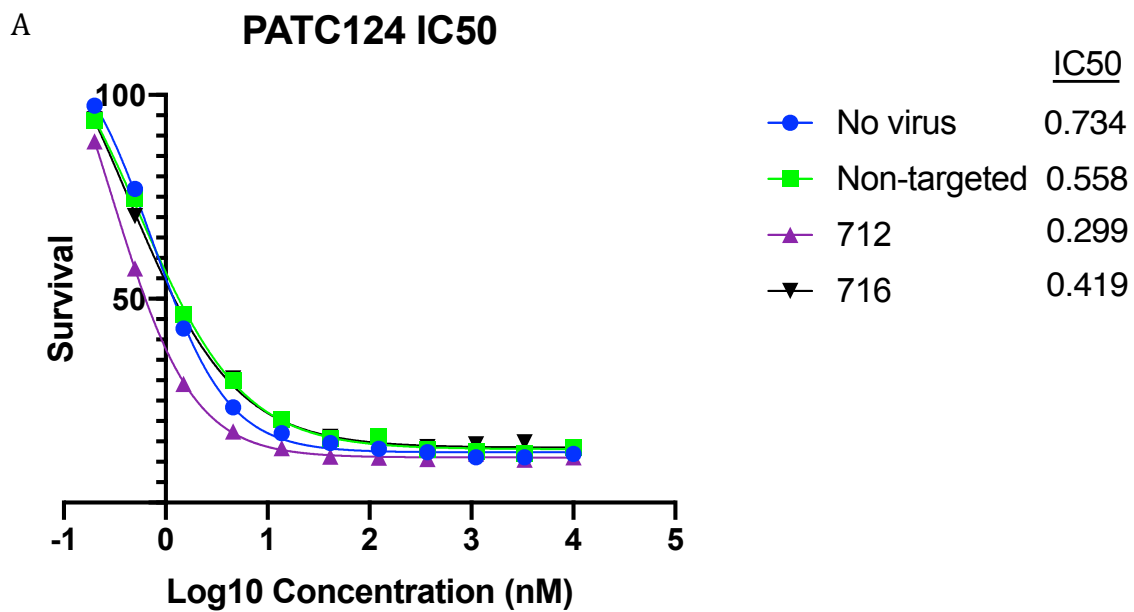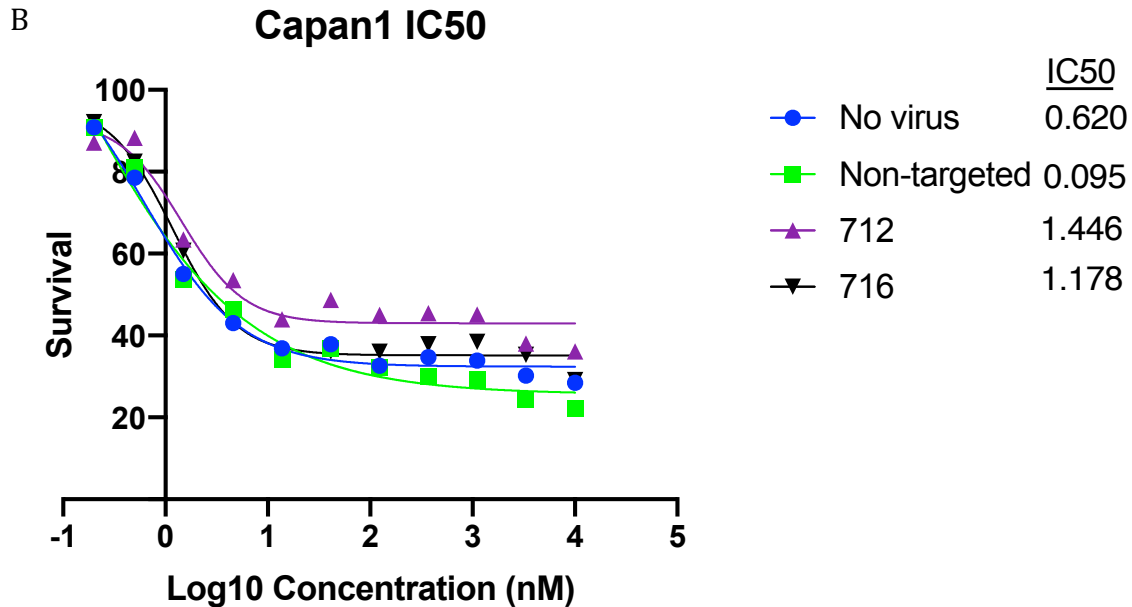
3.3.6 Western Blots Demonstrate Intact 53BP1 in all Cell Lines

Western blot was performed on PATC55 (*BRCA2* mutant), PATC124 (*BRCA1* mutant), and Capan-1 (*BRCA2* mutant) samples to assess for loss of 53BP1, a previously described mechanism of resistance to PARP inhibitor therapy in *BRCA1* mutants. All cell lines showed intact 53BP1 with approximately equivalent amounts of protein per sample (Figure 17).

3.3.7 Treating with Talazoparib at IC90 Does Not Alter BRCA2 VAF

PATC55 cell lines were plated on 100mm culture dishes and treated at 5-day intervals for 2 weeks. Resistant cells were harvested, DNA collected, and WES performed. Talazoparib-treated PDAC tumors retained *BRCA2* mutation with a VAF of 82%. This was comparable to the uninjected reference where the VAF was determined at 89%. Of note, coverage of *BRCA2* in the Talazoparib cohort was less than the pre-treated

controls accounting for slight decrease in *BRCA2* mutant VAF. No additional pathological secondary *BRCA* mutations were found in the treated cohort. There was no evidence of reversion of *BRCA* mutation to wild type.

Figure 17: Western blot demonstrating intact 53BP1 in all samples and *BRCA* mutants in PATC55 (*BRCA2* mutant), PATC124 (*BRCA1* mutant), and Capan-1 (*BRCA2* mutant) cell lines.
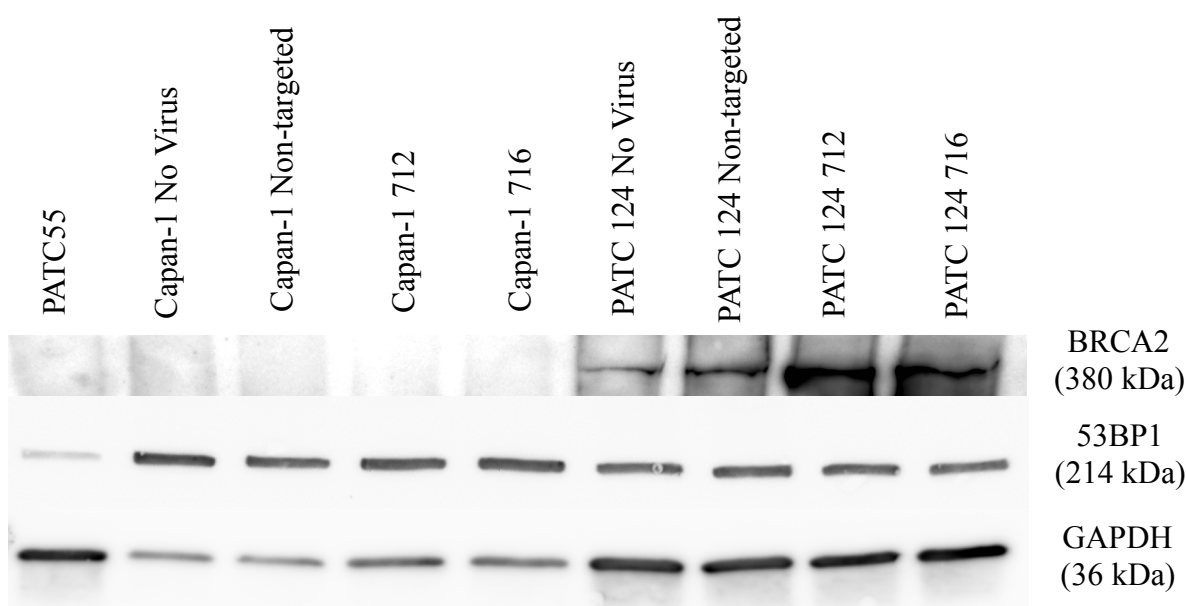
3.3.8 Treating with Talazoparib at IC90 Does Not Induce Novel Mutation and Does Not Alter Copy Number

PATC55 cells were treated in triplicate at an IC90 (100nM) every 5 days for two weeks and resistant cells were harvested, DNA extracted and sequenced. Mutect and Pindel were used to assess for induction of novel mutations in the Talazoparib-treated samples compared to Pre- and Vehicle-treated samples. There were no novel pathologic mutations or indels observed.

Sequenza was run to assess for copy number alterations between the three treatment cohorts. No significant change was seen in the copy number profiles between the three groups (Figure 18).

3.3.9 Single Cell Sequencing Shows Distinct Clusters Based on Treatment Group

PATC55 cells were treated at an IC90 (100nM) with Talazoparib for two weeks and triplicate samples were collected for single cell RNA sequencing. The goal was to sequence 1,000 cells per sample. Post filtering, 17,180 genes and 6,075 cells (2,998 Pre-treated, 1,724 Vehicle-treated, and 1,353 Talazoparib-treated) remained for downstream analysis. The gene drop-out rate was 47.52%. We performed unsupervised SNN clustering to create t-distributed stochastic neighbor embedding (TSNE) plots and determined there to be 11 distinct clusters that separated out by treatment group. Distribution did not seem to be dependent on triplicate sample or phase of the cell cycle (Figure 19).

3.3.10 UMAP Plots Show Two Distinct Cohorts Independent of Sample, Cell Cycle, Genes Covered, or Mitochondrial Content

UMAP plots were created to visualize the data based on cluster, triplicate, stage of cell cycle, genes covered, and mitochondrial content (Figure 20). Plots showed two distinct cohorts of cells that appeared to be independent of the triplicate, genes covered, or mitochondrial content eliminating these as causes of experimental bias. The cohorts also appeared independent of cell cycle with near even distribution between the two

groups (Figure 20D). The large majority of Talazoparib-treated cells were located in the larger cluster (Figure 20C).

Figure 18: Copy number profiles of Pre-Treated (A), Vehicle-Treated (B), and Talazoparib-Treated (C) PATC55 cells.
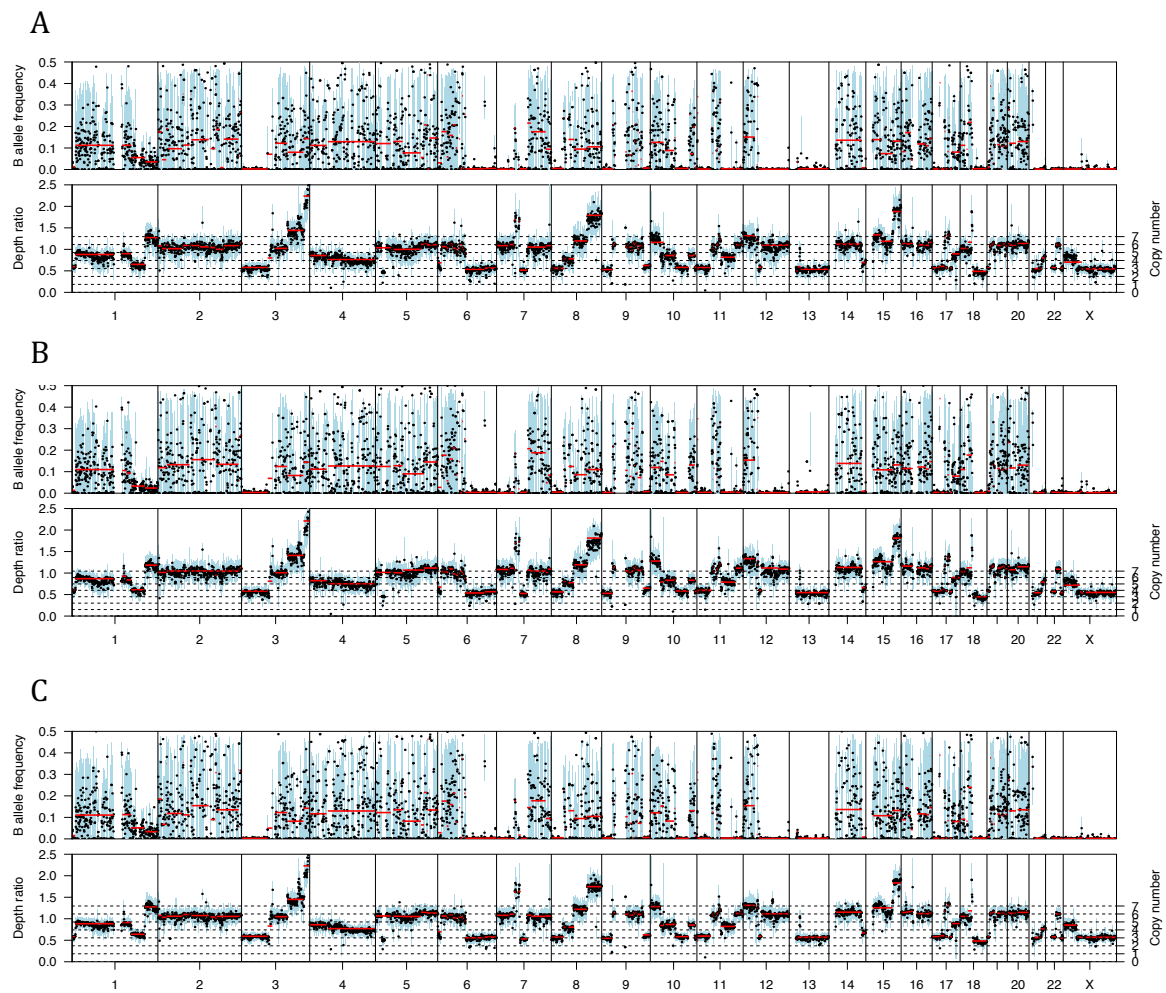
Figure 19: TSNE plots based on SNN unsupervised clustering (A) based on triplicate (B), treatment (C), and stage of cell cycle (D).
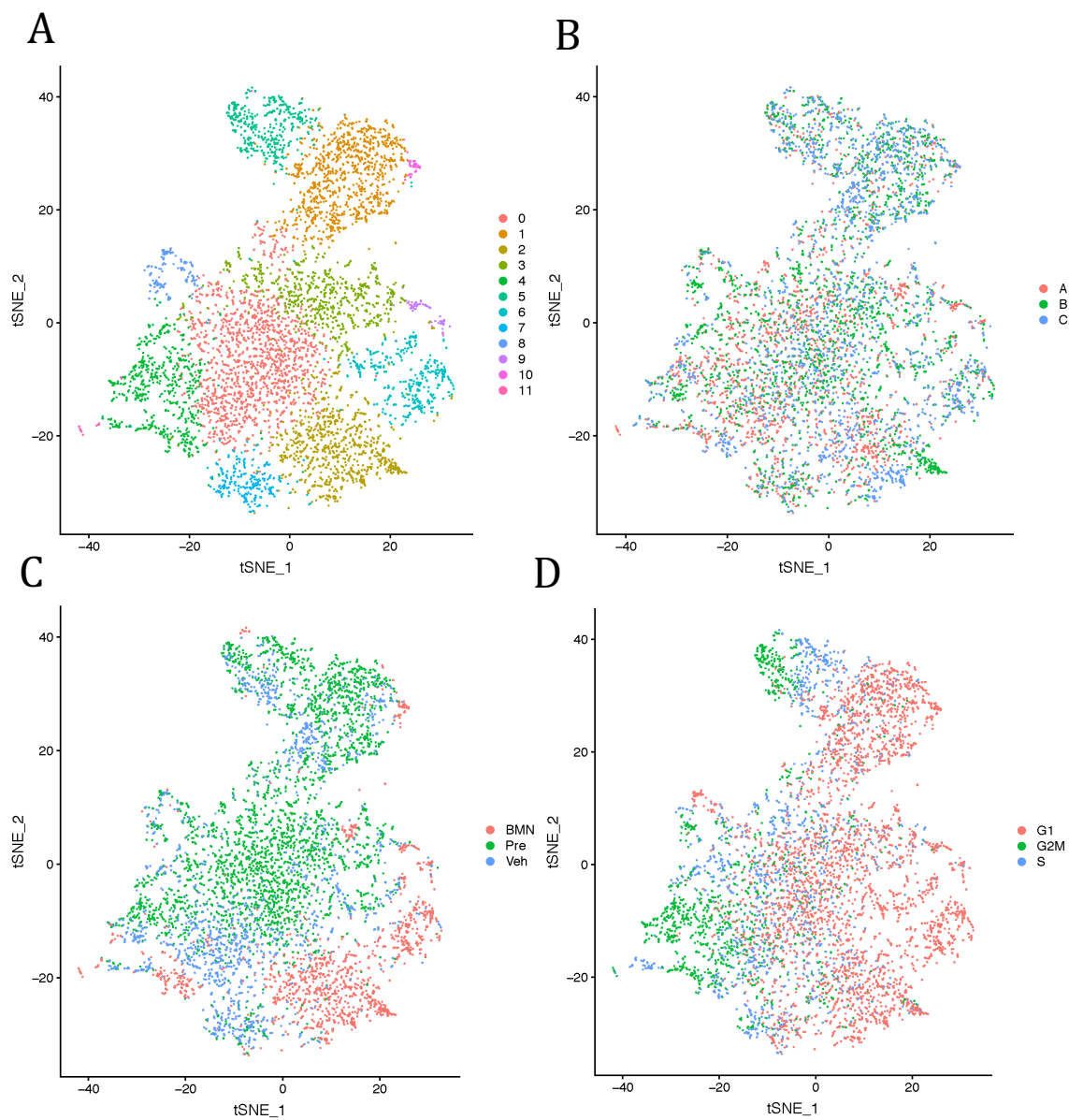
Figure 20: UMAP Plots by cluster (A), triplicate (B), treatment (C), stage of cell cycle (D), genes covered (E), or mitochondrial content (F).
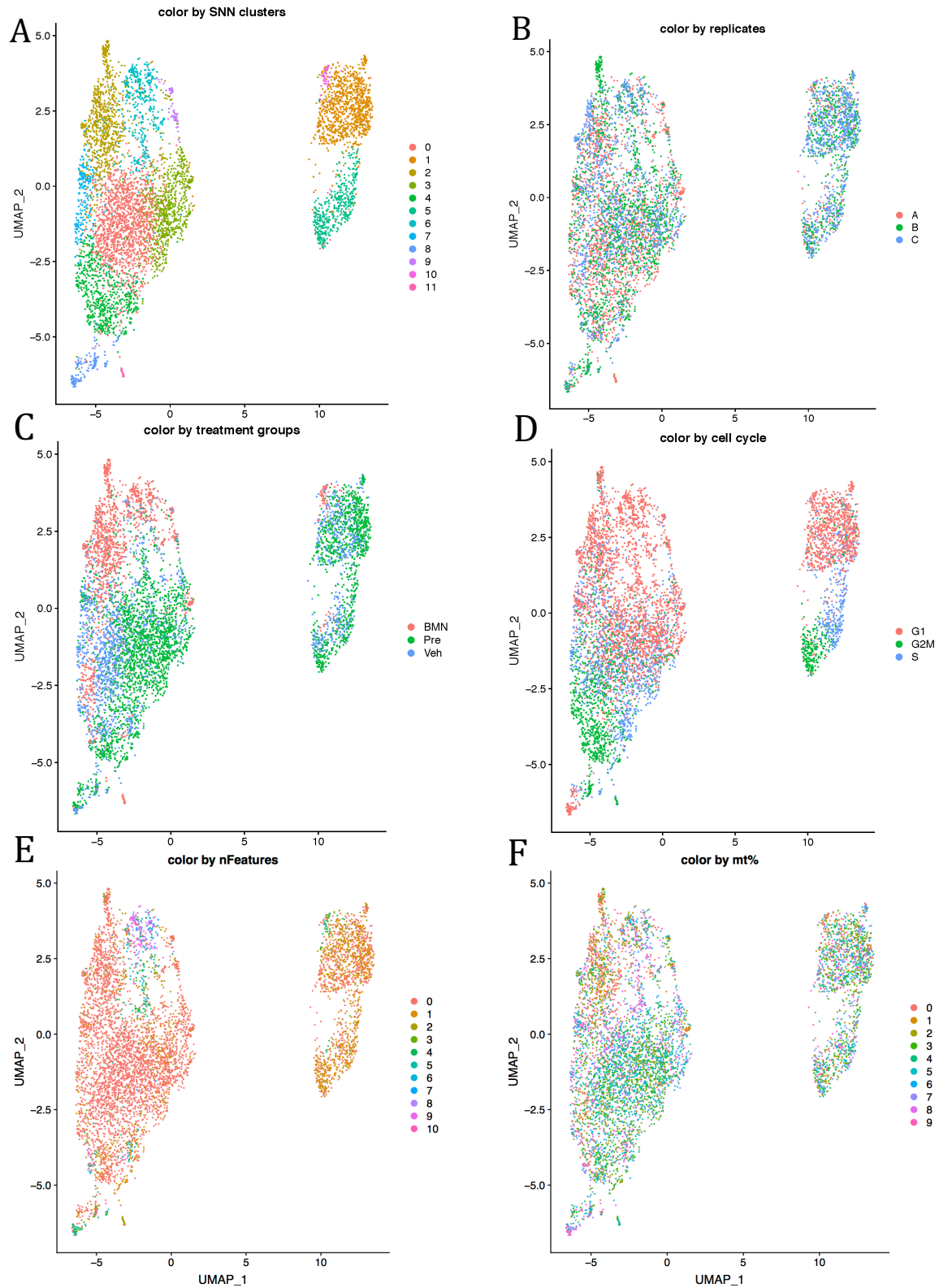
3.3.11 SNN and NMF Clustering Confirm Presence of Two Unique Cohorts of Cells with Distinct Gene Expression Profiles

Unsupervised clustering was performed using both SNN and NMF. SNN clustering showed three separate differential gene expression profiles based on treatment group with similarity between pre- and vehicle-treated groups (Figure 21). Talazoparib-treated cells had decreased MALAT1 and CAV1 expression, genes associated with aggressive pancreatic cancer and upregulation of B2M, HLA-A, HLA-B associated with immune induction. Most Talazoparib-treated cells also fell into the larger cohort as seen in the UMAP plot Figure 20C.

Clustering with NMF was done for each individual treatment group to confirm segregation of UMAP cohorts based on differentially expressed genes (Figure 22). UMAP plots were overlapped with NMF clustering to show DEGs between the two cohorts. In all treatment groups, there were distinct changes in gene expression between the smaller and larger cohorts with two clusters of cells in the larger cohort and one in the smaller in all treatment groups. There were markedly less cells in the smaller UMAP group in the group treated with Talazoparib (Figure 22C).

3.3.12 Pseudotime Analysis Shows Talazoparib is More Effective at Targeting Earlier Differentiated Cells

Psuedotime analysis was performed in order to create a branched trajectory that represents cellular decisions of differential gene expression over a theoretical time scale (Figure 23A). Cells appeared to develop with 3 major branch points with cells from the larger cohort appearing to branch off later in the trajectory (Figure 23B). The majority of

Talazoparib-treated cells also seemed to fall along a more advanced time scale with improved targeting of primitive cells with cells remaining after branched points and increasing differentially expressed genes (Figure 23C).

Figure 21: DEG heatmap using SNN clustering showing three distinct groups based on treatment.
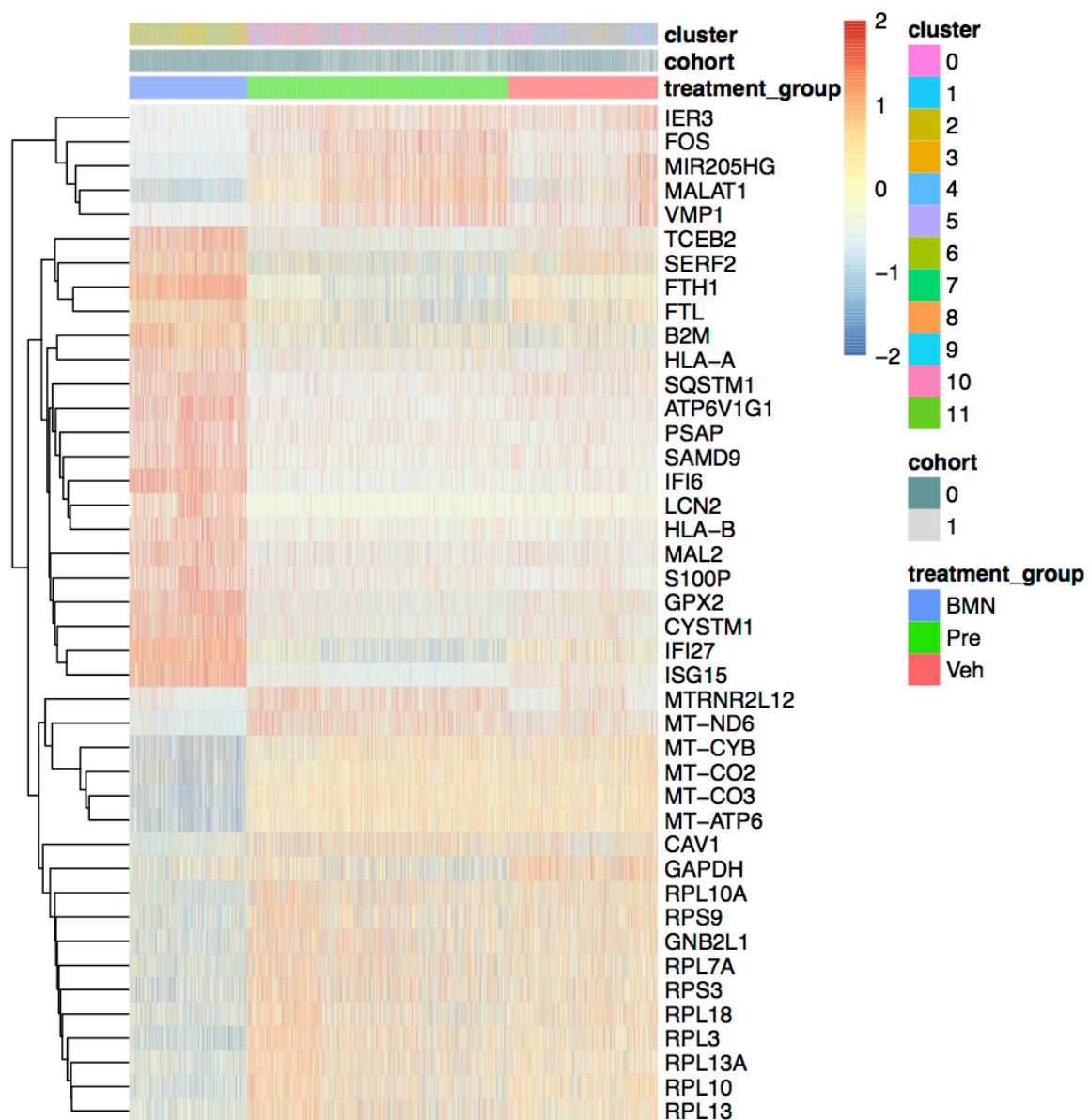
Figure 22: DEG heatmap using NMF clustering showing differentially expressed genes based for pre-treated (A), Vehicle-treated (B), and Talazoparib-treated (C) groups.
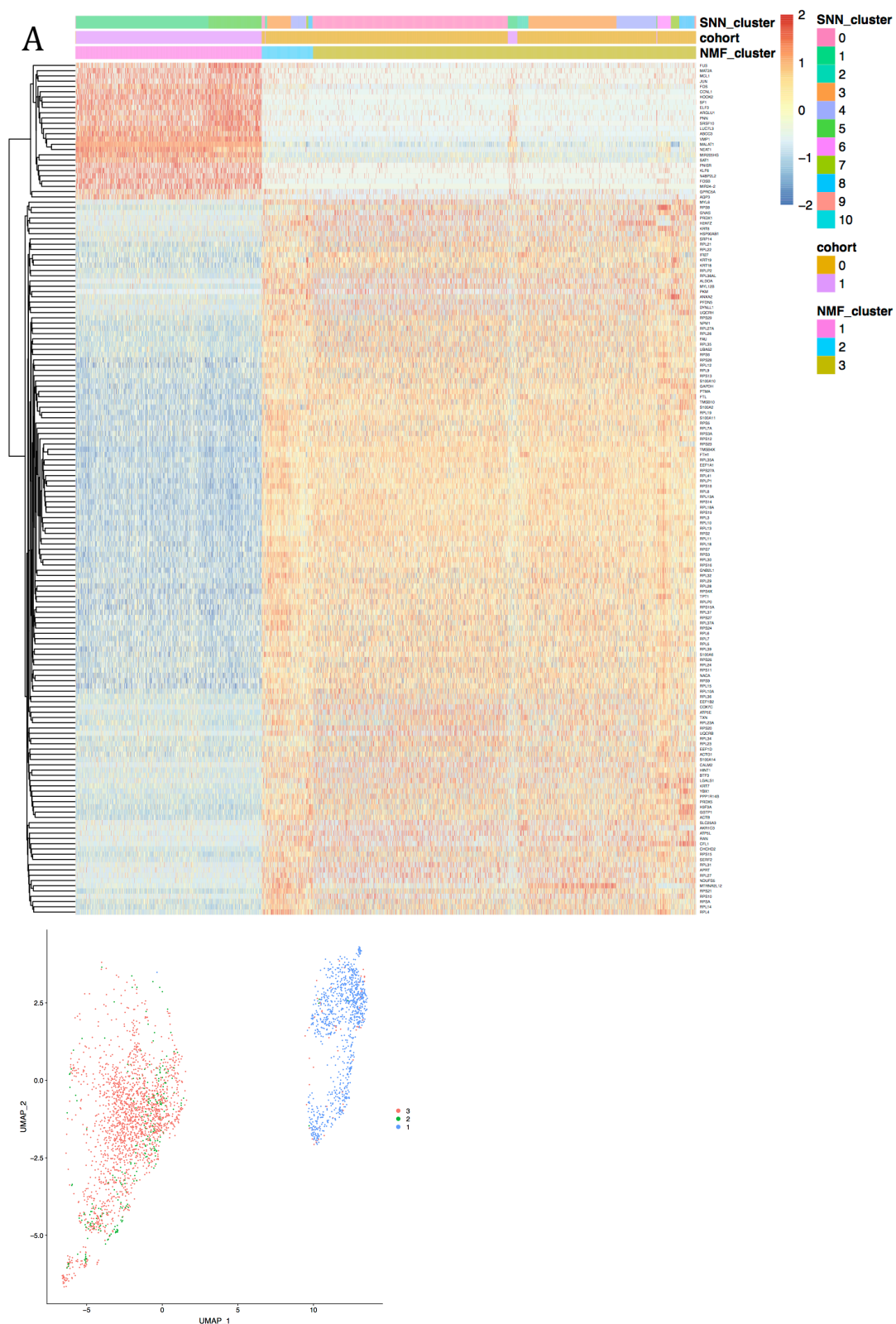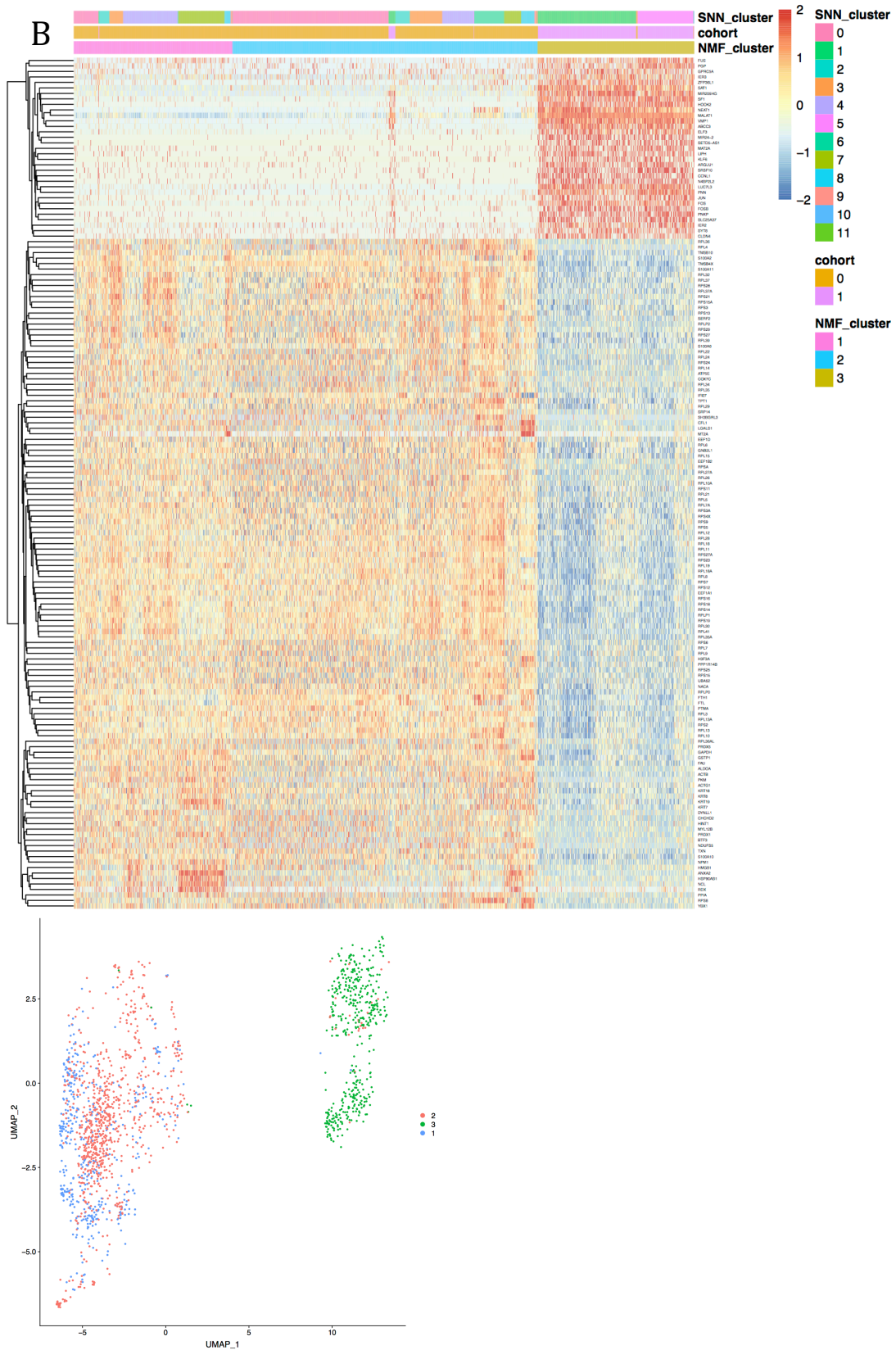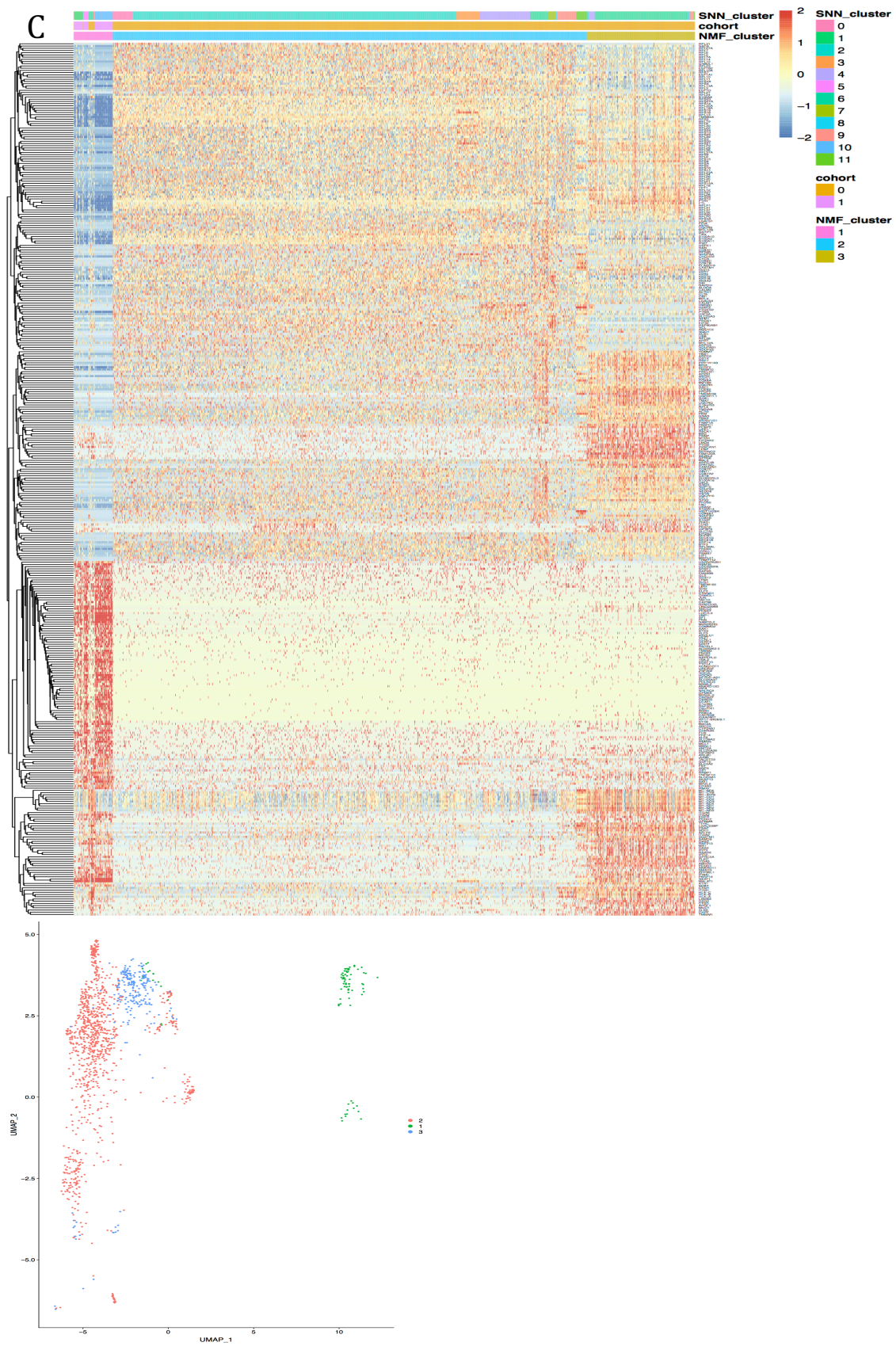
Figure 23: Pseudotime progression analysis (A) based on cohort (B) and treatment (C).
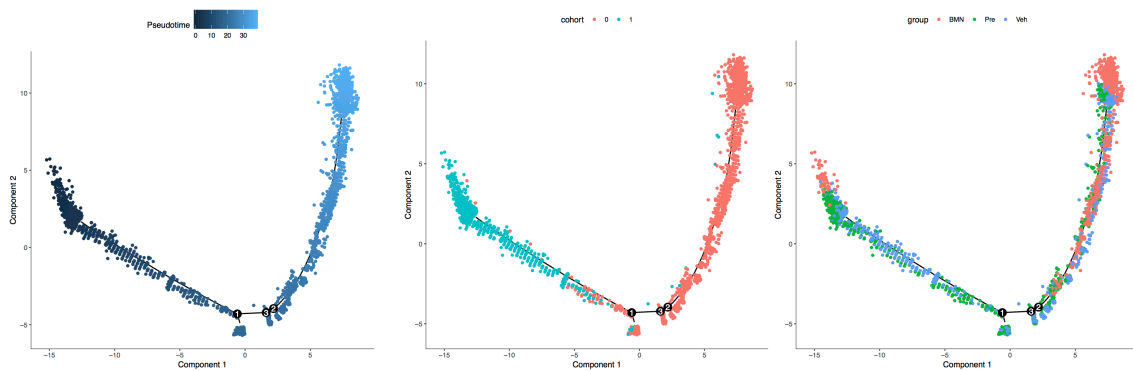
3.3.13 DNA Damage Response Gene Sensors are Upregulated in Response to Talazoparib Treatment

When assessing the differentially expressed DNA repair genes, there was no observed statistically significant difference between Vehicle- and Talazoparib-treated cells at the pathway level (Figure 24). However, when looking at the gene level, there was statistically significant upregulation of multiple DNA damage sensing genes including *Rad23B*, *Rad50*, and *XRCC5* in the Talazoparib-treated group (Figure 25). There was no statistically significant change in the expression of *BRCA1*, *BRCA2*, or *RIF1*.

3.3.14 High Levels of SHFM1 (DSS1) may be Associated with Primary Talazoparib Resistance

SHFM1, part of the 26S proteasome complex subunit, and known to function in BRCA-dependent and independent Rad51 loading of RPA, was the most highly expressed gene in all treatment groups (Figure 26A). There was also a statistically increased expression in the Talazoparib-treated group compared to both Pre-treated and

Vehicle-treated groups. Increased SHFM1 levels were found in the larger UMAP cohort as well (Figure 26B).

Figure 24: DEGs based on DNA repair pathway does not show statistical difference between treatment groups.
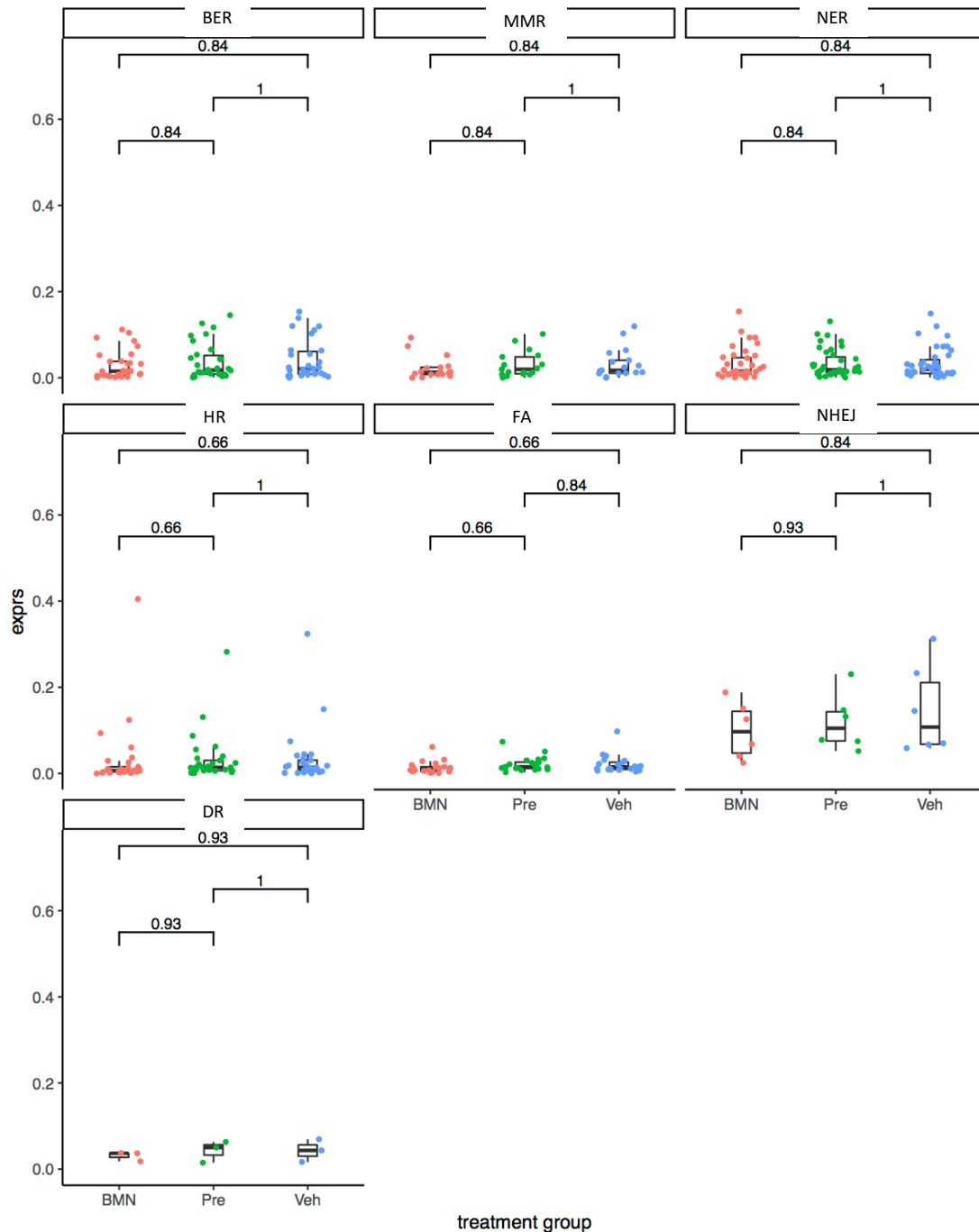
Figure 25: Differential expression of DNA Repair genes shows increased DNA damage sensing gene expression.
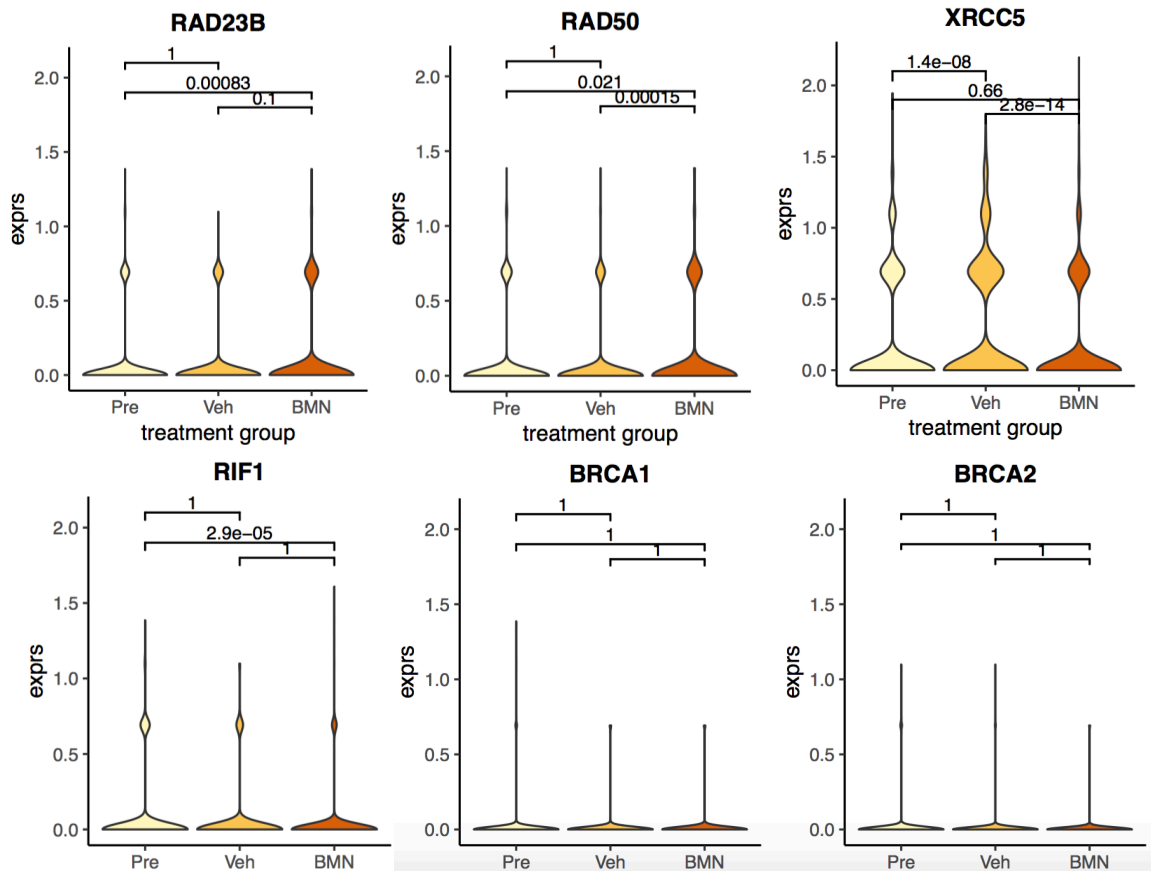
3.3.15 Combination Experiments with XPO-1 Inhibitor Selinexor and PARP Inhibitor Talazoparib Did Not Lead to Drug Synergy in BRCA1 or BRCA2 Cell Lines

We next tested the effect of dual XPO-1 and PARP inhibitor treatment on PATC124, *BRCA1* mutant or PATC55, *BRCA2* mutant cell lines using colony formation assays. The combined treatment did not appear to change the IC50 curves which essentially overlapped with the Talazoparib alone curves in both PATC124 (Figure 27A) and PATC55 (Figure 27B).

Figure 26: SHFM1 (DSS1) is the most highly expressed gene in all treatment groups (A) and TSNE plots show SHFM1 mostly expressed in larger UMAP cohort (B).
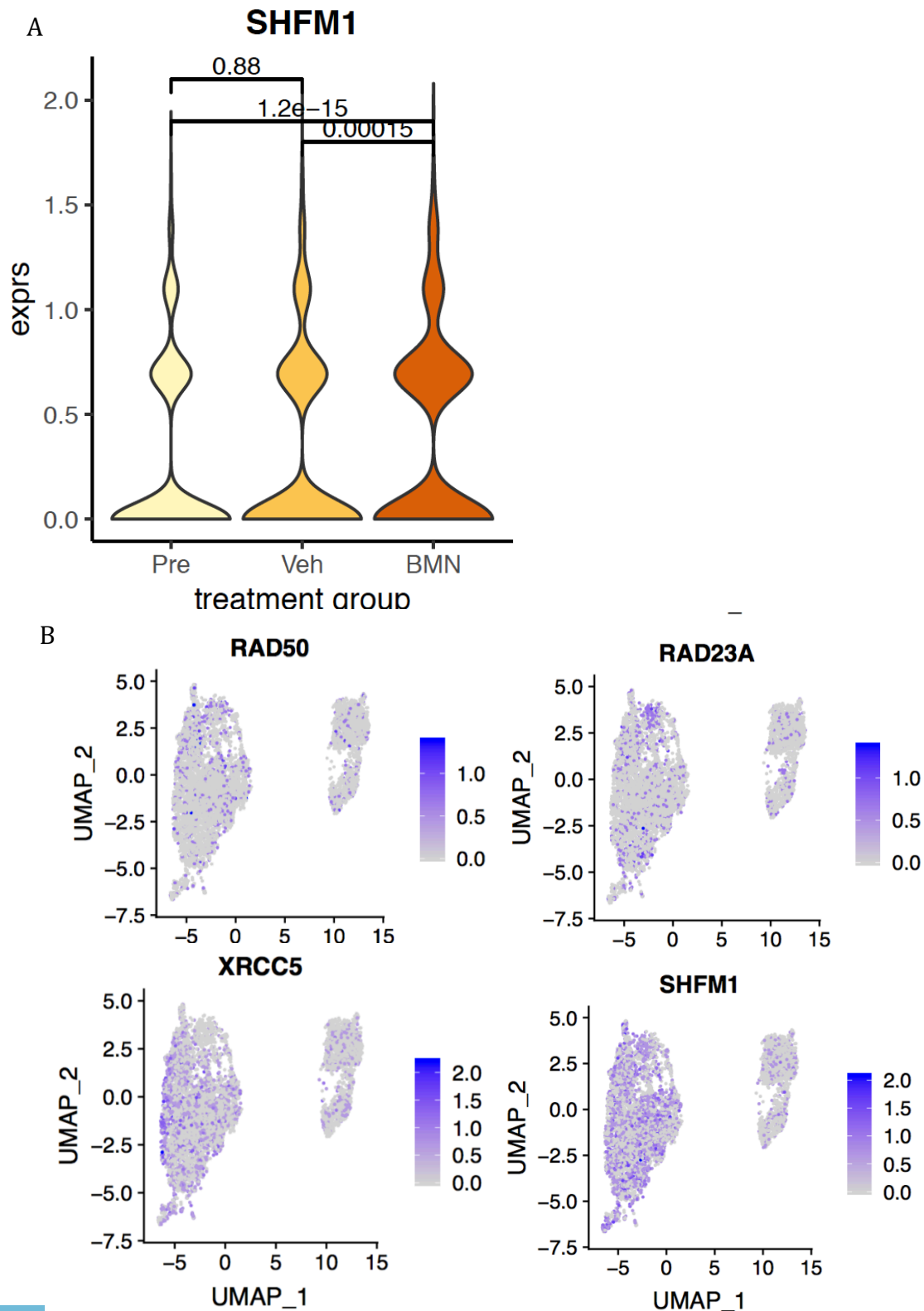
Figure 27: Colony formation assay of dual XPO-1 and PARP inhibitors in *BRCA1* (A)

and *BRCA2* (B) mutants.

A.

B.
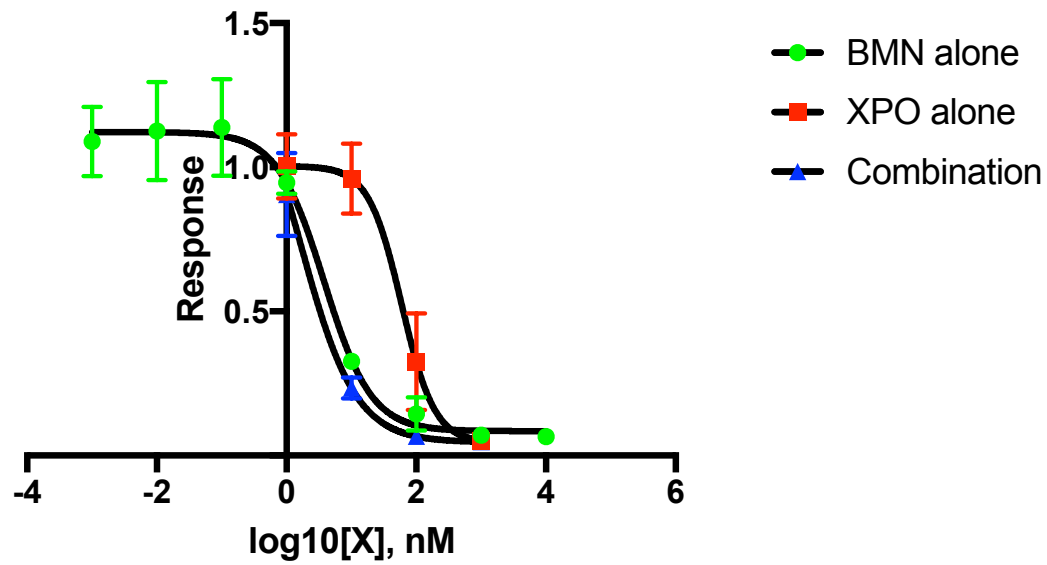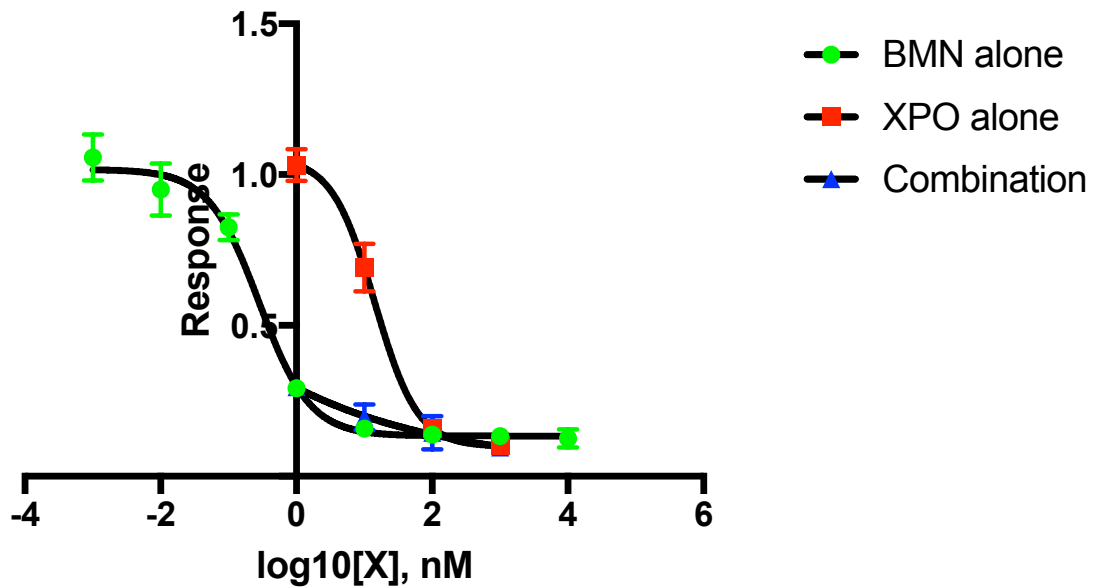
3.4 Discussion

We utilized patient-derived xenografts (PDXs) from *BRCA*-mutant tumors to test the response to the second generation PARP inhibitor, Talazoparib. As expected, *BRCA* wild type PDX models showed primary therapeutic resistance, whereas *BRCA*-mutant models appeared relatively sensitive to Talazoparib treatment. Consistent with the hypothesis that not all *BRCA* mutants respond equally to PARP inhibitor treatment, we found that, PATC55, a *BRCA2* mutant, had a resistant tail with about 30% cell survival after Talazoparib treatment.

I performed a thorough investigation of multiple mechanisms of resistance of PATC55 to Talazoparib at the DNA, RNA, and protein level. I explored the three most widely described mechanisms including reversion of the *BRCA* mutation to wild type, *TP53BP1* mutations that lead to restored genomic stability, and decreased SLFN11 expression[56,57,66,67,69]. I performed Talazoparib resistance assays and found no evidence of reversion of *BRCA* to wild type based on the relatively stable *BRCA2* mutation variant allele frequency between cohorts. There were no initial or induced *TP53BP1* mutations found. RNA sequencing data showed no change in SLFN11 expression levels between vehicle- and Talazoparib-treated samples. I therefore concluded that these previously reported mechanisms were not driving resistance in this model.

Upon further review of the original PATC55 Pindel data, a potentially pathologic *RIF1* p.L2344fs frameshift deletion was found. RIF1 is a protein downstream of 53BP1 that inhibits 3' to 5' DNA resection necessary for homologous recombination and therefore facilitating NHEJ repair[131]. The *RIF1* mutation was at the end of the gene in the *BRCA1* binding domain. I hypothesized that after Talazoparib treatment, the resistant

RIF1 mutant subclone would expand to dominate the population. On the contrary, the *RIF1* mutation VAF went down, corresponding with sensitivity to Talazoparib treatment. Additionally, at the RNA level, single cell sequencing showed no difference in the RIF1 expression in the Vehicle- versus Talazoparib-treated cells.

In the direct experiment, PATC124 (*BRCA1* mutant) and Capan-1 (*BRCA2* mutant) cells were transduced with an shRNA hairpin target against the *RIF1* gene to assess whether silencing *RIF1* leads to resistance against Talazoparib. In both cell lines, IC50 values were nearly overlapping with controls. Both of these direct and indirect experiments show that loss of *RIF1* does not appear to induce therapeutic resistance to Talazoparib therapy in either *BRCA1* or *BRCA2* mutants.

As we did not find evidence of resistance at the DNA level, we next performed single cell RNA to look for compensatory changes in RNA expression to PARP inhibitor treatment. Single cell RNA sequencing allows us to look at gene expression at a population level[132,133]. Here, I have used single cell RNA sequencing to evaluate for clusters of treatment resistant cells within a whole population and to assess the differential gene expression in the resistant cells in response to PARP inhibitor therapy.

I analyzed the genes in the 7 most common DNA repair pathways. There was not a statistically significant difference between cohorts at the pathway level, however I did find that subpopulations of treated cells had increased RNA expression of DNA damage sensor genes when compared to vehicle controls. The was a global upregulation of Rad23B, Rad50, and XRCC5. This may be compensation for the decreased DNA damage sensing through the BER pathway during PARP inhibition. Interestingly, we also found a particularly elevated level of SHFM1 in all cohorts, although this was most

pronounced in the Talazoparib-treated group. The increased gene expression also seemed to correlate to the larger UMAP cohort that containing the bulk of Talazoparib-treated cells.

SHFM1 has been shown to facilitate Rad51 loading of RPA in both a BRCA-dependent and independent manner[74,75]. High SHFM1 may help load RPA independently of BRCA in PATC55, a *BRCA2* mutant and subsequently lead to restoration of genomic stability and resistance to PARP inhibitor therapy. In breast cancer, Shen and colleagues found that shRNA to SHFM1 lead to Talazoparib sensitivity[26]. I plan to further investigate this finding with validation in a public pancreatic cancer RNA sequencing database such as TCGA, ICGC GEO, or ArrayExpress.

Chapter 4

Overall Discussion

Our current understanding of the pathologic molecular aberrations underlying hereditary pancreatic cancer is relatively limited to twelve genes previously described in 2015 in the Journal of Gastroenterology by Grant and colleagues[83]. The incidence of pathologic mutations has been reported between 5-10% of PDAC cases and mainly involve genes in the DNA damage repair pathways including *ATM*, *BRCA1*, *BRCA2*, *PALB2*, and *TP53*[103,104]. It has also been shown that there is a large amount of heterogeneity in hereditary pancreatic cancer which makes diagnosis difficult[104]. The NCCN recently updated national guidelines to include genetic counseling for all PDAC patients[134]. Therefore, the purpose of this dissertation was to both broaden our knowledge of the pathologic alterations associated with hereditary pancreatic cancer and to investigate a class of agents, PARP inhibitors, currently in use to treat hereditary cancers.

In Chapter 2, I conducted a 263-gene germline sequencing study of 133 metastatic pancreatic patients. I found a mutation rate of almost 20% when using a 263 cancer-associated gene panel in an unselected cohort of metastatic PDAC patients with a similar incidence (18.9%) of germline mutations in the TCGA validation cohort. I found a similar profile of mutations that have been previously reported in the literature to include, 3 *ATM*, 2 *BRCA1*, 2 *BRCA2*, 1 *CDKN2A*, 1 *PALB2*, and 1 *TP53* mutation. These mutations only accounted for about 8% of the sequenced cohort (10/133). We also discovered interesting and novel mutations in genes that included *AR*, *HNF1A*, and *SDHD*. There was, however, surprisingly little overlap with lower incidence mutations that occurred in the TCGA cohort. This supports Roberts and colleagues finding of a

large diversity of heterogeneous mutations in hereditary PDAC[104]. Such a large diversity may make targeted therapy difficult in this population with a variety of drivers of disease.

The two most commonly used chemotherapy regimens for metastatic pancreatic cancer are FOLFIRINOX and gem/nab-paclitaxel. In the clinic, the choice to treat patients with either regimen is usually based upon a patient's performance status, with those in better condition receiving the more difficult to tolerate, yet more effective FOLFIRINOX. It has been reported in the literature that hereditary pancreatic cancer patients have a better response to platinum therapy and also appears to have cross-sensitivity to PARP inhibitors[17,103]. However, many of the previous studies have looked at cisplatin containing platinum regimens, which are no longer used as part of SOC chemotherapy[17]. Due to this widely held belief, a majority of the patients we identified with a pathologic mutation, were placed on front-line FOLFIRINOX (85%). Additionally, by 2011, FOLFIRINOX become SOC for front-line metastatic pancreatic cancer while gem/nab-paclitaxel became FDA approved in 2013[91,92]. The overall response rate to FOLFIRINOX was 27.8% in our cohort. Only 4 patients, deemed to have deleterious mutations, received front-line gemcitabine and nab-paclitaxel and only two of these patients were evaluable for treatment response. This made comparison of response to the SOC regimens difficult and we did not see any difference in survival with one regimen or the other (Figure 3D).

Although not statistically significant, we have also provided evidence that a strong family history of 3 or more *BRCA*-related cancers may be a determinate of survival. Due to the subjective nature of family history, this may have contributed to the lack of OS significance. What was interesting, was that patients with DDR or cell cycle

check point mutations (*ATM, BRCA1, BRCA2, CDKN2A, CHEK2, PALB2*, and *ERCC4*) had a near doubling of the overall survival (17.9 versus 9.6 months, P = 0.03) compared to those without a mutation in these genes. Yurgelun and colleagues also found a near doubling in survival in those PDAC patients with DDR mutations, particularly in *ATM, BRCA1*, and *BRCA2 (34.4 vs 19.1 months* [103]. Survival in their study was significantly longer as they assessed surgically resectable patients and we assessed metastatic patients in our cohort. This argues for a biologically based overall survival benefit that may be due to a less aggressive tumor biology. Tumors may develop via impaired DNA damage repair leading to increased somatic mutation rates and abnormal cellular development rather than more aggressive canonical pathways of tumor development from pre-malignant lesions[14,15]. Patients may also have improved treatment response and therefore prolonged survival due to increased tumor vulnerability to platinum agents used in standard of care therapy. This genetic vulnerability and sensitivity to DNA damage may also confer response to PARP inhibitor treatment.

PARP inhibitors are a class of agents that block single-stranded DNA repair via the base excision repair pathway through inhibition of the PARP enzymes. Single stranded breaks may instead be converted to double stranded breaks that normally would be repaired using homologous recombination. In tumors with homologous recombination defects (i.e. *BRCA* mutants), there is an increased use of error prone DNA repair mechanisms such as non-homologous end joining and subsequent genomic instability and cell death[43]. Cross-sensitivity and cross-resistance has been shown between platinum and PARP inhibitor therapy and therefore are now undergoing testing in clinical trials. The phase III POLO trial, with the use of Olaparib in metastatic *BRCA*-mutant pancreatic

cancer has shown some promising clinical results. Those patients treated with Olaparib have shown an improved progression-free survival over placebo, however overall survival data is yet to mature[45,47]. Talazoparib, a second generation PARP inhibitor, is a highly efficacious PARP inhibitor due to its additional PARP trapping mechanism[135]. Talazoparib is currently FDA approved in *BRCA*-mutated, HER2-negative breast cancer[49]. This makes it an attractive compound to use in the highly aggressive pancreatic cancer.

It appears, however, that not all hereditary pancreatic cancer patients respond to treatment and often times they may develop resistance to therapy. We therefore decided to bring these familiar models into the *in vitro* and *in vivo* setting to test the sensitivity and resistance of hereditary PDAC to the second generation PARP inhibitor, Talazoparib. We utilized patient-derived xenografts (PDXs) from *BRCA*-mutant tumors from patients with known hereditary cancer syndromes PATC124 and PATC55, *BRCA1* and *BRCA2* mutants, respectively. PATC124 was derived from a patient with multiple primary, secondary, and tertiary family members with *BRCA*-related cancers. PATC55, a *BRCA2* mutant, displayed both a strong family history of multiple pancreatic, breast, and ovarian cancers as well as a personal history of bilateral breast cancer.

We then utilized colony formation assays to assess response to Talazoparib. As expected, *BRCA* wild type PDX models AsPC1, Capan-2 PATC53, PATC 69 showed therapeutic resistance (Figure 7A). Whereas PATC124 and Capan-1 both appeared to be very sensitive to Talazoparib treatment. However, PATC55, a *BRCA2* mutant, and expected to be sensitive, had a resistant tail (Figure 7B). This was consistent with the

hypothesis that not all *BRCA* mutants respond equally to PARP inhibitor treatment and some may have primary or induced resistance.

I subsequently performed a thorough investigation of multiple mechanisms of resistance at the DNA, RNA, and protein level. I first explored previously described mechanisms of resistance to Talazoparib therapy. The three most widely known mechanisms of resistance include reversion of the *BRCA* mutation to wild type, *TP53BP1* mutations that lead to restored genomic stability, and decreased SLFN11 expression[56,57,66,67,69]. I performed Talazoparib resistance assays (Figure 4) while treating at an IC90 dosage (100 nM). After two weeks I collected resistant cells and performed bulk DNA and single cell RNA sequencing and compared them to vehicle and pre-treatment controls. There was no evidence of reversion of the *BRCA* mutant to *BRCA* wild type status based on the finding of a relatively stable *BRCA2* mutation variant allele frequency between cohorts. This mechanism was previously described in the Capan-1 *BRCA2* mutant pancreatic cancer cell line that is deficient in HR DNA repair. In the case of Capan-1, the c.6174delT mutation, was flanked with frequent small tracts of homology possibly increasing the occurrence of error-prone repair in the region of the mutation. In PATC55, upon review of the surrounding DNA sequences, there was less homologous repeats in the region which may have made the development of this mechanism of resistance less likely.

Additionally, there was no evidence of initial or induced *TP53BP1* mutations found. It is possible that because PATC55 additionally had a pathologic *RIF1* mutation, loss of *TP53BP1* would lead to redundancy in the NHEJ pathway and therefore no selective pressure for this gene mutation would occur. Upon review of the RNA

sequencing data, there was no change in SLFN11 expression levels between vehicle- and Talazoparib-treated samples. I therefore concluded that it did not appear any of these previously reported mechanisms were at play and began to investigate novel mechanisms of therapeutic resistance to Talazoparib therapy.

I attempted to explore synthetic lethal partners to Talazoparib treatment in *BRCA-*mutants using a custom shRNA DNA RepairOme loss of function screen. The screen was able to target up to 350 DNA repair related genes. Tumors were harvested when mice were determined to be moribund or tumors reached the IACUC threshold of 2cm diameter. A QC was performed on the collected data. After analysis of the shRNA screen, it was determined that there was approximately 30% drop-out of shRNA tags, therefore rendering the screen unusable with a dropout threshold set at 10%. Upon further investigation, tumors were sent for Hematoxylin and Eosin (H&E) with the level of necrosis shown to be 20 to 30% in all tested tumors. The necrosis was at a microscopic level and therefore was not visualized upon gross dissection of tumors. As the quality of positive and negative controls could not be trusted, the screen was determined to have been unsuccessful.

Previous experimentation with Talazoparib in mice, independent of an additional shRNA screen, has been conducted over a total of 4 weeks, as was performed in this experiment[48]. Two dosing levels have frequently been used to treat mice, 0.165mg/kg by mouth twice daily and 0.33mg/kg by mouth daily. However, in our hands through previous experimentation by the Institute for Applied Cancer Science (IACS), the twice daily dose, lead to intolerability and death of approximately one mouse per week over 4 weeks. I therefore used a dose of 0.125mg/kg by mouth daily, intentionally sub-

therapeutic to avoid necrosis of the tumor. However, despite the use of the lower dosing schedule, and tolerability of treatment, necrosis levels still reached 20-30%. It is unclear whether this was due to drug effect or tumor outgrowth. One would hypothesize that this was due to outgrowth of tumor blood supply and subsequent necrosis as this effect was also seen in vehicle-treated controls. I therefore do not believe that changing the dosing level of the drug would have been an effective means to improve experimental outcomes. Additionally, although there was some difference in growth rate between tumors, this does not appear to have been substantial enough to change necrosis levels between the cohorts.

In the future, a better approach may have been taken by first performing an independent treatment time trial to evaluate the effect of Talazoparib and the degree of necrosis over time. Periodic assessment with H&E could be performed at weekly intervals to determine the appropriate treatment length prior to the development of necrosis. This could be performed on non-shRNA transduced tumors to determine the impact of the drug alone.

Looking for additional mechanisms of response and resistance, upon further review of the original PATC55 Pindel data, a potentially pathologic *RIF1* p.L2344fs frameshift deletion was found. RIF1 is a protein involved in double stranded DNA repair and acts downstream of 53BP1 to regulate NHEJ. RIF1 is responsible for inhibiting BRCA and shunting from HR to NHEJ during double stranded DNA repair. The *RIF1* mutation was found to be at the end of the gene in the *BRCA* binding domain and appeared to be in a subclonal population based on Sequenza and Pyclone analysis.

I then performed two different experiments to assess whether loss of RIF1 leads to resistance to Talazoparib therapy. I used an indirect approach by treating PATC55 (*RIF1* mutant) with a high dose of Talazoparib (IC90) and re-assessing the *RIF1* mutation VAF. I also used a direct approach by using a targeted shRNA against *RIF1* in *BRCA1* (PATC124) and *BRCA2* (Capan-1) mutants to assess for development of resistance. In the first approach, the VAF did not increase as expected if the sensitive wild type cells were depleted in response to Talazoparib treatment allowing the resistant *RIF1* mutant subclone to expand and dominate the population. On the contrary, although not statistically significant, the *RIF1* mutation VAF went down in the treated cohort (Table 7). Additionally, at the RNA level, single cell sequencing showed no difference in the RIF1 expression in the Vehicle- versus Talazoparib-treated cells when PATC55 was treated at an IC90 (Figure 25).

In the direct experiment, PATC124 (*BRCA1* mutant) and Capan-1 (*BRCA2* mutant) cells were transduced with an shRNA hairpin target against the *RIF1* gene to assess whether silencing the *RIF1* gene in either *BRCA1* or *BRCA2* mutants leads to resistance against Talazoparib. I performed western blots to confirm the gene silencing with 5 different shRNAs. In the end I chose two hairpins (#712 and #716) that showed greater than 60% silencing of RIF1 protein production when compared to the reference (Figures 14 and 15). I then treated the induced cells with Talazoparib over a 2-week period and compared the IC50 curves in compared to the non-targeted and non-transduced controls. In both cell lines, IC50 values were nearly overlapping with controls (Figure 16). Both of these direct and indirect experiments show that loss of

RIF1 does not appear to induce therapeutic resistance to Talazoparib therapy in either *BRCA1* or *BRCA2* mutants.

An alternative approach to finding mechanisms of resistance to this experiment would be to first perform Talazoparib treatment on PATC55 at an IC90 and collect surviving cells for DNA and RNA sequencing. A target could then be chosen based on the sequencing of the resistant cells and then the shRNA vector created against this target and incorporated into the wild type cell lines.

Conversely, rather than performing shRNA silencing of gene targets in wild type models, I could have performed a *RIF1* recovery experiment. Using a viral delivery system, wild type *RIF1* could have been transduced into the PATC55 cell line and production of RIF1 confirmed by western blot. With normal RIF1 protein production, repeat colony formation assays could have been performed in the context of Talazoparib to test for increased sensitivity to Talazoparib compared to mutants.

Single cell RNA sequencing has recently been developed with many uses in medical research and cancer biology. It allows us to look at gene expression at a population level both in normal tissue and in tumors[132,133]. In pancreatic cancer, Bernard and colleagues used single cell RNA sequencing to trace transcriptomic changes of a multistep progression from cystic PDAC precursors to pancreatic cancer[136]. Here, I have used single cell RNA sequencing to evaluate for clusters of treatment resistant cells within a whole population and to assess the differential gene expression in these resistant cells in response to PARP inhibitor therapy.

One thousand cells were sequenced per sample and experiments were performed in triplicate. After filtering, 17,180 genes and 6,075 cells (2,998 Pre-treated, 1,724

Vehicle-treated, and 1,353 Talazoparib-treated) remained for downstream analysis. After Talazoparib treatment and collection, there were only about 50% viable cells left in the sample so it is expected that less live cells were sequenced. The gene drop-out rate was 47.52%, which is expected for single cell RNA sequencing[137,138].

Principal component analysis was performed on the top 2,000 most variable genes and used for SNN clustering. TSNE plots showed 11 distinct clusters that separated out by treatment group. Distribution did not seem to be dependent on triplicate sample or phase of the cell cycle (Figure 19). A Uniform Manifold Approximation and Projection (UMAP) is a dimension reduction technique that can be used for visualization of single cell RNA sequencing data and place cells within clusters based on Euclidian distance from differential gene expression[123]. Figure 20 shows a UMAP with two distinct cohorts of cells. The majority of Talazoparib-treated cells were found in the larger of the two cohorts (Figure 20C). The cohorts did not seem dependent on sequencing coverage, mitochondrial content or phase of the cell cycle and had distinct differentially expressed genes based both on SNN and NMF clustering (Figures 21 and 22). Therefore the distinction between the cohorts does appear to be biologically based. SNN and NMF clustering showed Talazoparib-treated cells had low expression of MALAT-1, a long non-coding RNA that has been shown to promote aggressive pancreatic cancer growth and metastasis via autophagy stimulation as well as differences in expression of DNA repair genes[139].

At a pathway level, I analyzed the genes in the 7 most common DNA repair pathways. There did not seem to be a statistically significant difference between cohorts at the DNA repair pathway level (Figure 24). Other possible mechanisms of resistance

may be at play. We did find that subpopulations of treated cells had increased RNA expression of DNA damage sensors when compared to vehicle controls including Rad23B, Rad50, and XRCC5. This may allow for compensation for the decreased sensing through the BER pathway during PARP inhibition and lead to resistance to therapy.

Interestingly, we also found a particularly elevated level of SHFM1 in all cohorts, but most pronounced in the Talazoparib-treated group (Figure 26). The increased gene expression also seemed to correlate to the larger UMAP cohort that contained the bulk of Talazoparib-treated cells. SHFM1 has been shown to facilitate Rad51 loading of RPA in both a BRCA-dependent and independent manner[74,75]. High SHFM1 may compensate for BRCA loss and help load RPA independently. In PATC55, a *BRCA2* mutant high SHFM1 may therefore lead to restoration of genomic stability and resistance to PARP inhibitor therapy. In breast cancer, Shen and colleagues found that shRNA to SHFM1 lead to Talazoparib sensitivity[26]. In the future, tumor RNA expression levels of SHFM1, RAD23B, RAD50, and XRCC5 may be used to create a resistance signature, to predict Talazoparib resistance in *BRCA* mutant patients.

In order to mitigate resistance, one could also consider combined PARP inhibition with targeting of SHFM1. I believe this mechanism may be more important in *BRCA2* over *BRCA1* mutants due to the role of SHFM1 in stabilization of BRCA2 and therefore compensatory overexpression of SHFM1 when BRCA2 is deficient. Although direct SHFM1 inhibitors have yet to be developed, there are molecules currently being studied that interupt RPA's interaction site with BRCA and SHFM1[140]. This may lead impaired Rad51 loading, genomic instability, and restored sensitivity to PARP inhibition.

XPO-1 is an exporter protein that exports multiple oncoproteins and tumor suppressors from the nucleus. XPO-1 expression levels have been shown to be elevated in aggressive and proliferative pancreatic cancer[141]. We hypothesized that by blocking the exportation of BRCA from the nucleus, that we could salvage DNA repair and partially restore genomic stability. We tested whether the XPO-1 inhibitor, Selinexor, could induce therapeutic resistance to PARP inhibitor therapy when given in combination. We found, however, that the XPO-1 inhibitor did not appear to impact therapy as the inhibitor, single agent Talazoparib, and combination therapy had nearly overlapping IC50 curves. Additionally, in PATC55, when treated at an IC90 dosage of Talazoparib, resistant cells did not show down regulation of XPO-1 as would be expected if it were to lead to resistance to PARP therapy. As there did not appear to be upregulation of XPO-1 RNA expression in this model at baseline, it is possible that the Selinexor did not have adequate target and therefore minimal effect.

In this study I have performed a thorough investigation of multiple mechanisms of PARP inhibitor resistance at the DNA, RNA, and protein level. I have shown that *RIF1* loss does not appear to lead to PARP inhibitor resistance, however elevated gene expression levels of SHFM1 may be correlated with Talazoparib resistance, particularly in *BRCA2* mutants. I plan to validate this finding in the future.

Chapter 5

Conclusions and Future

Directions

Pancreatic adenocarcinoma remains a highly aggressive disease with a poor overall survival despite multi-modal therapy. In this study, I expanded upon our current knowledge of the germline pathologic mutations associated with hereditary pancreatic cancer. In an unselected cohort of pancreatic cancer patients, I have demonstrated a germline mutation rate of almost 20%. I also showed that patients with DNA damage repair gene mutations (*ATM*, *BRCA1,BRCA2*, *ERCC4*, and *PALB2*) had a statistically significant improved overall survival as compared to those patients without (16.8 versus 9.1 months, $P = 0.03$). I identified novel germline mutations that are prognostic for survival in pancreatic cancer patients. A family history of multiple breast, ovarian, and pancreatic cancers was associated with having DNA damage repair gene mutations and better overall survival.

I next characterized a group of patient-derived xenografts established from patient tumors at MDACC. Some of these cell lines were found to be from patients with *BRCA1* and *BRCA2* germline mutations with strong family histories of BRCA-related cancers. Treatment with radiation and assessment for induction of RAD51 foci showed deficiencies in homologous recombination pathways in *BRCA* mutants.

PARP inhibitors are a novel class of agents that block the single strand DNA repair base excision repair pathway. In hereditary pancreatic cancer patients with BRCA1 and BRCA2 mutations and homologous recombination double stranded DNA repair defects, this leads to genomic instability and cell death. PDX BRCA mutant models described above were tested for sensitivity and resistance to the second generation PARP inhibitor, Talazoparib.

However, not all response to Talazoparib was equal and resistance to treatment was seen in certain cell lines. Previously described mechanisms of resistance included reversion of the *BRCA* mutation to wild type, *TP53BP1* mutations that lead to restored genomic stability, and decreased SLFN11 expression. These mechanisms did not seem to be at play in this PDX model. XPO-1 is a nuclear exporter of proteins including *BRCA1*. We tested whether combination therapy with an XPO-1 (CRM1) inhibitor, Selinexor, would lead to increased BRCA1 levels inside the nucleus in *BRCA2* mutants leading to partial restoration of homologous recombination and therapeutic resistance to PARP inhibitors. Use of XPO-1, however, did not seem to impact response to Talazoparib.

Using a shRNA hairpin vector, I showed that in the Talazoparib-resistant *BRCA2* mutant cell line, PATC55, *BRCA2* and *RIF1* co-mutations did not appear to cause therapeutic resistance. When instead treating PATC55 with high concentrations of Talazoparib at an IC90 and collecting resistant cells for DNA and single cell RNA sequencing, I did demonstrate that high expression levels of SHFM1 (DSS1), however, may be associated with Talazoparib resistance.

In the future, I hope to validate my findings of high SHFM1 levels leading to resistance in hereditary pancreatic cancer by using a publicly available pancreatic cancer RNA sequencing database such as TCGA, ICGC GEO, or ArrayExpress to assess RNA expression levels in platinum or PARP-treated patients. I also plan to utilize the Genomics of Drug Sensitivity in Cancer database to look at SHFM1 levels in cell lines that show resistance to PARP inhibitors. With validation, SHFM1 levels may be used in a prospective manner to determine appropriate selection of PARP inhibitors in hereditary patients and anticipate response and resistance.

Appendix

Table A1: Patient characteristics with statistical comparison between sequenced and unsequenced cohorts among 233 patients.

Covariate	levels	Unsequenced	Sequenced	*P*-value
Sex	Male	58(58%)	78(58.6%)	0.92
	Female	42(42%)	55(41.4%)	.
Age at diagnosis	> 60	55(55%)	67(50.4%)	0.48
	≤ 60	45(45%)	66(49.6%)	.
ECOG	0,1	58(77.3%)	97(88.2%)	0.05
	≥ 2	17(22.7%)	13(11.8%)	.
First-line Treatment	F	58(58%)	95(71.4%)	0.03
	G	42(42%)	38(28.6%)	.
BRCA Group ≥ 3	N	96(96%)	127(95.5%)	0.85
	Y	4(4%)	6(4.5%)	.
Family history breast cancer	N	78(78%)	94(70.7%)	0.21
	Y	22(22%)	39(29.3%)	.
Family history ovarian cancer	N	97(97%)	127(95.5%)	0.55
	Y	3(3%)	6(4.5%)	.
Family history pancreatic cancer	N	87(87%)	114(85.7%)	0.78
	Y	13(13%)	19(14.3%)	.
Family history any cancer	N	19(19%)	26(19.5%)	0.92
	Y	81(81%)	107(80.5%)	.
Personal history of second cancer	N	90(90%)	124(93.2%)	0.37
	Y	10(10%)	9(6.8%)	.

Table A2: MDACC cohort list of variants of unknown significance.

Table S2. Variants of Unknown Significance Identified in Study Cohort			
Study ID	Gene	Variant	Variant Effect
FamilyHx25	ABL1	c.A797G	nonsynonymous SNV
FamilyHx26	ABL1	c.G185A	nonsynonymous SNV
FamilyHx3692	ABL1	c.C2486T	nonsynonymous SNV
FamilyHx38	ABL1	c.C2486T	nonsynonymous SNV
FamilyHx38	ABL2	c.A2350T	nonsynonymous SNV
FamilyHx74	ABL2	c.A2350T	nonsynonymous SNV
FamilyHx3728	ACVR1B	c.G1564A	nonsynonymous SNV
FamilyHx40	ACVR2A	c.C639A	nonsynonymous SNV
FamilyHx15	AJUBA	c.G1283A	nonsynonymous SNV
FamilyHx1	AKT2	c.G668A	nonsynonymous SNV
FamilyHx3688	ALK	c.C1437A	stop-gain
FamilyHx23	APC	c.A5213C	nonsynonymous SNV
FamilyHx37	APC	c.G1606A	nonsynonymous SNV
FamilyHx37	APC	c.A95G	nonsynonymous SNV
FamilyHx3748	APC	c.C7862G	nonsynonymous SNV
FamilyHx69	APC	c.A7471G	nonsynonymous SNV
FamilyHx3217	AR	c.1369_1371del	non-frameshift deletion
FamilyHx3837	AR	c.1369_1371del	non-frameshift deletion
FamilyHx70	AR	c.C1286A	nonsynonymous SNV
FamilyHx28	ARAF	c.G847A	nonsynonymous SNV
FamilyHx3881	ARAF	c.T1123A	nonsynonymous SNV
FamilyHx79	ARID1A	c.G4576A	nonsynonymous SNV
FamilyHx105	ARID1B	c.G2338A	nonsynonymous SNV
FamilyHx12	ARID1B	c.C4837G	nonsynonymous SNV
FamilyHx21	ARID2	c.C1718T	nonsynonymous SNV
FamilyHx3284	ARID2	c.G4705A	nonsynonymous SNV
FamilyHx98	ARID2	c.C1808T	nonsynonymous SNV
FamilyHx39	ASXL1	c.A734G	nonsynonymous SNV
FamilyHx76	ASXL1	c.G332A	nonsynonymous SNV
FamilyHx81	ATR	c.T2776C	nonsynonymous SNV
FamilyHx88	ATR	c.T5572C	nonsynonymous SNV
FamilyHx9	ATR	c.T4347A	nonsynonymous SNV
FamilyHx41	ATRX	c.A3641T	nonsynonymous SNV
FamilyHx51	AXIN1	c.G1063A	nonsynonymous SNV
FamilyHx54	AXIN1	c.C644T	nonsynonymous SNV
FamilyHx30	AXL	c.G1549A	nonsynonymous SNV
FamilyHx3736	BTK	c.G717T	nonsynonymous SNV

FamilyHx11	*CARD11*	c.C2060T	nonsynonymous SNV
FamilyHx3728	*CARD11*	c.G3025A	nonsynonymous SNV
FamilyHx50	*CARD11*	c.G3025A	nonsynonymous SNV
FamilyHx98	*CARD11*	c.G2735A	nonsynonymous SNV
FamilyHx3692	*CASP8*	c.A620G	nonsynonymous SNV
FamilyHx88	*CASP8*	c.A439G	nonsynonymous SNV
FamilyHx9	*CCNE1*	c.A779T	nonsynonymous SNV
FamilyHx3706	*CD79A*	c.C224T	nonsynonymous SNV
FamilyHx5	*CD79A*	c.T593C	nonsynonymous SNV
FamilyHx52	*CDC73*	c.G1333A	nonsynonymous SNV
FamilyHx10	*CDK12*	c.C2042T	nonsynonymous SNV
FamilyHx105	*CDK12*	c.C1513T	nonsynonymous SNV
FamilyHx66	*CDK12*	c.C3838A	nonsynonymous SNV
FamilyHx3921	*CDK6*	c.G328A	nonsynonymous SNV
FamilyHx55	*CDK6*	c.G328A	nonsynonymous SNV
FamilyHx25	*CHEK1*	c.G236A	stop-gain
FamilyHx3284	*CHEK1*	c.G163A	nonsynonymous SNV
FamilyHx15	*CIC*	c.C1979T	nonsynonymous SNV
FamilyHx3714	*CIC*	c.C1795T	nonsynonymous SNV
FamilyHx78	*CIC*	c.C3511T	nonsynonymous SNV
FamilyHx93	*CIC*	c.C2315T	nonsynonymous SNV
FamilyHx3437	*COL2A1*	c.A662C	nonsynonymous SNV
FamilyHx98	*COL2A1*	c.C4375T	nonsynonymous SNV
FamilyHx39	*CREBBP*	c.G6055A	nonsynonymous SNV
FamilyHx41	*CTCF*	c.C1318A	nonsynonymous SNV
FamilyHx10	*CTNNB1*	c.A860G	nonsynonymous SNV
FamilyHx81	*CTNNB1*	c.G583C	nonsynonymous SNV
FamilyHx103	*CYP2C19*	c.G1021C	nonsynonymous SNV
FamilyHx11	*CYP2C19*	c.C394T	nonsynonymous SNV
FamilyHx18	*DAXX*	c.G725T	nonsynonymous SNV
FamilyHx3921	*DDR2*	c.G784A	nonsynonymous SNV
FamilyHx53	*DDR2*	c.T476C	nonsynonymous SNV
FamilyHx3748	*DNMT3A*	c.A89C	nonsynonymous SNV
FamilyHx72	*EGFR*	c.G769A	nonsynonymous SNV
FamilyHx86	*EGFR*	c.C3405A	nonsynonymous SNV
FamilyHx3363	*ELF3*	c.G920A	nonsynonymous SNV
FamilyHx3605	*EP300*	c.6796_6798del	non-frameshift deletion
FamilyHx74	*EP300*	c.A5711C	nonsynonymous SNV
FamilyHx74	*EP300*	c.G7192A	nonsynonymous SNV
FamilyHx29	*EPHA2*	c.G1444A	nonsynonymous SNV
FamilyHx53	*EPHA2*	c.G2669A	nonsynonymous SNV

FamilyHx78	*EPHA2*	c.G2287A	nonsynonymous SNV
FamilyHx99	*EPHA3*	c.G621T	nonsynonymous SNV
FamilyHx3146	*EPHA5*	c.G988C	nonsynonymous SNV
FamilyHx3692	*ERBB2*	c.C3647A	nonsynonymous SNV
FamilyHx4	*ERBB2*	c.C3403T	nonsynonymous SNV
FamilyHx25	*ERBB3*	c.C3529A	nonsynonymous SNV
FamilyHx3413	*ERBB3*	c.G857A	nonsynonymous SNV
FamilyHx85	*ERBB3*	c.C1672T	nonsynonymous SNV
FamilyHx3660	*ERBB4*	c.T1122G	nonsynonymous SNV
FamilyHx3728	*ERBB4*	c.T1070C	nonsynonymous SNV
FamilyHx14	*ERCC2*	c.172dupC	frameshift insertion
FamilyHx90	*ERCC2*	c.G1847C	nonsynonymous SNV
FamilyHx3660	*ERCC3*	c.C275T	nonsynonymous SNV
FamilyHx3946	*ERCC3*	c.C2111T	nonsynonymous SNV
FamilyHx25	*ERCC4*	c.G1336T	nonsynonymous SNV
FamilyHx3146	*ERCC4*	c.T2749C	stop-loss
FamilyHx3736	*ERCC4*	c.A1728T	nonsynonymous SNV
FamilyHx51	*ERCC4*	c.T2117C	nonsynonymous SNV
FamilyHx99	*ERCC4*	c.T2117C	nonsynonymous SNV
FamilyHx106	*ERCC5*	c.A2101G	nonsynonymous SNV
FamilyHx3881	*ESR1*	c.A902G	nonsynonymous SNV
FamilyHx31	*FANCA*	c.G1874C	nonsynonymous SNV
FamilyHx41	*FANCA*	c.C577G	nonsynonymous SNV
FamilyHx59	*FANCA*	c.G3069T	nonsynonymous SNV
FamilyHx68	*FANCA*	c.G1460A	nonsynonymous SNV
FamilyHx77	*FANCA*	c.C4015T	nonsynonymous SNV
FamilyHx77	*FANCA*	c.C1266G	nonsynonymous SNV
FamilyHx77	*FANCA*	c.764_766del	non-frameshift deletion
FamilyHx99	*FANCA*	c.A3391G	nonsynonymous SNV
FamilyHx65	*FANCD2*	c.C2180T	nonsynonymous SNV
FamilyHx77	*FBXW7*	c.G176A	nonsynonymous SNV
FamilyHx91	*FBXW7*	c.T196A	nonsynonymous SNV
FamilyHx20	*FGFR1*	c.G853A	nonsynonymous SNV
FamilyHx42	*FGFR1*	c.C2557T	nonsynonymous SNV
FamilyHx3881	*FGFR2*	c.T1153C	nonsynonymous SNV
FamilyHx70	*FGFR2*	c.T1007C	nonsynonymous SNV
FamilyHx3837	*FGFR3*	c.T1156C	nonsynonymous SNV
FamilyHx68	*FGFR3*	c.C370T	nonsynonymous SNV
FamilyHx10	*FGFR4*	c.C2272T	nonsynonymous SNV
FamilyHx100	*FGFR4*	c.2394_2400del	frameshift deletion
FamilyHx43	*FGFR4*	c.C2272T	nonsynonymous SNV

FamilyHx52	*FGFR4*	c.T1384C	nonsynonymous SNV
FamilyHx71	*FGFR4*	c.C2167T	nonsynonymous SNV
FamilyHx74	*FGFR4*	c.G233A	nonsynonymous SNV
FamilyHx95	*FGFR4*	c.G982A	nonsynonymous SNV
FamilyHx101	*FH*	c.A358G	nonsynonymous SNV
FamilyHx3391	*FLT1*	c.A1867G	nonsynonymous SNV
FamilyHx3660	*FLT1*	c.A2945C	nonsynonymous SNV
FamilyHx61	*FLT1*	c.C3152T	nonsynonymous SNV
FamilyHx3736	*FLT3*	c.T2718A	nonsynonymous SNV
FamilyHx3706	*FLT4*	c.C2734G	nonsynonymous SNV
FamilyHx48	*FLT4*	c.C569T	nonsynonymous SNV
FamilyHx88	*FTO*	c.A428G	nonsynonymous SNV
FamilyHx14	*GABRA6*	c.G805A	nonsynonymous SNV
FamilyHx3284	*GABRA6*	c.G970A	nonsynonymous SNV
FamilyHx7	*GABRA6*	c.G805A	nonsynonymous SNV
FamilyHx75	*GABRA6*	c.A710G	nonsynonymous SNV
FamilyHx94	*GNAQ*	c.G718A	nonsynonymous SNV
FamilyHx51	*GNAS*	c.398_400del	non-frameshift deletion
FamilyHx77	*GNAS*	c.G196A	nonsynonymous SNV
FamilyHx95	*GNAS*	c.A484G	nonsynonymous SNV
FamilyHx23	*GSK3B*	c.T239C	nonsynonymous SNV
FamilyHx81	*GSK3B*	c.T239C	nonsynonymous SNV
FamilyHx3363	*HNF1A*	c.1490dupA	frameshift insertion
FamilyHx41	*HNF1A*	c.T1165G	nonsynonymous SNV
FamilyHx47	*HNF1A*	c.1490dupA	frameshift insertion
FamilyHx51	*HNF1A*	c.1490dupA	frameshift insertion
FamilyHx68	*HNF1A*	c.T1537C	nonsynonymous SNV
FamilyHx82	*HSP90AB1*	c.C1423T	nonsynonymous SNV
FamilyHx20	*IDH2*	c.G782A	nonsynonymous SNV
FamilyHx28	*IDH2*	c.C1304T	nonsynonymous SNV
FamilyHx100	*IGF1R*	c.G1162A	nonsynonymous SNV
FamilyHx101	*IGF1R*	c.A3173G	nonsynonymous SNV
FamilyHx28	*IGF1R*	c.C568T	nonsynonymous SNV
FamilyHx62	*IGF1R*	c.C568T	nonsynonymous SNV
FamilyHx98	*IGF1R*	c.A2240G	nonsynonymous SNV
FamilyHx25	*JAK1*	c.G247A	nonsynonymous SNV
FamilyHx18	*JAK2*	c.A3323G	nonsynonymous SNV
FamilyHx48	*JAK2*	c.G2600A	nonsynonymous SNV
FamilyHx99	*JAK2*	c.A3323G	nonsynonymous SNV
FamilyHx47	*JAK3*	c.G2152C	nonsynonymous SNV
FamilyHx67	*JAK3*	c.C2518T	nonsynonymous SNV

FamilyHx101	*KDM6A*	c.A1106G	nonsynonymous SNV
FamilyHx19	*KDM6A*	c.T866C	nonsynonymous SNV
FamilyHx47	*KDR*	c.G170C	nonsynonymous SNV
FamilyHx8	*KDR*	c.C2312T	nonsynonymous SNV
FamilyHx102	*KEAP1*	c.T1106C	nonsynonymous SNV
FamilyHx30	*KEAP1*	c.1858_1860del	non-frameshift deletion
FamilyHx32	*KEAP1*	c.C598T	nonsynonymous SNV
FamilyHx87	*KEAP1*	c.G1061A	nonsynonymous SNV
FamilyHx3363	*MAP2K2*	c.A1090G	nonsynonymous SNV
FamilyHx59	*MAP3K1*	c.A2441G	nonsynonymous SNV
FamilyHx94	*MAP3K13*	c.C1534A	nonsynonymous SNV
FamilyHx105	*MAP3K4*	c.3597_3599del	non-frameshift deletion
FamilyHx23	*MAP3K4*	c.C2942T	nonsynonymous SNV
FamilyHx55	*MAP3K4*	c.3597_3599del	non-frameshift deletion
FamilyHx93	*MAP3K4*	c.G1752T	nonsynonymous SNV
FamilyHx3363	*MCL1*	c.G121A	nonsynonymous SNV
FamilyHx21	*MED12*	c.C1312T	nonsynonymous SNV
FamilyHx86	*MEN1*	c.A680C	nonsynonymous SNV
FamilyHx18	*MET*	c.G561T	nonsynonymous SNV
FamilyHx3660	*MET*	c.G561T	nonsynonymous SNV
FamilyHx96	*MET*	c.G561T	nonsynonymous SNV
FamilyHx3946	*MPL*	c.C1621T	stop-gain
FamilyHx7	*MST1*	c.C1676A	nonsynonymous SNV
FamilyHx1	*MST1R*	c.C2947T	nonsynonymous SNV
FamilyHx23	*MST1R*	c.345delC	frameshift deletion
FamilyHx67	*MST1R*	c.T962C	nonsynonymous SNV
FamilyHx79	*MST1R*	c.C2476T	nonsynonymous SNV
FamilyHx12	*MTOR*	c.5445_5447del	non-frameshift deletion
FamilyHx82	*MTOR*	c.A4234G	nonsynonymous SNV
FamilyHx3217	*NCOR1*	c.G3408C	nonsynonymous SNV
FamilyHx33	*NCOR1*	c.T2792G	nonsynonymous SNV
FamilyHx34	*NCOR1*	c.G6544A	nonsynonymous SNV
FamilyHx3692	*NCOR1*	c.G6544A	nonsynonymous SNV
FamilyHx87	*NCOR1*	c.T2C	nonsynonymous SNV
FamilyHx90	*NCOR1*	c.T2792G	nonsynonymous SNV
FamilyHx106	*NF1*	c.A7087G	nonsynonymous SNV
FamilyHx3460	*NF2*	c.G713A	nonsynonymous SNV
FamilyHx27	*NOTCH1*	c.C5090T	nonsynonymous SNV
FamilyHx30	*NOTCH1*	c.G4795A	nonsynonymous SNV
FamilyHx34	*NOTCH1*	c.G5215A	nonsynonymous SNV
FamilyHx39	*NOTCH1*	c.G4049A	nonsynonymous SNV

FamilyHx41	*NOTCH1*	c.A1262G	nonsynonymous SNV
FamilyHx51	*NOTCH1*	c.G2900T	nonsynonymous SNV
FamilyHx51	*NOTCH1*	c.2901delG	frameshift deletion
FamilyHx70	*NOTCH1*	c.T5573C	nonsynonymous SNV
FamilyHx12	*NOTCH2*	c.C5491G	nonsynonymous SNV
FamilyHx61	*NOTCH2*	c.C2063T	nonsynonymous SNV
FamilyHx70	*NOTCH2*	c.G2830T	nonsynonymous SNV
FamilyHx76	*NOTCH3*	c.G1690A	nonsynonymous SNV
FamilyHx3728	*NOTCH4*	c.T190A	nonsynonymous SNV
FamilyHx12	*NSD1*	c.C362T	nonsynonymous SNV
FamilyHx3146	*NSD1*	c.A7764T	nonsynonymous SNV
FamilyHx2	*NTRK1*	c.C1808G	nonsynonymous SNV
FamilyHx33	*NTRK1*	c.G482A	nonsynonymous SNV
FamilyHx98	*NTRK3*	c.G1520A	nonsynonymous SNV
FamilyHx79	*PAX5*	c.C740T	nonsynonymous SNV
FamilyHx98	*PDGFRB*	c.A475G	nonsynonymous SNV
FamilyHx33	*PIK3CG*	c.G1427A	nonsynonymous SNV
FamilyHx41	*PIK3CG*	c.C1429T	nonsynonymous SNV
FamilyHx23	*PLCG1*	c.C828A	nonsynonymous SNV
FamilyHx102	*PPP2R1A*	c.C379T	nonsynonymous SNV
FamilyHx41	*PRDM1*	c.G1427A	nonsynonymous SNV
FamilyHx72	*PRDM1*	c.C1948A	nonsynonymous SNV
FamilyHx19	*PREX2*	c.A2597T	nonsynonymous SNV
FamilyHx33	*PREX2*	c.C2887T	nonsynonymous SNV
FamilyHx41	*PREX2*	c.G350A	nonsynonymous SNV
FamilyHx82	*PREX2*	c.A3056T	nonsynonymous SNV
FamilyHx95	*PREX2*	c.1002_1004del	non-frameshift deletion
FamilyHx41	*PRG4*	c.G3108C	nonsynonymous SNV
FamilyHx66	*PRG4*	c.G3569A	nonsynonymous SNV
FamilyHx3284	*PTK2*	c.G1343A	nonsynonymous SNV
FamilyHx3628	*PTK2*	c.G1879A	nonsynonymous SNV
FamilyHx91	*PTK2*	c.G1616C	nonsynonymous SNV
FamilyHx33	*PTPRB*	c.C5069T	nonsynonymous SNV
FamilyHx5	*PTPRB*	c.G2552A	nonsynonymous SNV
FamilyHx94	*PTPRB*	c.G2552A	nonsynonymous SNV
FamilyHx43	*RAD51C*	c.G335A	nonsynonymous SNV
FamilyHx3217	*RICTOR*	c.A4433G	nonsynonymous SNV
FamilyHx3837	*RICTOR*	c.C3835G	nonsynonymous SNV
FamilyHx53	*RICTOR*	c.C2719T	nonsynonymous SNV
FamilyHx54	*RICTOR*	c.A1420G	nonsynonymous SNV
FamilyHx65	*RICTOR*	c.A3085G	nonsynonymous SNV

FamilyHx75	*RICTOR*	c.G2618A	nonsynonymous SNV
FamilyHx3946	*RNF43*	c.C667T	nonsynonymous SNV
FamilyHx34	*ROS1*	c.T1708A	nonsynonymous SNV
FamilyHx3736	*ROS1*	c.C1958T	nonsynonymous SNV
FamilyHx42	*RPTOR*	c.G1960A	nonsynonymous SNV
FamilyHx43	*RPTOR*	c.G3451A	nonsynonymous SNV
FamilyHx55	*RPTOR*	c.C283G	nonsynonymous SNV
FamilyHx6	*RPTOR*	c.G2584A	nonsynonymous SNV
FamilyHx3	*RUNX1*	c.T155A	nonsynonymous SNV
FamilyHx16	*RUNX1T1*	c.T884C	nonsynonymous SNV
FamilyHx26	*RUNX1T1*	c.G121T	nonsynonymous SNV
FamilyHx104	*SETBP1*	c.G1198A	nonsynonymous SNV
FamilyHx3663	*SETBP1*	c.G3962A	nonsynonymous SNV
FamilyHx8	*SETD2*	c.G3307C	nonsynonymous SNV
FamilyHx9	*SETD2*	c.C19T	stop-gain
FamilyHx93	*SETD2*	c.G1415A	nonsynonymous SNV
FamilyHx53	*SMC3*	c.G3259A	nonsynonymous SNV
FamilyHx62	*SMO*	c.G808A	nonsynonymous SNV
FamilyHx67	*SMO*	c.G808A	nonsynonymous SNV
FamilyHx74	*SMO*	c.G808A	nonsynonymous SNV
FamilyHx81	*SMO*	c.C1921G	nonsynonymous SNV
FamilyHx39	*SOCS1*	c.G630C	nonsynonymous SNV
FamilyHx94	*SOS1*	c.C3697G	nonsynonymous SNV
FamilyHx69	*SOX9*	c.G817A	nonsynonymous SNV
FamilyHx104	*SPEN*	c.C166T	nonsynonymous SNV
FamilyHx3546	*SPEN*	c.G8110A	nonsynonymous SNV
FamilyHx3692	*SPEN*	c.C1299A	nonsynonymous SNV
FamilyHx3946	*SPEN*	c.C879G	nonsynonymous SNV
FamilyHx71	*SPEN*	c.C166T	nonsynonymous SNV
FamilyHx72	*SPEN*	c.C166T	nonsynonymous SNV
FamilyHx21	*SPOP*	c.C779T	nonsynonymous SNV
FamilyHx77	*SRC*	c.C875A	nonsynonymous SNV
FamilyHx29	*SUFU*	c.C434G	nonsynonymous SNV
FamilyHx3628	*SUFU*	c.G1028A	nonsynonymous SNV
FamilyHx58	*SUFU*	c.C925T	nonsynonymous SNV
FamilyHx75	*SYK*	c.G98A	nonsynonymous SNV
FamilyHx20	*TBC1D4*	c.G215A	nonsynonymous SNV
FamilyHx23	*TBC1D4*	c.C1901T	nonsynonymous SNV
FamilyHx3198	*TBC1D4*	c.C32T	nonsynonymous SNV
FamilyHx102	*TERT*	c.C292T	nonsynonymous SNV
FamilyHx48	*TERT*	c.C1336A	nonsynonymous SNV

FamilyHx23	*TET2*	c.A5009C	nonsynonymous SNV
FamilyHx35	*TET2*	c.T2662C	nonsynonymous SNV
FamilyHx63	*TET2*	c.T2662C	nonsynonymous SNV
FamilyHx69	*TET2*	c.A3314C	nonsynonymous SNV
FamilyHx99	*TNFAIP3*	c.G2090A	nonsynonymous SNV
FamilyHx65	*TOP1*	c.C241T	nonsynonymous SNV
FamilyHx74	*TOP1*	c.C241T	nonsynonymous SNV
FamilyHx69	*TSC1*	c.A1430C	nonsynonymous SNV
FamilyHx106	*TSC2*	c.C1342G	nonsynonymous SNV
FamilyHx23	*TSC2*	c.A149G	nonsynonymous SNV
FamilyHx33	*TSC2*	c.C368T	nonsynonymous SNV
FamilyHx3663	*TSC2*	c.C368T	nonsynonymous SNV
FamilyHx62	*WHSC1L1*	c.C779A	nonsynonymous SNV
FamilyHx9	*ZRSR2*	c.C620T	nonsynonymous SNV

Table A3: Univariate Cox proportional hazards model for overall survival among 133

patients (n deaths = 130).

Covariate	Hazard Ratio	95% CI		P value	N_death	N_total
Male vs. Female	1.13	0.79	1.61	0.50	131	133
Age at diagnosis ≤ 60 (vs. > 60)	0.96	0.68	1.35	0.81	131	133
Age at diagnosis ≤ 45 (vs. > 45)	0.57	0.30	1.07	0.08	131	133
ECOG ≥ 2 (vs. 0, 1)	2.62	1.43	4.82	0.002	109	110
First-line Treatment = Gem/nab-Paclitaxel (vs. FOLFIRINOX)	1.10	0.75	1.61	0.62	131	133
BRCA Group ≥3 (vs. < 3)	0.44	0.19	1.01	0.05	131	133
Family history breast cancer = Yes (vs. No)	0.79	0.54	1.15	0.22	131	133
Family history ovarian cancer = Yes (vs. No)	1.00	0.44	2.27	0.99	131	133
Family history pancreatic cancer = Yes (vs. No)	0.54	0.32	0.91	0.02	131	133

	HR	95% CI		P-value	N deaths	N total
Family history any cancer= Yes (vs. No)	0.60	0.39	0.94	0.02	131	133
Recurrent VUS=Yes (vs. No)	1.38	0.97	1.98	0.07	131	133
Personal History cancer =Yes (vs. No)	1.74	0.88	3.46	0.11	131	133
Ashkenazi Jewish heritage = Yes (vs. No)	0.79	0.35	1.80	0.58	127	129
Deleterious mutation = Yes (vs. No)	0.73	0.47	1.14	0.16	131	133
DDR mutation = Yes (vs. No)	0.44	0.22	0.91	0.03	131	133

Table A4: Univariate Cox proportional hazards model for overall survival among all 233 patients (n deaths=211).

Covariate	HR	95% CI		P-value	N deaths	N total
Male vs. Female	1.06	0.81	1.39	0.68	220	233
Age at diagnosis ≤ 60 (vs. > 60)	0.98	0.76	1.28	0.91	220	233
Age at diagnosis ≤ 45 (vs. > 45)	0.63	0.36	1.09	0.10	220	233
ECOG ≥ 2 (vs. 0, 1)*	1.99	1.33	2.98	0.001	177	185
First-line Treatment = Gem/nab-Paclitaxel (vs. FOLFIRINOX)	1.14	0.86	1.51	0.37	220	233
BRCA Group ≥3 (vs. < 3)	0.61	0.32	1.16	0.13	220	233
Family history breast cancer = Yes (vs. No)	1.00	0.74	1.35	0.98	220	233
Family history ovarian cancer = Yes (vs. No)	1.00	0.51	1.96	0.99	220	233
Family history pancreatic cancer = Yes (vs. No)	0.73	0.49	1.07	0.11	220	233

Family history any cancer= Yes (vs. No)	0.84	0.60	1.18	0.31	220	233
Recurrent VUS=Yes (vs. No)	1.38	0.97	1.98	0.07	131	133
Personal History cancer=Yes (vs. No)	1.45	0.89	2.35	0.14	220	233
Ashkenazi Jewish heritage = Yes (vs. No)	0.86	0.38	1.95	0.72	216	229
Deleterious mutation = Yes (vs. No)	0.83	0.54	1.27	0.39	220	233
DDR mutation = Yes (vs. No)	0.51	0.25	1.04	0.06	220	233

Table A5: Chemotherapy response rate by mutation status of sequenced cohort among

133 patients.

Chemotherapy and Mutation Status	No. of Patients	Percent (%)
FOLFIRINOX (n = 95)		
No Mutation	73	
Partial Response	22	30.1
Stable Disease	25	34.3
Progressive Disease	20	27.4
Not Evaluable	6	8.2
DDR Mutation Positive	14	
Partial Response*	5	35.7
Stable Disease	5	35.7
Progressive Disease	3	21.5
Not Evaluable	1	7.1
DDR Mutation Negative	8	
Partial Response	1	12.5
Stable Disease	2	25
Progressive Disease	4	50
Not Evaluable	1	12.5
Gemcitabine/nab-paclitaxel (n = 38)		
No Mutation	34	
Partial Response	9	26.5
Stable Disease	16	47

Progressive Disease	5	14.7
Not Evaluable	4	11.8
DDR Mutation Positive	1	
Stable Disease	1	100
DDR Mutation Negative	3	
Progressive Disease*	1	33.3
Not Evaluable	2	66.7

Table A6: Univariate logistic regression models for deleterious mutation among 133

sequenced subjects (n = 26 with deleterious mutation).

Variable	Odds ratio	95% CI	*P*-value
Male vs. Female	1.05	0.44 – 2.50	0.91
Age at diagnosis ≤ 60 (vs. > 60)	1.82	0.76 – 4.38	0.18
Age at diagnosis ≤ 45 (vs. > 45)	2.94	0.88 – 9.91	0.08
ECOG ≥ 2 (vs. 0, 1)	0.32	0.04 – 2.62	0.29
First-line Treatment = Gem/nab-Paclitaxel (vs. FOLFIRINOX)	0.39	0.13 – 1.22	0.11
BRCA Group ≥3 (vs. < 3)	4.53	0.86 – 23.85	0.08
Family history breast cancer = Yes (vs. No)	1.68	0.69 – 4.13	0.26
Family history ovarian cancer = Yes (vs. No)	0.82	0.09 – 7.30	0.86
Family history pancreatic cancer = Yes (vs. No)	2.16	0.74 – 6.39	0.16
Family history any cancer= Yes (vs. No)	1.03	0.35 – 3.04	0.96
Recurrent VUS=Yes (vs. No)	0.21	0.07 – 0.67	0.008
Personal History cancer =Yes (vs. No)	0.50	0.06 – 4.14	0.52

Variable	Odds ratio	95% CI	*P*-value
Ashkenazi Jewish heritage = Yes (vs. No)	3.22	0.68 – 15.43	0.14

Table A7: Multivariable logistic regression model for deleterious mutation among 133 sequenced subjects (n = 26 with deleterious mutation).

Variable	Odds ratio	95% CI	*P*-value
Recurrent VUS = Yes (vs. No)	0.20	0.06 – 0.62	0.005

Bibliography

1   Rezano, A., Kuwahara, K., Yamamoto-Ibusuki, M., Kitabatake, M., Moolthiya,
         P., Phimsen, S., Suda, T., Tone, S., Yamamoto, Y., Iwase, H. & Sakaguchi, N.
         Breast cancers with high DSS1 expression that potentially maintains BRCA2
         stability have poor prognosis in the relapse-free survival. *BMC Cancer* **13**,
         562, doi:10.1186/1471-2407-13-562 (2013).

2   Ma, Y. Y., Lin, H., Chang, F. M., Chang, T. C., Trieu, T., Pridgen, H. I., Zhang, Y.,
         Huang, J., Patino-Guzman, K., Diab, N., Cantu, A., Slaga, T. J. & Wei, S. J.
         Identification of the deleted in split hand/split foot 1 protein as a novel
         biomarker for human cervical cancer. *Carcinogenesis* **34**, 68-78,
         doi:10.1093/carcin/bgs279 (2013).

3   Siegel, R. L., Miller, K. D. & Jemal, A. Cancer statistics, 2019. *CA Cancer J Clin*
         69, 7-34, doi:10.3322/caac.21551 (2019).

4   Howlader N, N. A., Krapcho M, Miller D, Brest A, Yu M, Ruhl J, Tatalovich Z,
         Mariotto A, Lewis DR, Chen HS, Feuer EJ, Cronin KA (eds). SEER Cancer
         Statistics Review, 1975-2016, National Cancer Institute. Bethesda, MD,
         https://seer.cancer.gov/csr/1975_2016/, based on November 2018 SEER
         data submission, posted to the SEER web site, April 2019.

5   Rahib, L., Smith, B. D., Aizenberg, R., Rosenzweig, A. B., Fleshman, J. M. &
         Matrisian, L. M. Projecting cancer incidence and deaths to 2030: the
         unexpected burden of thyroid, liver, and pancreas cancers in the United
         States. *Cancer Res* **74**, 2913-2921, doi:10.1158/0008-5472.CAN-14-0155
         (2014).

6   Hassan, M. M., Bondy, M. L., Wolff, R. A., Abbruzzese, J. L., Vauthey, J. N., Pisters, P. W., Evans, D. B., Khan, R., Chou, T. H., Lenzi, R., Jiao, L. & Li, D. Risk factors for pancreatic cancer: case-control study. *Am J Gastroenterol* **102**, 2696-2707, doi:10.1111/j.1572-0241.2007.01510.x (2007).

7   June 30, 2019., N. C. I. P. D. Q. P. P. C. T.-f. H. P. A. a. h. w. c. g. t. p. h. p.-t.-p. o.

8   Walter, F. M., Mills, K., Mendonca, S. C., Abel, G. A., Basu, B., Carroll, N., Ballard, S., Lancaster, J., Hamilton, W., Rubin, G. P. & Emery, J. D. Symptoms and patient factors associated with diagnostic intervals for pancreatic cancer (SYMPTOM pancreatic study): a prospective cohort study. *Lancet Gastroenterol Hepatol* **1**, 298-306, doi:10.1016/S2468-1253(16)30079-6 (2016).

9   Miura, F., Takada, T., Amano, H., Yoshida, M., Furui, S. & Takeshita, K. Diagnosis of pancreatic cancer. *HPB (Oxford)* **8**, 337-342, doi:10.1080/13651820500540949 (2006).

10   Lall, C. G., Howard, T. J., Skandarajah, A., DeWitt, J. M., Aisen, A. M. & Sandrasegaran, K. New concepts in staging and treatment of locally advanced pancreatic head cancer. *AJR Am J Roentgenol* **189**, 1044-1050, doi:10.2214/AJR.07.2131 (2007).

11   Ryan, D. P., Hong, T. S. & Bardeesy, N. Pancreatic adenocarcinoma. *N Engl J Med* **371**, 1039-1049, doi:10.1056/NEJMra1404198 (2014).

12   Lopez, N. E., Prendergast, C. & Lowy, A. M. Borderline resectable pancreatic cancer: definitions and management. *World J Gastroenterol* **20**, 10740-10751, doi:10.3748/wjg.v20.i31.10740 (2014).

13   Neoptolemos, J. P., Palmer, D. H., Ghaneh, P., Psarelli, E. E., Valle, J. W.,
        Halloran, C. M., Faluyi, O., O'Reilly, D. A., Cunningham, D., Wadsley, J., Darby,
        S., Meyer, T., Gillmore, R., Anthoney, A., Lind, P., Glimelius, B., Falk, S., Izbicki,
        J. R., Middleton, G. W., Cummins, S., Ross, P. J., Wasan, H., McDonald, A.,
        Crosby, T., Ma, Y. T., Patel, K., Sherriff, D., Soomal, R., Borg, D., Sothi, S.,
        Hammel, P., Hackert, T., Jackson, R., Buchler, M. W. & European Study Group
        for Pancreatic, C. Comparison of adjuvant gemcitabine and capecitabine with
        gemcitabine monotherapy in patients with resected pancreatic cancer
        (ESPAC-4): a multicentre, open-label, randomised, phase 3 trial. *Lancet* **389**,
        1011-1024, doi:10.1016/S0140-6736(16)32409-6 (2017).

14   Maitra, A., Fukushima, N., Takaori, K. & Hruban, R. H. Precursors to invasive
        pancreatic cancer. *Adv Anat Pathol* **12**, 81-91 (2005).

15   Maitra, A. & Hruban, R. H. Pancreatic cancer. *Annu Rev Pathol* **3**, 157-188,
        doi:10.1146/annurev.pathmechdis.3.121806.154305 (2008).

16   Bailey, P., Chang, D. K., Nones, K., Johns, A. L., Patch, A. M., Gingras, M. C.,
        Miller, D. K., Christ, A. N., Bruxner, T. J., Quinn, M. C., Nourse, C., Murtaugh, L.
        C., Harliwong, I., Idrisoglu, S., Manning, S., Nourbakhsh, E., Wani, S., Fink, L.,
        Holmes, O., Chin, V., Anderson, M. J., Kazakoff, S., Leonard, C., Newell, F.,
        Waddell, N., Wood, S., Xu, Q., Wilson, P. J., Cloonan, N., Kassahn, K. S., Taylor,
        D., Quek, K., Robertson, A., Pantano, L., Mincarelli, L., Sanchez, L. N., Evers, L.,
        Wu, J., Pinese, M., Cowley, M. J., Jones, M. D., Colvin, E. K., Nagrial, A. M.,
        Humphrey, E. S., Chantrill, L. A., Mawson, A., Humphris, J., Chou, A., Pajic, M.,
        Scarlett, C. J., Pinho, A. V., Giry-Laterriere, M., Rooman, I., Samra, J. S., Kench, J.

G., Lovell, J. A., Merrett, N. D., Toon, C. W., Epari, K., Nguyen, N. Q., Barbour, A., Zeps, N., Moran-Jones, K., Jamieson, N. B., Graham, J. S., Duthie, F., Oien, K., Hair, J., Grutzmann, R., Maitra, A., Iacobuzio-Donahue, C. A., Wolfgang, C. L., Morgan, R. A., Lawlor, R. T., Corbo, V., Bassi, C., Rusev, B., Capelli, P., Salvia, R., Tortora, G., Mukhopadhyay, D., Petersen, G. M., Australian Pancreatic Cancer Genome, I., Munzy, D. M., Fisher, W. E., Karim, S. A., Eshleman, J. R., Hruban, R. H., Pilarsky, C., Morton, J. P., Sansom, O. J., Scarpa, A., Musgrove, E. A., Bailey, U. M., Hofmann, O., Sutherland, R. L., Wheeler, D. A., Gill, A. J., Gibbs, R. A., Pearson, J. V., Waddell, N., Biankin, A. V. & Grimmond, S. M. Genomic analyses identify molecular subtypes of pancreatic cancer. *Nature* **531**, 47-52, doi:10.1038/nature16965 (2016).

17   Waddell, N., Pajic, M., Patch, A. M., Chang, D. K., Kassahn, K. S., Bailey, P., Johns, A. L., Miller, D., Nones, K., Quek, K., Quinn, M. C., Robertson, A. J., Fadlullah, M. Z., Bruxner, T. J., Christ, A. N., Harliwong, I., Idrisoglu, S., Manning, S., Nourse, C., Nourbakhsh, E., Wani, S., Wilson, P. J., Markham, E., Cloonan, N., Anderson, M. J., Fink, J. L., Holmes, O., Kazakoff, S. H., Leonard, C., Newell, F., Poudel, B., Song, S., Taylor, D., Waddell, N., Wood, S., Xu, Q., Wu, J., Pinese, M., Cowley, M. J., Lee, H. C., Jones, M. D., Nagrial, A. M., Humphris, J., Chantrill, L. A., Chin, V., Steinmann, A. M., Mawson, A., Humphrey, E. S., Colvin, E. K., Chou, A., Scarlett, C. J., Pinho, A. V., Giry-Laterriere, M., Rooman, I., Samra, J. S., Kench, J. G., Pettitt, J. A., Merrett, N. D., Toon, C., Epari, K., Nguyen, N. Q., Barbour, A., Zeps, N., Jamieson, N. B., Graham, J. S., Niclou, S. P., Bjerkvig, R., Grutzmann, R., Aust, D., Hruban, R. H., Maitra, A., Iacobuzio-Donahue, C. A., Wolfgang, C. L., Morgan,

R. A., Lawlor, R. T., Corbo, V., Bassi, C., Falconi, M., Zamboni, G., Tortora, G., Tempero, M. A., Australian Pancreatic Cancer Genome, I., Gill, A. J., Eshleman, J. R., Pilarsky, C., Scarpa, A., Musgrove, E. A., Pearson, J. V., Biankin, A. V. & Grimmond, S. M. Whole genomes redefine the mutational landscape of pancreatic cancer. *Nature* **518**, 495-501, doi:10.1038/nature14169 (2015).

18   Yi, K. & Ju, Y. S. Patterns and mechanisms of structural variations in human cancer. *Exp Mol Med* **50**, 98, doi:10.1038/s12276-018-0112-3 (2018).

19   Futreal, P. A., Liu, Q., Shattuck-Eidens, D., Cochran, C., Harshman, K., Tavtigian, S., Bennett, L. M., Haugen-Strano, A., Swensen, J., Miki, Y. & et al. BRCA1 mutations in primary breast and ovarian carcinomas. *Science* **266**, 120-122, doi:10.1126/science.7939630 (1994).

20   Wooster, R., Bignell, G., Lancaster, J., Swift, S., Seal, S., Mangion, J., Collins, N., Gregory, S., Gumbs, C. & Micklem, G. Identification of the breast cancer susceptibility gene BRCA2. *Nature* **378**, 789-792, doi:10.1038/378789a0 (1995).

21   Lal, G., Liu, G., Schmocker, B., Kaurah, P., Ozcelik, H., Narod, S. A., Redston, M. & Gallinger, S. Inherited predisposition to pancreatic adenocarcinoma: role of family history and germ-line p16, BRCA1, and BRCA2 mutations. *Cancer Res* **60**, 409-416 (2000).

22   Easton, D. F., Matthews, F. E., Ford, D., Swerdlow, A. J. & Peto, J. Cancer mortality in relatives of women with ovarian cancer: the OPCS Study. Office of Population Censuses and Surveys. *Int J Cancer* **65**, 284-294,

doi:10.1002/(SICI)1097-0215(19960126)65:3<284::AID-IJC2>3.0.CO;2-W (1996).

23   Friedenson, B. BRCA1 and BRCA2 pathways and the risk of cancers other than breast or ovarian. *MedGenMed* **7**, 60 (2005).

24   Amundadottir, L. T., Thorvaldsson, S., Gudbjartsson, D. F., Sulem, P., Kristjansson, K., Arnason, S., Gulcher, J. R., Bjornsson, J., Kong, A., Thorsteinsdottir, U. & Stefansson, K. Cancer as a complex phenotype: pattern of cancer distribution within and beyond the nuclear family. *PLoS Med* **1**, e65, doi:10.1371/journal.pmed.0010065 (2004).

25   Iqbal, J., Ragone, A., Lubinski, J., Lynch, H. T., Moller, P., Ghadirian, P., Foulkes, W. D., Armel, S., Eisen, A., Neuhausen, S. L., Senter, L., Singer, C. F., Ainsworth, P., Kim-Sing, C., Tung, N., Friedman, E., Llacuachaqui, M., Ping, S., Narod, S. A. & Hereditary Breast Cancer Study, G. The incidence of pancreatic cancer in BRCA1 and BRCA2 mutation carriers. *Br J Cancer* **107**, 2005-2009, doi:10.1038/bjc.2012.483 (2012).

26   Oddoux, C., Struewing, J. P., Clayton, C. M., Neuhausen, S., Brody, L. C., Kaback, M., Haas, B., Norton, L., Borgen, P., Jhanwar, S., Goldgar, D., Ostrer, H. & Offit, K. The carrier frequency of the BRCA2 6174delT mutation among Ashkenazi Jewish individuals is approximately 1%. *Nat Genet* **14**, 188-190, doi:10.1038/ng1096-188 (1996).

27   Roa, B. B., Boyd, A. A., Volcik, K. & Richards, C. S. Ashkenazi Jewish population frequencies for common mutations in BRCA1 and BRCA2. *Nat Genet* **14**, 185-187, doi:10.1038/ng1096-185 (1996).

28   Murphy, K. M., Brune, K. A., Griffin, C., Sollenberger, J. E., Petersen, G. M.,
        Bansal, R., Hruban, R. H. & Kern, S. E. Evaluation of candidate genes MAP2K4,
        MADH4, ACVR1B, and BRCA2 in familial pancreatic cancer: deleterious
        BRCA2 mutations in 17%. *Cancer Res* **62**, 3789-3793 (2002).

29   Hahn, S. A., Greenhalf, B., Ellis, I., Sina-Frey, M., Rieder, H., Korte, B., Gerdes, B.,
        Kress, R., Ziegler, A., Raeburn, J. A., Campra, D., Grutzmann, R., Rehder, H.,
        Rothmund, M., Schmiegel, W., Neoptolemos, J. P. & Bartsch, D. K. BRCA2
        germline mutations in familial pancreatic carcinoma. *J Natl Cancer Inst* **95**,
        214-221, doi:10.1093/jnci/95.3.214 (2003).

30   Couch, F. J., Johnson, M. R., Rabe, K. G., Brune, K., de Andrade, M., Goggins, M.,
        Rothenmund, H., Gallinger, S., Klein, A., Petersen, G. M. & Hruban, R. H. The
        prevalence of BRCA2 mutations in familial pancreatic cancer. *Cancer
        Epidemiol Biomarkers Prev* **16**, 342-346, doi:10.1158/1055-9965.EPI-06-
        0783 (2007).

31   Solomon, S., Das, S., Brand, R. & Whitcomb, D. C. Inherited pancreatic cancer
        syndromes. *Cancer J* **18**, 485-491, doi:10.1097/PPO.0b013e318278c4a6
        (2012).

32   Fogelman, D., Sugar, E. A., Oliver, G., Shah, N., Klein, A., Alewine, C., Wang, H.,
        Javle, M., Shroff, R., Wolff, R. A., Abbruzzese, J. L., Laheru, D. & Diaz, L. A., Jr.
        Family history as a marker of platinum sensitivity in pancreatic
        adenocarcinoma. *Cancer Chemother Pharmacol* **76**, 489-498,
        doi:10.1007/s00280-015-2788-6 (2015).

33   Goggins, M., Schutte, M., Lu, J., Moskaluk, C. A., Weinstein, C. L., Petersen, G. M., Yeo, C. J., Jackson, C. E., Lynch, H. T., Hruban, R. H. & Kern, S. E. Germline BRCA2 gene mutations in patients with apparently sporadic pancreatic carcinomas. *Cancer Res* **56**, 5360-5364 (1996).

34   Shindo, K., Yu, J., Suenaga, M., Fesharakizadeh, S., Cho, C., Macgregor-Das, A., Siddiqui, A., Witmer, P. D., Tamura, K., Song, T. J., Navarro Almario, J. A., Brant, A., Borges, M., Ford, M., Barkley, T., He, J., Weiss, M. J., Wolfgang, C. L., Roberts, N. J., Hruban, R. H., Klein, A. P. & Goggins, M. Deleterious Germline Mutations in Patients With Apparently Sporadic Pancreatic Adenocarcinoma. *J Clin Oncol* **35**, 3382-3390, doi:10.1200/JCO.2017.72.3502 (2017).

35   Bannon, S. A., Montiel, M. F., Goldstein, J. B., Dong, W., Mork, M. E., Borras, E., Hasanov, M., Varadhachary, G. R., Maitra, A., Katz, M. H., Feng, L., Futreal, A., Fogelman, D. R., Vilar, E. & McAllister, F. High Prevalence of Hereditary Cancer Syndromes and Outcomes in Adults with Early-Onset Pancreatic Cancer. *Cancer Prev Res (Phila)* **11**, 679-686, doi:10.1158/1940-6207.CAPR-18-0014 (2018).

36   National Comprehensive Cancer Network. Pancreatic Adenocarcinoma (Version 2.2019). https://www.nccn.org/professionals/physician_gls/pdf/pancreatic.pdf Accessed June 19.

37   Goldstein, J. B., Zhao, L., Wang, X., Ghelman, Y., Overman M.J., Javle, M. M, Shroff, R.T., Varadhachary, G.R., Wolff, R.A., McAllister, F., Futreal, P.A., Fogelman, D.R. (in press). Germline DNA Sequencing Reveals Novel

Mutations Predictive of Overall Survival in a Cohort of Pancreatic Cancer Patients. Clinical Cancer Research.

38   Ame, J. C., Spenlehauer, C. & de Murcia, G. The PARP superfamily. *Bioessays* **26**, 882-893, doi:10.1002/bies.20085 (2004).

39   D'Amours, D., Desnoyers, S., D'Silva, I. & Poirier, G. G. Poly(ADP-ribosyl)ation reactions in the regulation of nuclear functions. *Biochem J* **342 (Pt 2)**, 249-268 (1999).

40   Heale, J. T., Ball, A. R., Jr., Schmiesing, J. A., Kim, J. S., Kong, X., Zhou, S., Hudson, D. F., Earnshaw, W. C. & Yokomori, K. Condensin I interacts with the PARP-1-XRCC1 complex and functions in DNA single-strand break repair. *Mol Cell* **21**, 837-848, doi:10.1016/j.molcel.2006.01.036 (2006).

41   Plummer, R. Poly(ADP-ribose) polymerase inhibition: a new direction for BRCA and triple-negative breast cancer? *Breast Cancer Res* **13**, 218, doi:10.1186/bcr2877 (2011).

42   Satoh, M. S. & Lindahl, T. Role of poly(ADP-ribose) formation in DNA repair. *Nature* **356**, 356-358, doi:10.1038/356356a0 (1992).

43   Jackson, S. P. & Bartek, J. The DNA-damage response in human biology and disease. *Nature* **461**, 1071-1078, doi:10.1038/nature08467 (2009).

44   Wahlberg, E., Karlberg, T., Kouznetsova, E., Markova, N., Macchiarulo, A., Thorsell, A. G., Pol, E., Frostell, A., Ekblad, T., Oncu, D., Kull, B., Robertson, G. M., Pellicciari, R., Schuler, H. & Weigelt, J. Family-wide chemical profiling and structural analysis of PARP and tankyrase inhibitors. *Nat Biotechnol* **30**, 283-288, doi:10.1038/nbt.2121 (2012).

45   Mukhopadhyay, A., Plummer, E. R., Elattar, A., Soohoo, S., Uzir, B., Quinn, J. E., McCluggage, W. G., Maxwell, P., Aneke, H., Curtin, N. J. & Edmondson, R. J. Clinicopathological features of homologous recombination-deficient epithelial ovarian cancers: sensitivity to PARP inhibitors, platinum, and survival. *Cancer Res* **72**, 5675-5682, doi:10.1158/0008-5472.CAN-12-0324 (2012).

46   Moore, K., Colombo, N., Scambia, G., Kim, B. G., Oaknin, A., Friedlander, M., Lisyanskaya, A., Floquet, A., Leary, A., Sonke, G. S., Gourley, C., Banerjee, S., Oza, A., Gonzalez-Martin, A., Aghajanian, C., Bradley, W., Mathews, C., Liu, J., Lowe, E. S., Bloomfield, R. & DiSilvestro, P. Maintenance Olaparib in Patients with Newly Diagnosed Advanced Ovarian Cancer. *N Engl J Med* **379**, 2495-2505, doi:10.1056/NEJMoa1810858 (2018).

47   Kindler, H. L., Hammel, P., Reni, M., Van Cutsem, E., Mercade T.M., Hall, M.J., Park, J.O., Hochhauser, D., Arnold, D., Oh, D.Y., Reinacher-Schick, A.C., Tortora, G., Algul, H., O'Reilly, E.M., McGuinness, D., Cui, K., Schlienger, K., Locker, G.Y., Golan, T. Olaparib as maintenance treatment following first-line platinum-based chemotherapy (PBC) in patients (pts) with a germline BRCA mutation and metastatic pancreatic cancer (mPC): Phase III POLO trial [abstract]. J Clin Oncol 37, 2019 (suppl; abstr LBA4).

48   Shen, Y., Rehman, F. L., Feng, Y., Boshuizen, J., Bajrami, I., Elliott, R., Wang, B., Lord, C. J., Post, L. E. & Ashworth, A. BMN 673, a novel and highly potent PARP1/2 inhibitor for the treatment of human cancers with DNA repair

deficiency. *Clin Cancer Res* **19**, 5003-5015, doi:10.1158/1078-0432.CCR-13-1391 (2013).

49   Litton, J. K., Rugo, H. S., Ettl, J., Hurvitz, S. A., Goncalves, A., Lee, K. H., Fehrenbacher, L., Yerushalmi, R., Mina, L. A., Martin, M., Roche, H., Im, Y. H., Quek, R. G. W., Markova, D., Tudor, I. C., Hannah, A. L., Eiermann, W. & Blum, J. L. Talazoparib in Patients with Advanced Breast Cancer and a Germline BRCA Mutation. *N Engl J Med* **379**, 753-763, doi:10.1056/NEJMoa1802905 (2018).

50   Bryant, H. E., Schultz, N., Thomas, H. D., Parker, K. M., Flower, D., Lopez, E., Kyle, S., Meuth, M., Curtin, N. J. & Helleday, T. Specific killing of BRCA2-deficient tumours with inhibitors of poly(ADP-ribose) polymerase. *Nature* **434**, 913-917, doi:10.1038/nature03443 (2005).

51   Farmer, H., McCabe, N., Lord, C. J., Tutt, A. N., Johnson, D. A., Richardson, T. B., Santarosa, M., Dillon, K. J., Hickson, I., Knights, C., Martin, N. M., Jackson, S. P., Smith, G. C. & Ashworth, A. Targeting the DNA repair defect in BRCA mutant cells as a therapeutic strategy. *Nature* **434**, 917-921, doi:10.1038/nature03445 (2005).

52   Madison, D. L., Stauffer, D. & Lundblad, J. R. The PARP inhibitor PJ34 causes a PARP1-independent, p21 dependent mitotic arrest. *DNA Repair (Amst)* **10**, 1003-1013, doi:10.1016/j.dnarep.2011.07.006 (2011).

53   Mason, P. J., Stevens, D., Diez, A., Knight, S. W., Scopes, D. A. & Vulliamy, T. J. Human hexose-6-phosphate dehydrogenase (glucose 1-dehydrogenase) encoded at 1p36: coding sequence and expression. *Blood Cells Mol Dis* **25**, 30-37, doi:10.1006/bcmd.1999.0224 (1999).

54   Banhegyi, G., Marcolongo, P., Fulceri, R., Hinds, C., Burchell, A. & Benedetti, A. Demonstration of a metabolically active glucose-6-phosphate pool in the lumen of liver microsomal vesicles. *J Biol Chem* **272**, 13584-13590, doi:10.1074/jbc.272.21.13584 (1997).

55   Knezevic, C. E., Wright, G., Rix, L. L. R., Kim, W., Kuenzi, B. M., Luo, Y., Watters, J. M., Koomen, J. M., Haura, E. B., Monteiro, A. N., Radu, C., Lawrence, H. R. & Rix, U. Proteome-wide Profiling of Clinical PARP Inhibitors Reveals Compound-Specific Secondary Targets. *Cell Chem Biol* **23**, 1490-1503, doi:10.1016/j.chembiol.2016.10.011 (2016).

56   Edwards, S. L., Brough, R., Lord, C. J., Natrajan, R., Vatcheva, R., Levine, D. A., Boyd, J., Reis-Filho, J. S. & Ashworth, A. Resistance to therapy caused by intragenic deletion in BRCA2. *Nature* **451**, 1111-1115, doi:10.1038/nature06548 (2008).

57   Swisher, E. M., Sakai, W., Karlan, B. Y., Wurz, K., Urban, N. & Taniguchi, T. Secondary BRCA1 mutations in BRCA1-mutated ovarian carcinomas with platinum resistance. *Cancer Res* **68**, 2581-2586, doi:10.1158/0008-5472.CAN-08-0088 (2008).

58   Sakai, W., Swisher, E. M., Karlan, B. Y., Agarwal, M. K., Higgins, J., Friedman, C., Villegas, E., Jacquemont, C., Farrugia, D. J., Couch, F. J., Urban, N. & Taniguchi, T. Secondary mutations as a mechanism of cisplatin resistance in BRCA2-mutated cancers. *Nature* **451**, 1116-1120, doi:10.1038/nature06633 (2008).

59   Huertas, P. DNA resection in eukaryotes: deciding how to fix the break. *Nat Struct Mol Biol* **17**, 11-16, doi:10.1038/nsmb.1710 (2010).

60   Williams, R. S., Dodson, G. E., Limbo, O., Yamada, Y., Williams, J. S., Guenther, G., Classen, S., Glover, J. N., Iwasaki, H., Russell, P. & Tainer, J. A. Nbs1 flexibly tethers Ctp1 and Mre11-Rad50 to coordinate DNA double-strand break processing and repair. *Cell* **139**, 87-99, doi:10.1016/j.cell.2009.07.033 (2009).

61   Sartori, A. A., Lukas, C., Coates, J., Mistrik, M., Fu, S., Bartek, J., Baer, R., Lukas, J. & Jackson, S. P. Human CtIP promotes DNA end resection. *Nature* **450**, 509-514, doi:10.1038/nature06337 (2007).

62   Yuan, J. & Chen, J. N terminus of CtIP is critical for homologous recombination-mediated double-strand break repair. *J Biol Chem* **284**, 31746-31752, doi:10.1074/jbc.M109.023424 (2009).

63   Huertas, P. & Jackson, S. P. Human CtIP mediates cell cycle control of DNA end resection and double strand break repair. *J Biol Chem* **284**, 9558-9565, doi:10.1074/jbc.M808906200 (2009).

64   D'Andrea, A. D. Mechanisms of PARP inhibitor sensitivity and resistance. *DNA Repair (Amst)* **71**, 172-176, doi:10.1016/j.dnarep.2018.08.021 (2018).

65   Chapman, J. R., Barral, P., Vannier, J. B., Borel, V., Steger, M., Tomas-Loba, A., Sartori, A. A., Adams, I. R., Batista, F. D. & Boulton, S. J. RIF1 is essential for 53BP1-dependent nonhomologous end joining and suppression of DNA double-strand break resection. *Mol Cell* **49**, 858-871, doi:10.1016/j.molcel.2013.01.002 (2013).

66   Johnson, N., Johnson, S. F., Yao, W., Li, Y. C., Choi, Y. E., Bernhardy, A. J., Wang, Y., Capelletti, M., Sarosiek, K. A., Moreau, L. A., Chowdhury, D.,

Wickramanayake, A., Harrell, M. I., Liu, J. F., D'Andrea, A. D., Miron, A., Swisher, E. M. & Shapiro, G. I. Stabilization of mutant BRCA1 protein confers PARP inhibitor and platinum resistance. *Proc Natl Acad Sci U S A* **110**, 17041-17046, doi:10.1073/pnas.1305170110 (2013).

67   Bouwman, P., Aly, A., Escandell, J. M., Pieterse, M., Bartkova, J., van der Gulden, H., Hiddingh, S., Thanasoula, M., Kulkarni, A., Yang, Q., Haffty, B. G., Tommiska, J., Blomqvist, C., Drapkin, R., Adams, D. J., Nevanlinna, H., Bartek, J., Tarsounas, M., Ganesan, S. & Jonkers, J. 53BP1 loss rescues BRCA1 deficiency and is associated with triple-negative and BRCA-mutated breast cancers. *Nat Struct Mol Biol* **17**, 688-695, doi:10.1038/nsmb.1831 (2010).

68   Mu, Y., Lou, J., Srivastava, M., Zhao, B., Feng, X. H., Liu, T., Chen, J. & Huang, J. SLFN11 inhibits checkpoint maintenance and homologous recombination repair. *EMBO Rep* **17**, 94-109, doi:10.15252/embr.201540964 (2016).

69   Murai, J., Feng, Y., Yu, G. K., Ru, Y., Tang, S. W., Shen, Y. & Pommier, Y. Resistance to PARP inhibitors by SLFN11 inactivation can be overcome by ATR inhibition. *Oncotarget* **7**, 76534-76550, doi:10.18632/oncotarget.12266 (2016).

70   Feng, L., Fong, K. W., Wang, J., Wang, W. & Chen, J. RIF1 counteracts BRCA1-mediated end resection during DNA repair. *J Biol Chem* **288**, 11135-11143, doi:10.1074/jbc.M113.457440 (2013).

71   Xu, D., Muniandy, P., Leo, E., Yin, J., Thangavel, S., Shen, X., Ii, M., Agama, K., Guo, R., Fox, D., 3rd, Meetei, A. R., Wilson, L., Nguyen, H., Weng, N. P., Brill, S. J., Li, L., Vindigni, A., Pommier, Y., Seidman, M. & Wang, W. Rif1 provides a new

DNA-binding interface for the Bloom syndrome complex to maintain normal replication. *EMBO J* **29**, 3140-3155, doi:10.1038/emboj.2010.186 (2010).

72   Han, J., Ruan, C., Huen, M. S. Y., Wang, J., Xie, A., Fu, C., Liu, T. & Huang, J. BRCA2 antagonizes classical and alternative nonhomologous end-joining to prevent gross genomic instability. *Nat Commun* **8**, 1470, doi:10.1038/s41467-017-01759-y (2017).

73   Sone, T., Saeki, Y., Toh-e, A. & Yokosawa, H. Sem1p is a novel subunit of the 26 S proteasome from Saccharomyces cerevisiae. *J Biol Chem* **279**, 28807-28816, doi:10.1074/jbc.M403165200 (2004).

74   Siaud, N., Barbera, M. A., Egashira, A., Lam, I., Christ, N., Schlacher, K., Xia, B. & Jasin, M. Plasticity of BRCA2 function in homologous recombination: genetic interactions of the PALB2 and DNA binding domains. *PLoS Genet* **7**, e1002409, doi:10.1371/journal.pgen.1002409 (2011).

75   Krogan, N. J., Lam, M. H., Fillingham, J., Keogh, M. C., Gebbia, M., Li, J., Datta, N., Cagney, G., Buratowski, S., Emili, A. & Greenblatt, J. F. Proteasome involvement in the repair of DNA double-strand breaks. *Mol Cell* **16**, 1027-1034, doi:10.1016/j.molcel.2004.11.033 (2004).

76   Martens-de Kemp, S. R., Brink, A., van der Meulen, I. H., de Menezes, R. X., Te Beest, D. E., Leemans, C. R., van Beusechem, V. W., Braakhuis, B. J. & Brakenhoff, R. H. The FA/BRCA Pathway Identified as the Major Predictor of Cisplatin Response in Head and Neck Cancer by Functional Genomics. *Mol Cancer Ther* **16**, 540-550, doi:10.1158/1535-7163.MCT-16-0457 (2017).

77   Nguyen, K. T., Holloway, M. P. & Altura, R. A. The CRM1 nuclear export protein in normal development and disease. *Int J Biochem Mol Biol* **3**, 137-151 (2012).

78   Noske, A., Weichert, W., Niesporek, S., Roske, A., Buckendahl, A. C., Koch, I., Sehouli, J., Dietel, M. & Denkert, C. Expression of the nuclear export protein chromosomal region maintenance/exportin 1/Xpo1 is a prognostic factor in human ovarian cancer. *Cancer* **112**, 1733-1743, doi:10.1002/cncr.23354 (2008).

79   Huang, W. Y., Yue, L., Qiu, W. S., Wang, L. W., Zhou, X. H. & Sun, Y. J. Prognostic value of CRM1 in pancreas cancer. *Clin Invest Med* **32**, E315 (2009).

80   Abdul Razak, A. R., Mau-Soerensen, M., Gabrail, N. Y., Gerecitano, J. F., Shields, A. F., Unger, T. J., Saint-Martin, J. R., Carlson, R., Landesman, Y., McCauley, D., Rashal, T., Lassen, U., Kim, R., Stayner, L. A., Mirza, M. R., Kauffman, M., Shacham, S. & Mahipal, A. First-in-Class, First-in-Human Phase I Study of Selinexor, a Selective Inhibitor of Nuclear Export, in Patients With Advanced Solid Tumors. *J Clin Oncol* **34**, 4142-4150, doi:10.1200/JCO.2015.65.3949 (2016).

81   Shafique, M., Ismail-Khan, R., Extermann, M., Sullivan, D., Goodridge, D., Boulware, D., Hogue, D., Soliman, H., Khong, H. & Han, H. S. A Phase II Trial of Selinexor (KPT-330) for Metastatic Triple-Negative Breast Cancer. *Oncologist*, doi:10.1634/theoncologist.2019-0231 (2019).

82   Brand, R. E., Lerch, M. M., Rubinstein, W. S., Neoptolemos, J. P., Whitcomb, D. C., Hruban, R. H., Brentnall, T. A., Lynch, H. T., Canto, M. I. & Participants of the

Fourth International Symposium of Inherited Diseases of the, P. Advances in counselling and surveillance of patients at risk for pancreatic cancer. *Gut* **56**, 1460-1469, doi:10.1136/gut.2006.108456 (2007).

83   Grant, R. C., Selander, I., Connor, A. A., Selvarajah, S., Borgida, A., Briollais, L., Petersen, G. M., Lerner-Ellis, J., Holter, S. & Gallinger, S. Prevalence of germline mutations in cancer predisposition genes in patients with pancreatic cancer. *Gastroenterology* **148**, 556-564, doi:10.1053/j.gastro.2014.11.042 (2015).

84   Kastrinos, F., Mukherjee, B., Tayob, N., Wang, F., Sparr, J., Raymond, V. M., Bandipalliam, P., Stoffel, E. M., Gruber, S. B. & Syngal, S. Risk of pancreatic cancer in families with Lynch syndrome. *JAMA* **302**, 1790-1795, doi:10.1001/jama.2009.1529 (2009).

85   Lin, K. M., Shashidharan, M., Thorson, A. G., Ternent, C. A., Blatchford, G. J., Christensen, M. A., Watson, P., Lemon, S. J., Franklin, B., Karr, B., Lynch, J. & Lynch, H. T. Cumulative incidence of colorectal and extracolonic cancers in MLH1 and MSH2 mutation carriers of hereditary nonpolyposis colorectal cancer. *J Gastrointest Surg* **2**, 67-71 (1998).

86   Moran, A., O'Hara, C., Khan, S., Shack, L., Woodward, E., Maher, E. R., Lalloo, F. & Evans, D. G. Risk of cancer other than breast or ovarian in individuals with BRCA1 and BRCA2 mutations. *Fam Cancer* **11**, 235-242, doi:10.1007/s10689-011-9506-2 (2012).

87   Roberts, N. J., Jiao, Y., Yu, J., Kopelovich, L., Petersen, G. M., Bondy, M. L., Gallinger, S., Schwartz, A. G., Syngal, S., Cote, M. L., Axilbund, J., Schulick, R.,

Ali, S. Z., Eshleman, J. R., Velculescu, V. E., Goggins, M., Vogelstein, B., Papadopoulos, N., Hruban, R. H., Kinzler, K. W. & Klein, A. P. ATM mutations in patients with hereditary pancreatic cancer. *Cancer Discov* **2**, 41-46, doi:10.1158/2159-8290.CD-11-0194 (2012).

88   Shindo, K., Yu, J., Suenaga, M., Fesharakizadeh, S., Cho, C., Macgregor-Das, A., Siddiqui, A., Witmer, P. D., Tamura, K., Song, T. J., Navarro Almario, J. A., Brant, A., Borges, M., Ford, M., Barkley, T., He, J., Weiss, M. J., Wolfgang, C. L., Roberts, N. J., Hruban, R. H., Klein, A. P. & Goggins, M. Deleterious Germline Mutations in Patients With Apparently Sporadic Pancreatic Adenocarcinoma. *J Clin Oncol*, JCO2017723502, doi:10.1200/JCO.2017.72.3502 (2017).

89   Network., N. C. C. *Genetic/Familial High-Risk Assessment: Breast and Ovarian (Version 2.2019)* <https://www.nccn.org/professionals/physician_gls/pdf/genetics_screening.pdf> (

90   Hampel, H., Bennett, R. L., Buchanan, A., Pearlman, R., Wiesner, G. L., Guideline Development Group, A. C. o. M. G., Genomics Professional, P., Guidelines, C. & National Society of Genetic Counselors Practice Guidelines, C. A practice guideline from the American College of Medical Genetics and Genomics and the National Society of Genetic Counselors: referral indications for cancer predisposition assessment. *Genet Med* **17**, 70-87, doi:10.1038/gim.2014.147 (2015).

91   Conroy, T., Desseigne, F., Ychou, M., Bouche, O., Guimbaud, R., Becouarn, Y., Adenis, A., Raoul, J. L., Gourgou-Bourgade, S., de la Fouchardiere, C.,

Bennouna, J., Bachet, J. B., Khemissa-Akouz, F., Pere-Verge, D., Delbaldo, C., Assenat, E., Chauffert, B., Michel, P., Montoto-Grillot, C., Ducreux, M., Groupe Tumeurs Digestives of, U. & Intergroup, P. FOLFIRINOX versus gemcitabine for metastatic pancreatic cancer. *N Engl J Med* **364**, 1817-1825, doi:10.1056/NEJMoa1011923 (2011).

92   Von Hoff, D. D., Ervin, T., Arena, F. P., Chiorean, E. G., Infante, J., Moore, M., Seay, T., Tjulandin, S. A., Ma, W. W., Saleh, M. N., Harris, M., Reni, M., Dowden, S., Laheru, D., Bahary, N., Ramanathan, R. K., Tabernero, J., Hidalgo, M., Goldstein, D., Van Cutsem, E., Wei, X., Iglesias, J. & Renschler, M. F. Increased survival in pancreatic cancer with nab-paclitaxel plus gemcitabine. *N Engl J Med* **369**, 1691-1703, doi:10.1056/NEJMoa1304369 (2013).

93   Chen, K., Meric-Bernstam, F., Zhao, H., Zhang, Q., Ezzeddine, N., Tang, L. Y., Qi, Y., Mao, Y., Chen, T., Chong, Z., Zhou, W., Zheng, X., Johnson, A., Aldape, K. D., Routbort, M. J., Luthra, R., Kopetz, S., Davies, M. A., de Groot, J., Moulder, S., Vinod, R., Farhangfar, C. J., Shaw, K. M., Mendelsohn, J., Mills, G. B. & Eterovic, A. K. Clinical actionability enhanced through deep targeted sequencing of solid tumors. *Clin Chem* **61**, 544-553, doi:10.1373/clinchem.2014.231100 (2015).

94   Li, H. & Durbin, R. Fast and accurate short read alignment with Burrows-Wheeler transform. *Bioinformatics* **25**, 1754-1760, doi:10.1093/bioinformatics/btp324 (2009).

95   DePristo, M. A., Banks, E., Poplin, R., Garimella, K. V., Maguire, J. R., Hartl, C., Philippakis, A. A., del Angel, G., Rivas, M. A., Hanna, M., McKenna, A., Fennell,

T. J., Kernytsky, A. M., Sivachenko, A. Y., Cibulskis, K., Gabriel, S. B., Altshuler, D. & Daly, M. J. A framework for variation discovery and genotyping using next-generation DNA sequencing data. *Nat Genet* **43**, 491-498, doi:10.1038/ng.806 (2011).

96   Rimmer, A., Phan, H., Mathieson, I., Iqbal, Z., Twigg, S. R. F., Consortium, W. G. S., Wilkie, A. O. M., McVean, G. & Lunter, G. Integrating mapping-, assembly- and haplotype-based approaches for calling variants in clinical sequencing applications. *Nat Genet* **46**, 912-918, doi:10.1038/ng.3036 (2014).

97   Richards, S., Aziz, N., Bale, S., Bick, D., Das, S., Gastier-Foster, J., Grody, W. W., Hegde, M., Lyon, E., Spector, E., Voelkerding, K., Rehm, H. L. & Committee, A. L. Q. A. Standards and guidelines for the interpretation of sequence variants: a joint consensus recommendation of the American College of Medical Genetics and Genomics and the Association for Molecular Pathology. *Genet Med* **17**, 405-424, doi:10.1038/gim.2015.30 (2015).

98   Eggington, J. M., Bowles, K. R., Moyes, K., Manley, S., Esterling, L., Sizemore, S., Rosenthal, E., Theisen, A., Saam, J., Arnell, C., Pruss, D., Bennett, J., Burbidge, L. A., Roa, B. & Wenstrup, R. J. A comprehensive laboratory-based program for classification of variants of uncertain significance in hereditary cancer genes. *Clin Genet* **86**, 229-237, doi:10.1111/cge.12315 (2014).

99   Stenson, P. D., Ball, E. V., Mort, M., Phillips, A. D., Shiel, J. A., Thomas, N. S., Abeysinghe, S., Krawczak, M. & Cooper, D. N. Human Gene Mutation Database (HGMD): 2003 update. *Hum Mutat* **21**, 577-581, doi:10.1002/humu.10212 (2003).

100   Landrum, M. J., Lee, J. M., Benson, M., Brown, G., Chao, C., Chitipiralla, S., Gu, B., Hart, J., Hoffman, D., Hoover, J., Jang, W., Katz, K., Ovetsky, M., Riley, G., Sethi, A., Tully, R., Villamarin-Salomon, R., Rubinstein, W. & Maglott, D. R. ClinVar: public archive of interpretations of clinically relevant variants. *Nucleic Acids Res* **44**, D862-868, doi:10.1093/nar/gkv1222 (2016).

101   Beroud, C., Letovsky, S. I., Braastad, C. D., Caputo, S. M., Beaudoux, O., Bignon, Y. J., Bressac-De Paillerets, B., Bronner, M., Buell, C. M., Collod-Beroud, G., Coulet, F., Derive, N., Divincenzo, C., Elzinga, C. D., Garrec, C., Houdayer, C., Karbassi, I., Lizard, S., Love, A., Muller, D., Nagan, N., Nery, C. R., Rai, G., Revillion, F., Salgado, D., Sevenet, N., Sinilnikova, O., Sobol, H., Stoppa-Lyonnet, D., Toulas, C., Trautman, E., Vaur, D., Vilquin, P., Weymouth, K. S., Willis, A., Laboratory Corporation of America Variant Classification, G., Quest Diagnostics Variant Classification, G., Network, U. G. G. B. L., Eisenberg, M. & Strom, C. M. BRCA Share: A Collection of Clinical BRCA Gene Variants. *Hum Mutat* **37**, 1318-1328, doi:10.1002/humu.23113 (2016).

102   Hu, C., Hart, S. N., Polley, E. C., Gnanaolivu, R., Shimelis, H., Lee, K. Y., Lilyquist, J., Na, J., Moore, R., Antwi, S. O., Bamlet, W. R., Chaffee, K. G., DiCarlo, J., Wu, Z., Samara, R., Kasi, P. M., McWilliams, R. R., Petersen, G. M. & Couch, F. J. Association Between Inherited Germline Mutations in Cancer Predisposition Genes and Risk of Pancreatic Cancer. *JAMA* **319**, 2401-2409, doi:10.1001/jama.2018.6228 (2018).

103   Yurgelun, M. B., Chittenden, A. B., Morales-Oyarvide, V., Rubinson, D. A., Dunne, R. F., Kozak, M. M., Qian, Z. R., Welch, M. W., Brais, L. K., Da Silva, A.,

Bui, J. L., Yuan, C., Li, T., Li, W., Masuda, A., Gu, M., Bullock, A. J., Chang, D. T., Clancy, T. E., Linehan, D. C., Findeis-Hosey, J. J., Doyle, L. A., Thorner, A. R., Ducar, M. D., Wollison, B. M., Khalaf, N., Perez, K., Syngal, S., Aguirre, A. J., Hahn, W. C., Meyerson, M. L., Fuchs, C. S., Ogino, S., Hornick, J. L., Hezel, A. F., Koong, A. C., Nowak, J. A. & Wolpin, B. M. Germline cancer susceptibility gene variants, somatic second hits, and survival outcomes in patients with resected pancreatic cancer. *Genet Med* **21**, 213-223, doi:10.1038/s41436-018-0009-5 (2019).

104   Roberts, N. J., Norris, A. L., Petersen, G. M., Bondy, M. L., Brand, R., Gallinger, S., Kurtz, R. C., Olson, S. H., Rustgi, A. K., Schwartz, A. G., Stoffel, E., Syngal, S., Zogopoulos, G., Ali, S. Z., Axilbund, J., Chaffee, K. G., Chen, Y. C., Cote, M. L., Childs, E. J., Douville, C., Goes, F. S., Herman, J. M., Iacobuzio-Donahue, C., Kramer, M., Makohon-Moore, A., McCombie, R. W., McMahon, K. W., Niknafs, N., Parla, J., Pirooznia, M., Potash, J. B., Rhim, A. D., Smith, A. L., Wang, Y., Wolfgang, C. L., Wood, L. D., Zandi, P. P., Goggins, M., Karchin, R., Eshleman, J. R., Papadopoulos, N., Kinzler, K. W., Vogelstein, B., Hruban, R. H. & Klein, A. P. Whole Genome Sequencing Defines the Genetic Heterogeneity of Familial Pancreatic Cancer. *Cancer Discov* **6**, 166-175, doi:10.1158/2159-8290.CD-15-0402 (2016).

105   Hwang, R. F., Wang, H., Lara, A., Gomez, H., Chang, T., Sieffert, N., Moon, Y., Ram, S., Zimmerman, S., Lee, J. H., Pisters, P. W., Tamm, E. P., Fleming, J. B., Abbruzzese, J. L. & Evans, D. B. Development of an integrated biospecimen

bank and multidisciplinary clinical database for pancreatic cancer. *Ann Surg Oncol* **15**, 1356-1366, doi:10.1245/s10434-008-9833-1 (2008).

106   Barber, L. J., Rosa Rosa, J. M., Kozarewa, I., Fenwick, K., Assiotis, I., Mitsopoulos, C., Sims, D., Hakas, J., Zvelebil, M., Lord, C. J. & Ashworth, A. Comprehensive genomic analysis of a BRCA2 deficient human pancreatic cancer. *PLoS One* **6**, e21639, doi:10.1371/journal.pone.0021639 (2011).

107   Deer, E. L., Gonzalez-Hernandez, J., Coursen, J. D., Shea, J. E., Ngatia, J., Scaife, C. L., Firpo, M. A. & Mulvihill, S. J. Phenotype and genotype of pancreatic cancer cell lines. *Pancreas* **39**, 425-435, doi:10.1097/MPA.0b013e3181c15963 (2010).

108   Fogh, J., Fogh, J. M. & Orfeo, T. One hundred and twenty-seven cultured human tumor cell lines producing tumors in nude mice. *J Natl Cancer Inst* **59**, 221-226 (1977).

109   Dahiya, R., Kwak, K. S., Byrd, J. C., Ho, S., Yoon, W. H. & Kim, Y. S. Mucin synthesis and secretion in various human epithelial cancer cell lines that express the MUC-1 mucin gene. *Cancer Res* **53**, 1437-1443 (1993).

110   Chen, W. H., Horoszewicz, J. S., Leong, S. S., Shimano, T., Penetrante, R., Sanders, W. H., Berjian, R., Douglass, H. O., Martin, E. W. & Chu, T. M. Human pancreatic adenocarcinoma: in vitro and in vivo morphology of a new tumor line established from ascites. *In Vitro* **18**, 24-34 (1982).

111   Cibulskis, K., Lawrence, M. S., Carter, S. L., Sivachenko, A., Jaffe, D., Sougnez, C., Gabriel, S., Meyerson, M., Lander, E. S. & Getz, G. Sensitive detection of

somatic point mutations in impure and heterogeneous cancer samples. *Nat Biotechnol* **31**, 213-219, doi:10.1038/nbt.2514 (2013).

112   Ye, K., Schulz, M. H., Long, Q., Apweiler, R. & Ning, Z. Pindel: a pattern growth approach to detect break points of large deletions and medium sized insertions from paired-end short reads. *Bioinformatics* **25**, 2865-2871, doi:10.1093/bioinformatics/btp394 (2009).

113   Wang, K., Li, M. & Hakonarson, H. ANNOVAR: functional annotation of genetic variants from high-throughput sequencing data. *Nucleic Acids Res* **38**, e164, doi:10.1093/nar/gkq603 (2010).

114   Quinlan, A. R. & Hall, I. M. BEDTools: a flexible suite of utilities for comparing genomic features. *Bioinformatics* **26**, 841-842, doi:10.1093/bioinformatics/btq033 (2010).

115   Gildemeister, O. S., Sage, J. M. & Knight, K. L. Cellular redistribution of Rad51 in response to DNA damage: novel role for Rad51C. *J Biol Chem* **284**, 31945-31952, doi:10.1074/jbc.M109.024646 (2009).

116   Graeser, M., McCarthy, A., Lord, C. J., Savage, K., Hills, M., Salter, J., Orr, N., Parton, M., Smith, I. E., Reis-Filho, J. S., Dowsett, M., Ashworth, A. & Turner, N. C. A marker of homologous recombination predicts pathologic complete response to neoadjuvant chemotherapy in primary breast cancer. *Clin Cancer Res* **16**, 6159-6168, doi:10.1158/1078-0432.CCR-10-1027 (2010).

117   Tashiro, S., Walter, J., Shinohara, A., Kamada, N. & Cremer, T. Rad51 accumulation at sites of DNA damage and in postreplicative chromatin. *J Cell Biol* **150**, 283-291 (2000).

118   Roth, A., Khattra, J., Yap, D., Wan, A., Laks, E., Biele, J., Ha, G., Aparicio, S., Bouchard-Cote, A. & Shah, S. P. PyClone: statistical inference of clonal population structure in cancer. *Nat Methods* **11**, 396-398, doi:10.1038/nmeth.2883 (2014).

119   Jamal-Hanjani, M., Wilson, G. A., McGranahan, N., Birkbak, N. J., Watkins, T. B. K., Veeriah, S., Shafi, S., Johnson, D. H., Mitter, R., Rosenthal, R., Salm, M., Horswell, S., Escudero, M., Matthews, N., Rowan, A., Chambers, T., Moore, D. A., Turajlic, S., Xu, H., Lee, S. M., Forster, M. D., Ahmad, T., Hiley, C. T., Abbosh, C., Falzon, M., Borg, E., Marafioti, T., Lawrence, D., Hayward, M., Kolvekar, S., Panagiotopoulos, N., Janes, S. M., Thakrar, R., Ahmed, A., Blackhall, F., Summers, Y., Shah, R., Joseph, L., Quinn, A. M., Crosbie, P. A., Naidu, B., Middleton, G., Langman, G., Trotter, S., Nicolson, M., Remmen, H., Kerr, K., Chetty, M., Gomersall, L., Fennell, D. A., Nakas, A., Rathinam, S., Anand, G., Khan, S., Russell, P., Ezhil, V., Ismail, B., Irvin-Sellers, M., Prakash, V., Lester, J. F., Kornaszewska, M., Attanoos, R., Adams, H., Davies, H., Dentro, S., Taniere, P., O'Sullivan, B., Lowe, H. L., Hartley, J. A., Iles, N., Bell, H., Ngai, Y., Shaw, J. A., Herrero, J., Szallasi, Z., Schwarz, R. F., Stewart, A., Quezada, S. A., Le Quesne, J., Van Loo, P., Dive, C., Hackshaw, A., Swanton, C. & Consortium, T. R. Tracking the Evolution of Non-Small-Cell Lung Cancer. *N Engl J Med* **376**, 2109-2121, doi:10.1056/NEJMoa1616288 (2017).

120   Murtaza, M., Dawson, S. J., Pogrebniak, K., Rueda, O. M., Provenzano, E., Grant, J., Chin, S. F., Tsui, D. W. Y., Marass, F., Gale, D., Ali, H. R., Shah, P., Contente-Cuomo, T., Farahani, H., Shumansky, K., Kingsbury, Z., Humphray, S., Bentley,

D., Shah, S. P., Wallis, M., Rosenfeld, N. & Caldas, C. Multifocal clonal evolution characterized using circulating tumour DNA in a case of metastatic breast cancer. *Nat Commun* **6**, 8760, doi:10.1038/ncomms9760 (2015).

121   Butler, A., Hoffman, P., Smibert, P., Papalexi, E. & Satija, R. Integrating single-cell transcriptomic data across different conditions, technologies, and species. *Nat Biotechnol* **36**, 411-420, doi:10.1038/nbt.4096 (2018).

122   Stuart, T., Butler, A., Hoffman, P., Hafemeister, C., Papalexi, E., Mauck, W. M., 3rd, Hao, Y., Stoeckius, M., Smibert, P. & Satija, R. Comprehensive Integration of Single-Cell Data. *Cell* **177**, 1888-1902 e1821, doi:10.1016/j.cell.2019.05.031 (2019).

123   McInnes, L., Healy, J., Saul, N. & Großberger, L. UMAP: uniform manifold approximation and projection. J. Open Source Softw. 3, 861 (2018).

124   Hanzelmann, S., Castelo, R. & Guinney, J. GSVA: gene set variation analysis for microarray and RNA-seq data. *BMC Bioinformatics* **14**, 7, doi:10.1186/1471-2105-14-7 (2013).

125   Brunet, J. P., Tamayo, P., Golub, T. R. & Mesirov, J. P. Metagenes and molecular pattern discovery using matrix factorization. *Proc Natl Acad Sci U S A* **101**, 4164-4169, doi:10.1073/pnas.0308531101 (2004).

126   Gaujoux, R. & Seoighe, C. A flexible R package for nonnegative matrix factorization. *BMC Bioinformatics* **11**, 367, doi:10.1186/1471-2105-11-367 (2010).

127   Qiu, X., Hill, A., Packer, J., Lin, D., Ma, Y. A. & Trapnell, C. Single-cell mRNA quantification and differential analysis with Census. *Nat Methods* **14**, 309-315, doi:10.1038/nmeth.4150 (2017).

128   Qiu, X., Mao, Q., Tang, Y., Wang, L., Chawla, R., Pliner, H. A. & Trapnell, C. Reversed graph embedding resolves complex single-cell trajectories. *Nat Methods* **14**, 979-982, doi:10.1038/nmeth.4402 (2017).

129   Trapnell, C., Cacchiarelli, D., Grimsby, J., Pokharel, P., Li, S., Morse, M., Lennon, N. J., Livak, K. J., Mikkelsen, T. S. & Rinn, J. L. The dynamics and regulators of cell fate decisions are revealed by pseudotemporal ordering of single cells. *Nat Biotechnol* **32**, 381-386, doi:10.1038/nbt.2859 (2014).

130   Kim, M. P., Evans, D. B., Wang, H., Abbruzzese, J. L., Fleming, J. B. & Gallick, G. E. Generation of orthotopic and heterotopic human pancreatic cancer xenografts in immunodeficient mice. *Nat Protoc* **4**, 1670-1680, doi:10.1038/nprot.2009.171 (2009).

131   Kumar, R. & Cheok, C. F. RIF1: a novel regulatory factor for DNA replication and DNA damage response signaling. *DNA Repair (Amst)* **15**, 54-59, doi:10.1016/j.dnarep.2013.12.004 (2014).

132   Vento-Tormo, R., Efremova, M., Botting, R. A., Turco, M. Y., Vento-Tormo, M., Meyer, K. B., Park, J. E., Stephenson, E., Polanski, K., Goncalves, A., Gardner, L., Holmqvist, S., Henriksson, J., Zou, A., Sharkey, A. M., Millar, B., Innes, B., Wood, L., Wilbrey-Clark, A., Payne, R. P., Ivarsson, M. A., Lisgo, S., Filby, A., Rowitch, D. H., Bulmer, J. N., Wright, G. J., Stubbington, M. J. T., Haniffa, M., Moffett, A. & Teichmann, S. A. Single-cell reconstruction of the early maternal-fetal

interface in humans. *Nature* **563**, 347-353, doi:10.1038/s41586-018-0698-6 (2018).

133   Paulson, K. G., Voillet, V., McAfee, M. S., Hunter, D. S., Wagener, F. D., Perdicchio, M., Valente, W. J., Koelle, S. J., Church, C. D., Vandeven, N., Thomas, H., Colunga, A. G., Iyer, J. G., Yee, C., Kulikauskas, R., Koelle, D. M., Pierce, R. H., Bielas, J. H., Greenberg, P. D., Bhatia, S., Gottardo, R., Nghiem, P. & Chapuis, A. G. Acquired cancer resistance to combination immunotherapy from transcriptional loss of class I HLA. *Nat Commun* **9**, 3868, doi:10.1038/s41467-018-06300-3 (2018).

134   June, N. N. G. F. H.-R. A. B. a. O. V. A. f. h. w. n. o. p. p. g. p. g. s. p. a.

135   Hopkins, T. A., Shi, Y., Rodriguez, L. E., Solomon, L. R., Donawho, C. K., DiGiammarino, E. L., Panchal, S. C., Wilsbacher, J. L., Gao, W., Olson, A. M., Stolarik, D. F., Osterling, D. J., Johnson, E. F. & Maag, D. Mechanistic Dissection of PARP1 Trapping and the Impact on In Vivo Tolerability and Efficacy of PARP Inhibitors. *Mol Cancer Res* **13**, 1465-1477, doi:10.1158/1541-7786.MCR-15-0191-T (2015).

136   Bernard, V., Semaan, A., Huang, J., San Lucas, F. A., Mulu, F. C., Stephens, B. M., Guerrero, P. A., Huang, Y., Zhao, J., Kamyabi, N., Sen, S., Scheet, P. A., Taniguchi, C. M., Kim, M. P., Tzeng, C. W., Katz, M. H., Singhi, A. D., Maitra, A. & Alvarez, H. A. Single-Cell Transcriptomics of Pancreatic Cancer Precursors Demonstrates Epithelial and Microenvironmental Heterogeneity as an Early Event in Neoplastic Progression. *Clin Cancer Res* **25**, 2194-2205, doi:10.1158/1078-0432.CCR-18-1955 (2019).

137   Chen, G., Ning, B. & Shi, T. Single-Cell RNA-Seq Technologies and Related

Computational Data Analysis. *Front Genet* **10**, 317,

doi:10.3389/fgene.2019.00317 (2019).

138   Haque, A., Engel, J., Teichmann, S. A. & Lonnberg, T. A practical guide to

single-cell RNA-sequencing for biomedical research and clinical applications.

Genome Med **9**, 75, doi:10.1186/s13073-017-0467-4 (2017).

139   Li, L., Chen, H., Gao, Y., Wang, Y. W., Zhang, G. Q., Pan, S. H., Ji, L., Kong, R.,

Wang, G., Jia, Y. H., Bai, X. W. & Sun, B. Long Noncoding RNA MALAT1

Promotes Aggressive Pancreatic Cancer Proliferation and Metastasis via the

Stimulation of Autophagy. *Mol Cancer Ther* **15**, 2232-2243,

doi:10.1158/1535-7163.MCT-16-0008 (2016).

140   Glanzer, J. G., Liu, S. & Oakley, G. G. Small molecule inhibitor of the RPA70 N-

terminal protein interaction domain discovered using in silico and in vitro

methods. *Bioorg Med Chem* **19**, 2589-2595, doi:10.1016/j.bmc.2011.03.012

(2011).

141   Saulino, D. M., Younes, P. S., Bailey, J. M. & Younes, M. CRM1/XPO1 expression

in pancreatic adenocarcinoma correlates with survivin expression and the

proliferative activity. *Oncotarget* **9**, 21289-21295,

doi:10.18632/oncotarget.25088 (2018).

Vita

Jennifer B Goldstein was born in New York City, New York on November 17, 1981 to Ivan Rick Goldstein and Joyce Leigh LeVine Goldstein. After graduating from Oak Park High School in Oak Park, California she enrolled at The University of California at San Diego (UCSD) where she completed her undergraduate work. Jennifer graduated with a Bachelor of Science degree from UCSD, majoring in General Biology and minoring in Psychology and graduated in 2003. After graduation she spent two years performing research in the neuroscience basic science research laboratory of Marla Feller, Ph.D. Jennifer was accepted and enrolled in George Washington University School of Medicine and Health Sciences graduating in 2009. Jennifer then completed her internship and residency in Internal Medicine at The University of California at Los Angeles School of Medicine Department of Internal Medicine graduating in 2012. Jennifer then was accepted for a Hematology and Medical Oncology fellowship position at The University of Texas MD Anderson Cancer Center and began her training in 2012. She completed the fellowship in June of 2015. She entered The University of Texas Health Science Center Graduate School of Biomedical Sciences in 2013 under the mentorship of Andy Futreal, Ph.D. Jennifer plans to continue her career in academic medicine.

Permanent Address:

6425 Bayberry Street

Oak Park, CA 91377